Clarke Modet

Carrera 11 No. 86-53, Piso 3
Edificio Segovia
110221 Bogotá, **Colombia**
T (+57) 1 618 10 88
F (+57) 1 635 08 24

P- 2021/36795

SUPERINTENDENCIA DE INDUSTRIA Y COMERCIO
DIRECCIÓN DE NUEVAS CREACIONES
E. S. D.

Re: Expediente No. **NC2021/0017366**
Solicitud de patente a nombre de **AMGEN INC**

CLARKE MODET & CO COLOMBIA SAS, por intermedio de CAROLINA MERCEDES DAZA MONTALVO mayor de edad, identificada con cédula de ciudadanía número 39.808.557, abogada en ejercicio portadora de la tarjeta profesional número 141.563, actuando como apoderada de la sociedad AMGEN INC domiciliado en California, Estados Unidos de América, solicitante de la patente de referencia, en respuesta al oficio Nº **3985** notificado electrónicamente el 26 de marzo de 2025, relativo a los requisitos sustantivos de la solicitud, respetuosamente me permito presentar la siguiente información:

1. **Modificación al capítulo reivindicatorio:**

Con fundamento en la facultad que confiere el artículo 34 de la Decisión 486 al solicitante para modificar la solicitud de patente en cualquier momento del trámite, presento junto a este memorial un nuevo capítulo reivindicatorio que consta de diecisiete (17) reivindicaciones, el cual reemplaza completamente el documento presentado el 12 de febrero de 2025. Específicamente, se realizaron las siguientes modificaciones:

1.1 Se modificó la reivindicación 1 con el fin de:

1.1.1 Hacer referencia a que el compuesto corresponde a la Forma I del antropoisómero M del Compuesto 1. Dicha modificación se sustenta en las páginas 37, 43 y Ejemplo 1 de la descripción.

1.1.2 Reemplazar la referencia a que el número de picos del patrón de difracción de polvo de rayos X es "*al menos tres*" por el rango de "*tres a dieciocho*" de conformidad con los picos allí reclamados.

Clarke Modet

Carrera 11 No. 86-53, Piso 3
Edificio Segovia
110221 Bogotá, **Colombia**
T (+57) 1 618 10 88
F (+57) 1 635 08 24

1.1.3 Reemplazar el término "*usando*" por "*con*" para referirse a que la difracción de polvo de rayos X se realiza con una longitud de onda de rayos X de 1.54 Å.

1.1.4 Reemplazar la referencia a que el número de picos del RMN en estado sólido de ^{13}C es de "*al menos tres"* por el rango de "*tres a treinta y dos"* de conformidad con los picos allí reclamados.

1.2 Se eliminaron las reivindicaciones 2, 7, 11. Además se ajustó la numeración del documento.

1.3 Se modificó la antigua reivindicación 4 (nueva reivindicación 3) con el fin de reemplazar la referencia a que el número de picos del patrón de difracción de polvo de rayos X es "*al menos cinco*" por el rango de "*cinco a dieciocho*" de conformidad con los picos allí reclamados.

1.4 Se modificó la antigua reivindicación 5 (nueva reivindicación 4) con el fin de reemplazar la referencia a que el número de picos del patrón de difracción de polvo de rayos X es "*al menos siete*" por el rango de "*siete a dieciocho*" de conformidad con los picos allí reclamados.

1.5 Se modificó la antigua reivindicación 8 (nueva reivindicación 6) con el fin de reemplazar la referencia a que el número de picos del RMN en estado sólido de ^{13}C de "*al menos cinco*" por el rango de "*cinco a treinta y dos*" de conformidad con los picos allí reclamados.

1.6 Se modificó la antigua reivindicación 9 (nueva reivindicación 7) con el fin de reemplazar la referencia a que el número de picos del RMN en estado sólido de ^{13}C de "*al* menos *siete*" por el rango de "*siete a treinta y dos*" de conformidad con los picos allí reclamados.

Estas modificaciones no amplían de ninguna manera la materia objeto de la presente solicitud, ya que se encuentran sustentadas tanto en la descripción como en el listado de secuencias, y se realizan con el fin de definir la materia reclamada de forma clara y superar las objeciones planteadas por el examinador en su concepto técnico.

Clarke Modet

Carrera 11 No. 86-53, Piso 3
Edificio Segovia
110221 Bogotá, **Colombia**
T (+57) 1 618 10 88
F (+57) 1 635 08 24

2. Pago de tasas

Considerando que el presente memorial se presenta junto con modificaciones a las reivindicaciones, se adjunta recibo por concepto de pago de tasa de modificación a la solicitud, según lo establecido en la **Resolución 59669 de 2020.**

Ahora, en relación con el número de reivindicaciones, atentamente me permito resaltar que junto a la presente respuesta no se realiza el pago de la tasa por concepto de reivindicaciones adicionales, dado que el nuevo capítulo reivindicatorio cuenta con un menor número de cláusulas que el presentado y estudiado anteriormente por su despacho.

Por otra parte, es deseo del solicitante requerir que, si el examinador considera que aún existen motivos que impidan la concesión de la solicitud, proceda a emitir un nuevo examen de patentabilidad, para lo cual se anexa el respectivo pago de nuevo examen.

3. Claridad y concisión de las reivindicaciones

El solicitante manifiesta que mediante la presentación del nuevo capítulo reivindicatorio quedan subsanadas la totalidad de las objeciones presentadas por el examinador en su concepto técnico, de modo tal que las nuevas reivindicaciones reclaman de manera clara y concisa la invención descrita. Con respecto a las objeciones específicas del examinador, me permito manifestar lo siguiente:

3.1 El examinador indica que el alcance de la reivindicación 1 y sus dependientes se refiere específicamente a la Forma I anhidra cristalina del atropisómero M del compuesto (1). Por tanto, solicita que se especifique expresamente esta forma para una definición más clara del material a proteger.

Con el fin de facilitar la continuación del trámite, el solicitante ha decidido acoger la sugerencia del examinador y ha modificado la redacción de la reivindicación para especificar que el compuesto corresponde a la forma cristalina (Forma I) del atropisómero M del 6-fluoro-7-(2-fluoro-6-hidroxifenil)-1-(4-metil-2-(2-propanil)-3-piridinil)-4-((2S)-2-metil-4-(2-propenoil)-1-piperazinil)pirido[2,3-d]pirimidin-2(1H)-ona, es decir, la Forma I del atropisómero M del Compuesto 1. En este sentido, se solicita respetuosamente considerar superada la objeción correspondiente.

Clarke Modet

Carrera 11 No. 86-53, Piso 3
Edificio Segovia
110221 Bogotá, **Colombia**
T (+57) 1 618 10 88
F (+57) 1 635 08 24

3.2 El examinador observa que la reivindicación 1 incluye tres características alternativas (a, b o c), lo cual genera ambigüedad respecto al alcance de la protección. Dado que se refiere a un único material, el examinador recomienda eliminar el carácter opcional y redactar la reivindicación de forma acumulativa.

El solicitante manifiesta respetuosamente su desacuerdo con la objeción planteada. En este sentido, desea aclarar que el alcance de la reivindicación 1 es claro y se encuentra debidamente definido, ya que el compuesto al que hace referencia corresponde específicamente a la Forma I del atropisómero M del Compuesto 1.

Asimismo, se precisa que dicha reivindicación establece tres métodos independientes para caracterizar e identificar la forma reivindicada. Cada uno de los métodos señalados, (a), (b) y (c), es, por sí solo, suficiente para identificar la forma cristalina objeto de protección. Cabe resaltar que los métodos indicados son técnicas reconocidas y ampliamente utilizadas en el campo de la ciencia del polimorfismo, siendo prácticas estándar en la caracterización de formas sólidas (véanse, por ejemplo: Du et al., 2022, y Gil et al.,2019, que se encuentran para facilidad de consulta en los anexos de este memorial).

Dichos métodos representan alternativas válidas de caracterización que no se excluyen entre sí ni introducen ambigüedad respecto a la estructura de la forma protegida. Por el contrario, permiten confirmar con mayor solidez la identidad del compuesto reivindicado. En este contexto, el uso del conector "o" resulta técnicamente adecuado y justificado. Por lo tanto, se solicita respetuosamente que la presente objeción sea retirada.

3.3 El examinador objeta la reivindicación 1 por el uso de la expresión "*...usando una longitud de...*", ya que puede interpretarse como una reivindicación de uso, lo cual no es patentable. Se sugiere suprimir dicha expresión y ajustar la redacción.

Con el fin de evitar hacer referencia a materia no patentable, el solicitante ha decidido reemplazar el término "*usando*" por "*con*", de modo que la expresión correspondiente indique que la difracción de rayos X en polvo se lleva a cabo con una longitud de onda de 1.54 Å. En este sentido, se solicita amablemente que la presente objeción sea considerada como superada.

3.4 Las reivindicaciones 1, 2, 4-5 y 7 a 9 utilizan el término *"al menos",* el cual se considera impreciso e insuficiente para delimitar la invención respecto al estado

Clarke Modet

Carrera 11 No. 86-53, Piso 3
Edificio Segovia
110221 Bogotá, **Colombia**
T (+57) 1 618 10 88
F (+57) 1 635 08 24

de la técnica. Por ende, el examinador recomienda reemplazarlo por valores o rangos definidos.

Al respecto, el solicitante respetuosamente manifiesta su desacuerdo, pero con el fin de contribuir al adecuado avance del trámite, se ha decidido modificar el capítulo reivindicatorio para eliminar el término "*al menos*", sustituyéndolo por rangos concretos en relación con la cantidad de picos observados en el espectro de RMN en estado sólido de 13C y en el patrón de difracción de rayos X en polvo, según corresponda.

Dichas modificaciones se detallan en la Sección 1 del presente escrito de modificación a las reivindicaciones. En este sentido, se solicita amablemente que la objeción sea considerada como superada.

3.5 El examinador señala que las reivindicaciones 2, 7 y 11 repiten el material ya definido en la reivindicación 1 sin añadir características técnicas adicionales, generando falta de concisión. Se recomienda eliminarlas o redefinirlas con aportes técnicos concretos.

El solicitante en este sentido manifiesta respetuosamente su desacuerdo, sin embargo, únicamente con el propósito de agilizar el trámite del presente expediente, el solicitante eliminó las reivindicaciones 2, 7 y 11. Por ende es posible considerar superada la presente objeción.

3.6 El examinador considera que las reivindicaciones 3 a 7, así como 8 a 10, aunque están formuladas correctamente, se consideran redundantes, ya que protegen esencialmente la misma materia. De ahí que el examinador sugiere consolidarlas para mejorar la claridad y evitar repeticiones innecesarias.

El solicitante manifiesta respetuosamente su desacuerdo con la objeción del examinador, toda vez que las reivindicaciones 3 a 7 y 8 a 10 corresponden a realizaciones preferidas de la invención. Dichas reivindicaciones especifican picos particulares dentro del patrón de difracción de rayos X en polvo y del espectro de RMN en estado sólido de 13C, los cuales son coherentes con el rango definido en la reivindicación independiente 1.

En consecuencia, estas reivindicaciones no introducen ambigüedad ni redundancia, sino que describen características estructurales particulares del compuesto objeto de protección, que el solicitante desea reivindicar como parte del alcance estructural

Clarke Modet

Carrera 11 No. 86-53, Piso 3
Edificio Segovia
110221 Bogotá, **Colombia**
T (+57) 1 618 10 88
F (+57) 1 635 08 24

derivado de la reivindicación 1, de la cual dependen. Por lo anterior, se solicita respetuosamente que se retire la objeción formulada.

3.8 El examinador indica que estas reivindicaciones 16 a 20 no están respaldadas suficientemente en la descripción, ya que no se evidencia una composición que incluya un excipiente farmacéuticamente aceptable, ni se describen todas las combinaciones posibles. Recuerda que no basta con mencionar la materia, sino que debe estar técnicamente descrita. Por ello, sugiere eliminarlas.

Respetuosamente, el solicitante manifiesta su desacuerdo con la objeción formulada por el examinador. Como se indicó previamente, los ejemplos incluidos en la solicitud tienen como objetivo ilustrar el desarrollo de la invención, sin limitar su alcance. Exigir que cada característica, compuesto o composición individual sea evaluado explícitamente para demostrar que forma parte de la invención constituye, a nuestro juicio, una interpretación excesivamente restrictiva e inconsistente con el marco normativo aplicable.

En este sentido, reiteramos que la suficiencia de la descripción debe evaluarse a la luz de lo dispuesto en la página 124 de la Guía de Examen de Patentabilidad, la cual establece que:

> *"Si en la descripción se omite información que es necesaria para poner en práctica la invención y que no puede ser suplida por el conocimiento general de la persona del oficio normalmente versada en la materia, se considerará que la invención no está suficientemente descrita".*

Por lo tanto, la solicitud debe interpretarse desde la perspectiva de una persona con conocimientos técnicos en el área. En este caso, un experto en polimorfismo y desarrollo farmacéutico comprendería sin dificultad cómo formular una composición farmacéutica que contenga el compuesto reivindicado como principio activo, basándose tanto en la enseñanza incluida en la solicitud como en sus conocimientos generales.

Desde esta óptica, una persona versada en la materia consideraría que la descripción brinda soporte suficiente, ya que no se limita a mencionar superficialmente las composiciones farmacéuticas. Por el contrario, la descripción ofrece una discusión detallada en distintas secciones, como el segundo párrafo de la página 14, las líneas 24 de la página 15 hasta la página 16, así como las realizaciones 13 a 16 en la página 20. Estas secciones evidencian claramente que las composiciones farmacéuticas

Clarke Modet

Carrera 11 No. 86-53, Piso 3
Edificio Segovia
110221 Bogotá, **Colombia**
T (+57) 1 618 10 88
F (+57) 1 635 08 24

constituyen una modalidad integral de la invención y están respaldadas por el contenido técnico divulgado.

Adicionalmente, cabe resaltar que según la Guía de Patentabilidad Colombiana de 2023 (p. 108):

> *"Si la reivindicación se refiere a "composición caracterizada porque contiene X" (siendo X un principio activo nuevo e inventivo) no necesita mencionar la presencia de los excipientes."*

Por ende, no requiere especificar los excipientes para considerarse suficientemente definida. En consecuencia, al haberse reconocido el nivel inventivo del compuesto, la reivindicación dirigida a la composición farmacéutica que lo contiene como ingrediente activo debe entenderse como suficientemente sustentada, sin necesidad de mayor especificidad. Una persona con conocimientos en el área sabría incorporar los excipientes adecuados con base en la información divulgada y su conocimiento técnico. Por lo anterior, se solicita respetuosamente que se reconsidere la objeción formulada en relación con las reivindicaciones 16 a 20.

En vista de lo anterior, las objeciones relacionadas con la claridad, la concisión y el soporte en la descripción del capítulo reivindicatorio, han quedado completamente superadas.

4. Descripción

El examinador indica que la descripción no divulga la materia reclamada de manera suficiente para que una persona normalmente versada en la materia pueda ejecutarla o reproducirla, por lo que no cumpliría con las disposiciones del Art. 28 de la Decisión Andina 486.

<u>Objeciones del examinador:</u>
El examinador señala que la descripción no presenta evidencia técnica que respalde el desarrollo de una composición que combine el compuesto de la reivindicación 1 con un excipiente farmacéuticamente aceptable, tal como lo definen las reivindicaciones 16 a 20.
Aclara además que no se incluyen ejemplificaciones de dicha composición en el documento. Por lo tanto, una persona versada en la materia requeriría realizar una

Clarke Modet

Carrera 11 No. 86-53, Piso 3
Edificio Segovia
110221 Bogotá, **Colombia**
T (+57) 1 618 10 88
F (+57) 1 635 08 24

cantidad excesiva e injustificada de ensayos de prueba y error para llevar a cabo la invención, lo que afecta el cumplimiento del requisito de suficiencia descriptiva.

Argumentos del solicitante:

En este sentido, manifestamos nuestro total desacuerdo con la objeción planteada, ya que, como se expuso en la Sección 2 del presente memorial, la suficiencia del soporte de la descripción debe evaluarse desde la perspectiva de una persona con conocimientos técnicos en el área. En este caso, un experto en polimorfismo y desarrollo farmacéutico comprendería sin dificultad cómo formular una composición farmacéutica que contenga el compuesto reivindicado como principio activo, basándose tanto en las enseñanzas incluidas en la solicitud como en su conocimiento general en el campo, sin requerir ejemplos explícitos para saber cómo estructurar adecuadamente una composición.

Desde esta óptica, una persona versada en la materia consideraría que la descripción brinda soporte técnico suficiente, ya que no se limita a mencionar superficialmente las composiciones farmacéuticas, como ha sido evidenciado en las citas aportadas previamente en este documento.

Asimismo, el artículo 51 de la Decisión 486 establece que:

> *"El alcance de la protección conferida por la patente estará determinado por el tenor de las reivindicaciones. La descripción, los dibujos y, en su caso, el listado de secuencias o el depósito de material biológico servirán para interpretarlas."*

Este fundamento refuerza el argumento de que una persona experta, con base en su experiencia y en la información técnica contenida en la solicitud, incluyendo las múltiples realizaciones descritas, sabría determinar los excipientes adecuados para formular la composición reivindicada, incluso si estos no han sido ejemplificados expresamente. Por lo anterior, se solicita respetuosamente que se reconsidere la objeción formulada respecto a las reivindicaciones relacionadas con las composiciones farmacéuticas.

De esta manera, la materia divulgada en la descripción ahora se relaciona de una manera más cercana con la materia definida en el capítulo reivindicatorio. Por lo tanto, la descripción proporciona toda la información necesaria para llevar a cabo la invención y cumple con los requisitos legales establecidos en la Decisión Andina 486.

5. Nivel inventivo

Clarke Modet

Carrera 11 No. 86-53, Piso 3
Edificio Segovia
110221 Bogotá, **Colombia**
T (+57) 1 618 10 88
F (+57) 1 635 08 24

El examinador ha indicado que las reivindicaciones 1 a 20 carecerían de nivel inventivo en vista de las enseñanzas del documento D1 (US2018334454A1) y D3 (US2018362529A1).

Con respecto a lo anterior, me permito resaltar las disposiciones del artículo 18 de la Decisión 486 de la Comisión de la Comunidad Andina, que establecen que "*se considerará que la invención tiene nivel inventivo, si para una persona del oficio normalmente versada en la materia técnica correspondiente, esa invención no hubiese resultado obvia ni se hubiese derivado de manera evidente del estado de la técnica*".

Lo anterior significa que el análisis de nivel inventivo **NO** es una comparación de los objetos de las anterioridades y la solicitud en estudio. Por el contrario, el análisis de nivel inventivo **debe demostrar** la obviedad de la invención y establecer cómo ésta no contiene un salto cualitativo, que demuestre su altura inventiva, teniendo en cuenta que se hace **necesario demostrar** que la invención analizada carece de nivel inventivo y hubiese sido obvia para una persona versada en la materia.

El análisis del examinador

El examinador considera que la invención definida en la reivindicación 1 carece de nivel inventivo frente al documento D1, identificado como el estado de la técnica más cercano. D1 divulga el compuesto base (6-fluoro-7-(2-fluoro-6-hidroxifenil)-...), incluyendo un atropisómero y su correspondiente sal farmacéuticamente aceptable, así como su utilidad como inhibidor de KRAS G12C en el tratamiento de diversos tipos de cáncer.

La diferencia entre la invención y D1 radica en que la solicitud actual reivindica una forma cristalina específica (Forma I) del compuesto, caracterizada mediante un patrón de difracción de rayos X en polvo. Sin embargo, el examinador señala que no se presentan ejemplos experimentales ni resultados técnicos concluyentes que demuestren un efecto técnico inesperado o una mejora funcional derivada de dicha forma cristalina en comparación con la forma amorfa conocida.

Adicionalmente, el documento D3 enseña métodos ampliamente conocidos para obtener y caracterizar formas sólidas cristalinas de compuestos farmacéuticos, incluyendo análisis DRXP, TGA, DSC, IR, RMN, SEM, entre otros. D3 también demuestra que

Clarke Modet

Carrera 11 No. 86-53, Piso 3
Edificio Segovia
110221 Bogotá, **Colombia**
T (+57) 1 618 10 88
F (+57) 1 635 08 24

obtener polimorfos con propiedades deseables, como estabilidad y solubilidad, es parte del conocimiento general en el campo.

En este contexto, el examinador considera que una persona versada en la materia tendría una motivación clara para aplicar los conocimientos sobre polimorfismo revelados en D3 al compuesto conocido en D1, con una expectativa razonable de éxito al obtener nuevas formas cristalinas. En ausencia de un efecto técnico distintivo y sorpresivo, dicha modificación se considera una solución obvia.

En cuanto a las reivindicaciones dependientes 2 a 15, el examinador señala que no aportan características adicionales que confieran nivel inventivo al compuesto de la reivindicación 1. Estas reivindicaciones se consideran redundantes o derivadas de lo ya conocido.

Finalmente, la reivindicación 16, que se refiere a una composición farmacéutica que incluye el compuesto y un excipiente farmacéuticamente aceptable, también se considera obvia. Tanto D1 como D3 divulgan composiciones similares y no se proporciona en la solicitud evidencia experimental que demuestre un efecto técnico específico atribuible a la composición reclamada.

Argumentos del solicitante:

El solicitante manifiesta su desacuerdo con la objeción del examinador. En primer lugar, el solicitante destaca que la identificación de formas particulares de un compuesto específico, como es el caso de la invención reivindicada, a pesar de lo afirmado por el examinador, ha sido y sigue siendo un proceso altamente impredecible, como lo evidencian diversas referencias científicas (véanse los documentos adjuntos):

- Byrn et al. 1995 señalan que: *"Las sustancias farmacéuticas sólidas exhiben una amplia y en gran parte impredecible variedad de propiedades en estado sólido."*.
- Maddox, en *Nature* (vol. 335, 1988, p. 201), indica que: *"A pesar de ciertos avances en el campo, sigue siendo en general imposible predecir la estructura de incluso los sólidos cristalinos más simples a partir del conocimiento de su composición química."*

Clarke Modet

Carrera 11 No. 86-53, Piso 3
Edificio Segovia
110221 Bogotá, **Colombia**
T (+57) 1 618 10 88
F (+57) 1 635 08 24

- Bernstein, en su libro *"Polymorphism in Molecular Crystals"*, menciona que: *"Aunque no sorprende que muchos materiales farmacéuticos importantes presenten polimorfismo, cada compuesto representa una nueva situación. Nuestro entendimiento sobre el fenómeno del polimorfismo aún no permite predecir con confianza si un compuesto será polimórfico, cómo obtener nuevos polimorfos, ni cuáles serán sus propiedades."*
- Byrn et al., 1994, afirman que *"existe muy poca información disponible que permita predecir de forma general la estabilidad de compuestos en estado sólido, y menos aún de sus diferentes formas sólidas o formulaciones."*
- Más recientemente, Cruz-Cabeza et al. concluyen que, en teoría, se quisiera mapear computacionalmente el paisaje polimórfico de un compuesto y predecir sus condiciones de cristalización. Sin embargo, en la práctica, los modelos computacionales son complejos, las relaciones estructura-propiedad no son fácilmente predecibles, y el diseño racional de procesos de cristalización sigue siendo un reto ingenieril.

Adicionalmente, como lo evidencian Byrn et al., muchos factores afectan la formación de formas polimórficas, tales como: composición y polaridad del solvente, concentración o sobresaturación, temperatura (incluyendo el perfil y la tasa de enfriamiento), aditivos, semillas, pH y agitación. Por ende, la combinación de estos factores genera un número prácticamente infinito de posibilidades. Por tanto, descubrir la existencia de una forma cristalina específica y cómo obtenerla implica un esfuerzo significativo y enfrentar obstáculos impredecibles, lo cual no puede considerarse obvio para una persona normalmente versada en la materia.

El estado de la técnica respalda la idea de que, aunque ciertas técnicas están disponibles, no existe guía alguna que permita a la persona versada en la materia seleccionar condiciones que conduzcan al descubrimiento de una forma polimórfica específica, y mucho menos de una adecuada para el desarrollo farmacéutico, como es el caso de la forma cristalina específica del atropisómero M del Compuesto 1 reivindicado, y con una expectativa razonable de éxito. Esta conclusión también se ve respaldada por la información contenida en la descripción de la solicitud.

Clarke Modet

Carrera 11 No. 86-53, Piso 3
Edificio Segovia
110221 Bogotá, **Colombia**
T (+57) 1 618 10 88
F (+57) 1 635 08 24

A pesar de esta falta de orientación en el arte previo, el solicitante diseñó y ejecutó un exhaustivo estudio de cribado de polimorfos y sales del compuesto AMG 510 (ver último párrafo de la página 41 de la descripción). Se identificaron numerosas formas salinas, anhidras, hidratadas y solvatadas. La solicitud describe específicamente 17 ejemplos que resultan en diferentes formas del atropisómero M del compuesto 1. Cabe destacar que la mayoría de los intentos condujeron a hidratos o solvatos (ejemplos 5 a 17). Solo los ejemplos 2 a 4 condujeron a formas anhidras y libres de solvente, y solo una de ellas —la Forma I— presentó características adecuadas para el desarrollo.

Tal como se detalla en la pagína 42 de la solicitud, la Forma I del atropisómero M del Compuesto 1 presenta propiedades sorprendentes y no previsibles, siendo la forma polimórfica más termodinámicamente estable. También es menos higroscópica que las Formas II y III, estable química y físicamente en estado sólido, resistente a condiciones de estrés durante 14 días, y compatible con excipientes durante al menos 4 semanas. Además, mostró estabilidad frente a luz UV y visible. AMG 510, también conocido como sotorasib, fue aprobado en diversos países, incluyendo EE. UU., como el primer tratamiento dirigido para cáncer de pulmón no microcítico localmente avanzado o metastásico con mutación KRAS G12C.

Más aún, la Forma I, tal como se describe y reclama, no fue obtenida por métodos rutinarios, como lo afirma erróneamente el examinador. De acuerdo con el ejemplo 2 de la página 44 de la solicitud, la Forma I anhidra se obtuvo en un proceso de tres pasos: (1) conversión del atropisómero M a forma amorfa; (2) conversión de la forma amorfa en la Forma II anhidra; y (3) conversión de la Forma II en la Forma I mediante tratamiento en agua a 90 °C por 2 horas y posterior agitación. Cada paso requirió condiciones específicas y no evidentes.

Por tanto, la obtención de la Forma I anhidra y cristalina del compuesto AMG 510 no fue resultado de procedimientos evidentes o rutinarios, sino de una serie de pasos complejos y no predecibles, que permitieron descubrir una forma con propiedades extraordinarias y apta para su desarrollo como un medicamento de primera clase.
En consecuencia, se solicita el reconocimiento del nivel inventivo de la invención tal como está definida frente a los documentos D1 y D3, y que la objeción sea retirada.

Clarke Modet

Carrera 11 No. 86-53, Piso 3
Edificio Segovia
110221 Bogotá, **Colombia**
T (+57) 1 618 10 88
F (+57) 1 635 08 24

Teniendo en cuenta lo anteriormente expuesto, queda claro que las características técnicas de la materia definida en el capítulo reivindicatorio presentado junto al presente memorial no se derivan de manera obvia o evidente de las enseñanzas de D1 y D2. Por lo tanto, el objeto reclamado cumple con el requisito de Nivel inventivo establecido en el Art. 18 de la Decisión 486.

6. Conclusión

Con las modificaciones introducidas y los argumentos presentados puede concluirse que:

i) El nuevo pliego reivindicatorio se ajusta a las disposiciones del Artículo 34 de la Decisión 486/00;

ii) La invención de la presente solicitud es clara y cuenta con el debido sustento en el capítulo descriptivo, a la vez que se encuentra divulgada de manera suficientemente completa, cumpliendo así con los requerimientos de los Artículos 30 y 28 de la Decisión 486;

iii) La invención de la presente solicitud no resulta obvia ni se derivada de manera evidente del estado de la técnica, cumpliendo así con los requerimientos del Artículo 18 de la Decisión 486.

Por tanto, atentamente me permito solicitar a ese Despacho otorgar el privilegio de patente solicitado a la solicitud en estudio, toda vez que cumple a cabalidad con los requerimientos de la Decisión 486 de 2000.

Asimismo, respetuosamente solicito a ese Despacho pronunciarse en relación con todos los argumentos presentados en este memorial dando estricta aplicación al principio del debido proceso consagrado en el artículo 29 de la Constitución Nacional.

7. Anexos

- Nuevo capítulo reivindicatorio conformado por diecisiete (17) reivindicaciones.

Clarke Modet +

Carrera 11 No. 86-53, Piso 3
Edificio Segovia
110221 Bogotá, **Colombia**
T (+57) 1 618 10 88
F (+57) 1 635 08 24

- Du et al., 19F Solid-state NMR characterization of pharmaceutical solids, Solid State Nuclear Magnetic Resonance, Vol. 120, 2022, 101796;
- Gil et al., 13C Solid State Nuclear Magnetic Resonance as a Tool for Studying Polymorphism in Pharmaceuticals, Arch Phar & Pharmacol Res., 2(4): 2019
- Byrn et al., "Pharmaceutical Solids: A Strategic Approach to Regulatory Considerations", Pharmaceutical Research, 1995, vol. 12, págs. 945-954
- MADDOX, John. Crystals from first principles. *Nature*, 1988, vol. 335, no 6187, p. 201-201.
- Bernstein, en su libro *"Polymorphism in Molecular Crystals"* (2002, Capítulo 7, p. 241),
- Byrn et al., en otro artículo (*"Solid-State Pharmaceutical Chemistry"*, Chem. Mater., 1994, vol. 6, pp. 1148-1158),
- *Cruz-Cabeza et al., Commun. Chem. 3, 142 (2020)*
- Recibo de pago por concepto de modificaciones a las reivindicaciones y nuevo examen de patentabilidad.

Señora Directora,



CAROLINA DAZA MONTALVO
C.C. 66.783.790 de Palmira Valle
TP-141563 CSJ
notificaciones@clarkemodet.com.co

REIVINDICACIONES

1. Un compuesto, en donde el compuesto es una forma cristalina del atropisómero M del 6-fluoro-7-(2-fluoro-6-hidroxifenil)-1-(4-metil-2-(2-propanil)-3-piridinil)-4-((2S)-2-metil-4-(2-propenoil)-1-piperazinil)pirido[2,3-d]pirimidin-2(1H)-ona (Forma I del antropisómero M del Compuesto 1), donde el compuesto está caracterizado por a) un patrón de difracción de polvo de rayos X que comprende tres a dieciocho picos seleccionados de entre 8.8, 9.0, 10.8, 12.0, 12.6, 12.8, 13.6, 14.2, 15.0, 15.4, 18.0, 18.6, 18.7, 19.0, 19.9, 20.0, 22.9, y 25.0 ± 0.2 grados 2 theta según lo medido por difracción de polvo de rayos X con una longitud de onda de rayos X de 1.54 Å; o b) una RMN en estado sólido de ^{13}C que comprende tres a treinta y dos picos seleccionados de picos a 12, 13, 16, 21, 23, 31, 33, 38, 42, 44, 47, 50, 54, 107, 110, 111, 123, 124, 127, 128, 132, 145, 146, 150, 154, 156, 158, 160, 162, 166, 167.7, y 168 ppm; o c) una RMN en estado sólido de ^{19}F que comprende picos a -109 y -120 ppm.

2. El compuesto de la reivindicación 1, en donde el compuesto está caracterizado por un patrón de difracción de polvo de rayos X que comprende picos a 9.0, 12.0, 12.6, y 19.0 ± 0.2 grados 2 theta según lo medido por difracción de polvo de rayos X con una longitud de onda de rayos X de 1.54 Å.

3. El compuesto de la reivindicación 1, en donde el compuesto está caracterizado por un patrón de difracción de polvo de rayos X que comprende de cinco a dieciocho picos seleccionados de 8.8, 9.0, 10.8, 12.0, 12.6, 12.8, 13.6, 14.2, 15.0, 15.4, 18.0, 18.6, 18.7, 19.0, 19.9, 20.0, 22.9, y 25.0 ± 0.2 grados 2 theta según lo medido por difracción de polvo de rayos X con una longitud de onda de rayos X de 1.54 Å.

4. El compuesto de la reivindicación 1, en donde el compuesto está caracterizado por un patrón de difracción de polvo de rayos X que comprende de siete a dieciocho picos seleccionados de 8.8, 9.0, 10.8, 12.0, 12.6, 12.8, 13.6, 14.2, 15.0, 15.4, 18.0, 18.6, 18.7, 19.0, 19.9, 20.0, 22.9, y 25.0 ± 0.2 grados 2 theta según lo medido por difracción de polvo de rayos X con una longitud de onda de rayos X de 1.54 Å.

5. El compuesto de la reivindicación 1, en donde el compuesto está caracterizado por un patrón de difracción de polvo de rayos X que comprende picos a 8.8, 9.0, 10.8, 12.0, 12.6, 12.8, 13.6, 14.2, 15.0, 15.4, 18.0, 18.6, 18.7, 19.0, 19.9, 20.0, 22.9, y 25.0 ± 0.2 grados 2 theta según lo medido por difracción de polvo de rayos X con una longitud de onda de rayos X de 1.54 Å.

6. El compuesto de la reivindicación 1, en donde el compuesto está caracterizado por una RMN en estado sólido de ^{13}C que comprende de cinco a treinta y dos picos seleccionados de picos a 12, 13, 16, 21, 23, 31, 33, 38, 42, 44, 47, 50, 54, 107, 110, 111, 123, 124, 127, 128, 132, 145, 146, 150, 154, 156, 158, 160, 162, 166, 167.7, y 168 ppm.

7. El compuesto de la reivindicación 1, en donde el compuesto está caracterizado por una RMN en estado sólido de ^{13}C que comprende de siete a treinta y dos picos seleccionados de picos a 12, 13, 16, 21, 23, 31, 33, 38, 42, 44, 47, 50, 54, 107, 110, 111, 123, 124, 127, 128, 132, 145, 146, 150, 154, 156, 158, 160, 162, 166, 167.7, y 168 ppm

8. El compuesto de la reivindicación 1, en donde el compuesto está caracterizado por una RMN en estado sólido de ^{13}C que comprende picos a 12, 13, 16, 21, 23, 31, 33, 38, 42, 44, 47, 50, 54, 107, 110, 111, 123, 124, 127, 128, 132, 145, 146, 150, 154, 156, 158, 160, 162, 166, 167.7, y 168 ppm.

9. El compuesto de la reivindicación 1, en donde el compuesto está caracterizado por una RMN en estado sólido de ^{19}F que comprende picos a -49, -60, -79, -90, -109, -120, -138, -150, -168, y -179 ppm según lo medido a una frecuencia de giro de 14 kHz.

10. El compuesto de una cualquiera de las reivindicaciones 1-9, en donde el compuesto está caracterizado por un termograma de calorimetría diferencial de barrido que comprende una endoterma con un inicio de 293 °C.

11. El compuesto de una cualquiera de las reivindicaciones 1-10, en donde el compuesto está caracterizado por un termograma de análisis termogravimétrico que comprende una pérdida de peso del 0.2 % cuando se calienta de 25 °C a 275 °C.

12. El compuesto de una cualquiera de las reivindicaciones 1-11, en donde el compuesto es puro.

13. Una composición farmacéutica que comprende el compuesto de una cualquiera de las reivindicaciones 1-12 y un excipiente farmacéuticamente aceptable.

14. La composición farmacéutica de la reivindicación 13, donde la composición farmacéutica es una forma de dosificación para administración oral.

15. La composición farmacéutica de la reivindicación 14, donde la forma de dosificación es una forma de dosificación sólida.

16. La composición farmacéutica de la reivindicación 15, donde la forma de dosificación es un comprimido.

17. La composición farmacéutica de una cualquiera de las reivindicaciones 13-16, donde la composición farmacéutica comprende 120 mg del compuesto.

Solid State Nuclear Magnetic Resonance 120 (2022) 101796

Contents lists available at ScienceDirect

Solid State Nuclear Magnetic Resonance

journal homepage: www.elsevier.com/locate/ssnmr

Trends

^{19}F Solid-state NMR characterization of pharmaceutical solids☆

Yong Du [a], Yongchao Su [a,b,c,d,*]

[a] Analytical Research and Development, Merck & Co., Inc., Rahway, NJ, 07065, United States
[b] Department of Industrial and Physical Pharmacy, College of Pharmacy, Purdue University, IN, 47907, United States
[c] Division of Molecular Pharmaceutics and Drug Delivery, College of Pharmacy, The University of Texas at Austin, Austin, TX, 78712, United States
[d] Department of Pharmaceutical Sciences, School of Pharmacy, University of Connecticut, Storrs, CT, 06269, United States

ARTICLE INFO

Keywords:
Solid-state analysis
Pharmaceuticals
Drug substances
Drug products
Polymorphism
Amorphous solid dispersion
Quantification
^{19}F NMR

ABSTRACT

Solid-state NMR has been increasingly recognized as a high-resolution and versatile spectroscopic tool to characterize drug substances and products. However, the analysis of pharmaceutical materials is often carried out at natural isotopic abundance and a relatively low drug loading in multi-component systems and therefore suffers from challenges of low sensitivity. The fact that fluorinated therapeutics are well represented in pipeline drugs and commercial products offers an excellent opportunity to utilize fluorine as a molecular probe for pharmaceutical analysis. We aim to review recent advancements of ^{19}F magic angle spinning NMR methods in modern drug research and development. Applications to polymorph screening at the micromolar level, structural elucidation, and investigation of molecular interactions at the Ångström to submicron resolution in drug delivery, stability, and quality will be discussed.

1. Introduction

Pharmaceutical formulations are composed of active pharmaceutical ingredients (APIs) and several functional or inert excipients. Drug products should have desired efficacy, bioavailability, manufacturability, and physical and chemical stability from manufacturing to the end of shelf life [1–4]. These critical attributes depend significantly on the physicochemical, mechanical, and biopharmaceutical properties of pharmaceutical materials. Solid dosage formulations, including tablets, capsules, and implants, represent the principal choices in drug development [5,6]. Compared to other forms, solid dosages possess various advantages, for example, enhanced stability, ease of administration, and low cost of manufacturing, packaging, and shipping [1].

Many factors can modulate the physicochemical properties of the solid dosage drug product, including forms of API, selection of excipients, and processing strategies [7–9]. Most drugs are formulated as crystalline or amorphous forms in solid dosages. Currently, up to 90% of the new drug development candidates exhibit poor aqueous solubility, classified as class II or class IV compounds in the Biopharmaceutics Classification System (BCS), as illustrated in Fig. 1 [10,11]. Undesired inter-conversion between crystalline and amorphous forms, e.g., different crystalline polymorphic or amorphous forms, can occur during manufacturing, shipping, and storage [12–15]. Such phase conversions may result in notable differences in pharmaceutical attributes, including stability, solubility, and bioavailability. In this regard, mechanisms responsible for the phase transformation need to be understood further to provide insight into the processability and storage to ensure drug product quality. To enhance the aqueous solubility of BCS II and IV compounds, amorphous solid dispersion (ASD), where amorphous API is distributed in a polymer matrix, is widely utilized as a formulation strategy [16–19]. Both API and excipients could experience changes in property profiles due to the altered structural and dynamic behaviors in the amorphization process [18,20,21]. For example, compared to neat amorphous API, the physical and chemical stability of ASD products is vastly improved. At the same time, the molecular mobility is significantly reduced with the presence of polymeric additives in the dispersion. Such changes are often related to the molecular interactions between API and excipient [19,22]. Therefore, atomic-level mechanistic understanding of molecular structure and interactions is vital for excipient selection and formulation design. Overall, in-depth knowledge of the molecular and physicochemical properties of drug substances and products can provide rationales for developing a robust and bioavailable drug product with optimal stability and therapeutic efficacy.

Many techiniques, including solid-state nuclear magnetic resonance

☆ Trends Article for ***Solid State Nuclear Magnetic Resonance*** May 18th, 2022.

* Corresponding author. Analytical Research and Development, Merck & Co., Inc., Rahway, NJ, 07065, United States.
E-mail address: yongchao.su@merck.com (Y. Su).

https://doi.org/10.1016/j.ssnmr.2022.101796
Received 9 April 2022; Received in revised form 18 May 2022; Accepted 19 May 2022
Available online 25 May 2022
0926-2040/© 2022 Elsevier Inc. All rights reserved.

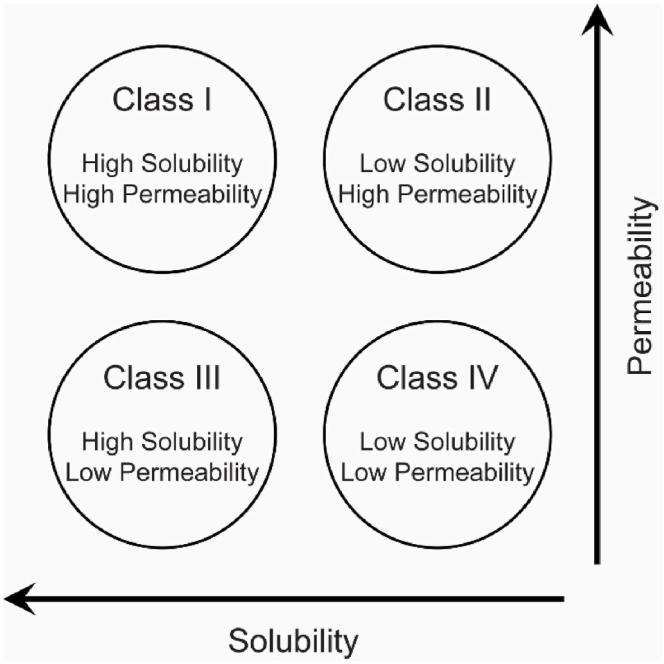


Fig. 1. A schematic diagram of the Biopharmaceutics Classification System (BCS). Note that most modern drugs in BCS class II and IV are formulated in amorphous forms to enhance the aqueous solubility. The structural basis of amorphous-to-crystalline inter-conversions and physicochemical stability of amorphous APIs within the polymer matrix remains largely unexplored.

(ssNMR) spectroscopy, differential scanning calorimetry (DSC), thermogravimetric analysis (TGA), X-ray diffraction (XRD), infrared (IR), and Raman spectroscopy, and optical and electron microscopies, are available to characterize solid-state properties of drug substances and products [16,23–25]. In most cases, a combined toolbox of these techniques is required to analyze pharmaceutical properties comprehensively [20]. Among these techniques, ssNMR has evolved into a valuable method in pharmaceutical analysis in the last three decades throughout the research and development of a drug from its candidate stage to the final commercialized product and sometimes even post-commercialization development [26–28]. Firstly, ssNMR has a long history of providing fingerprint features to distinguish API polymorphism [28–30]. Furthermore, the inherent quantitative nature and high sensitivity of ssNMR enable both the detection and quantification of API form changes in drug substances and products [31,32]. Secondly, the relaxation and spin diffusion measurement in ssNMR is a powerful method to measure the miscibility and homogeneity in solid dispersions at a nanometer scale [33–35]. Lastly, ssNMR is an advanced technique for investigating structure and dynamics in stability- and delivery-related problems. Information regarding molecular packing and interactions can be readily revealed at the molecular or atomic level [20,26].

Despite the increasing applications of ssNMR in pharmaceutical sciences, the inherent low sensitivity of NMR and the multiple components and relatively low drug loading of natural abundance materials present a significant challenge. Most pharmaceutical ssNMR analyses are performed on spin ½ nuclei, including ^{1}H, ^{13}C, ^{15}N, ^{19}F, and ^{31}P. ^{1}H detection has not yet become a routine practice in material characterizations, even though fast magic angle spinning (MAS) enables ^{1}H-based methods. Commonly used ^{13}C and ^{15}N methods often require a relatively long experimental time and cannot be routinely extended to multidimensional experiments for their low sensitivity. In contrast, ^{19}F has many remarkable advantages. It has a high gyromagnetic ratio (γ) and 100% natural abundance (compared to ^{13}C at 1.07% and ^{15}N at 0.37%). The NMR receptivity of ^{19}F is only 1.2-fold weaker than that of ^{1}H and roughly 4900-fold stronger than ^{13}C's. Moreover, ^{19}F resonance is also quite sensitive to the local structural and electronic environment around the fluorine nuclei, where the chemical shift range can span more than 300 ppm [36–38]. In addition, the utility of ^{19}F ssNMR in the pharmaceutical field has a particular advantage. Fluorine atoms are mostly absent in the pharmaceutical excipients, allowing spectral collection and analysis without interference from the excipient [26]. Lastly, the large share (approximately 25%–30%) of fluorine-containing pharmaceuticals on the market also endows the extensive utilization of ^{19}F ssNMR in the pharmaceutical analysis [39,40].

^{19}F ssNMR has been widely utilized in materials and biological systems studies to probe information on structure, dynamics, folding, and interactions at an atomic resolution [41–46]. ^{19}F ssNMR in pharmaceutical sciences emerged about two decades ago and recently gained substantial attention [26,47]. In this review, we will first introduce fluorinated pharmaceuticals. We will then elaborate on ^{19}F ssNMR in pharmaceutical research and development. These include identifying and quantifying different API forms and unraveling structural details such as conformational behavior, molecular interactions, and miscibility and mobility of API in solid dispersions. Moreover, the characterization of fluorinated API molecules in various drug delivery systems will be discussed, followed by how ^{19}F ssNMR is utilized to uncover mechanisms of drug action in lipid membranes. Finally, two state-of-the-art techniques, fast MAS and dynamic nuclear polarization (DNP), are highlighted to improve the sensitivity and resolution of ^{19}F ssNMR.

2. Fluorinated pharmaceutical compounds

Fluorine plays a critical role in medicinal chemistry and has the largest electronegativity and oxidation potential. Liu and coworkers have nicely reviewed the fluorine-containing molecules for various therapeutical areas in the last two decades [39,40]. The selective substitution of fluorine for hydrogen or hydroxyl groups can customize the properties of small organic compounds significantly [39]. Three main advantages are generally gathered when introducing fluorine in the molecular structure concerning drug design [39,48]. Firstly, as the most electronegative element, fluorine can alter the physicochemical properties of small molecules readily, resulting in changes of the acidity and basicity, stereo conformation, pKa, dipole moment, chemical reactivity, etc. Secondly, the metabolic stability of the drug candidates can be boosted with fluorine substitution in the structure, where the C–F bond is more resistant to being attacked than the C–H bond. Thirdly, the introduction of fluorine can increase the binding affinity of a drug candidate with target proteins due to its large polarity. These changes induced via fluorination have driven many advancements in fluorine medicinal chemistry to improve the therapeutic efficacy and pharmacological properties of small molecule drugs [39,40]. It has been estimated that fluorinated drugs hold a vast market share, representing almost 25% of pharmaceuticals containing fluorine atoms or fluoroalkyl groups [39,40]. Moreover, nearly 30% of newly approved drugs (excluding biopharmaceutical products) have been fluorinated in recent years [40,49].

We have included 11 representative fluorine-containing drugs (Fig. 2A–K) that are top-selling on the market and studied by ^{19}F ssNMR. For example, atorvastatin (Lipitor®), mainly treating high cholesterol and preventing heart attacks, was the best-selling drug globally in 2008 [39]. Meanwhile, atorvastatin solid formulations have been extensively analyzed by various solid-state analytical techniques, including ^{19}F ssNMR, for the many known crystalline and amorphous forms [50–52]. These APIs can be classified into different categories based on the site of fluorination. For example, these substitutions happen at the fluorine atom (e.g., atorvastatin), trifluoromethyl group (e.g., flutamide (Eulexin®)), and both the fluorine atom and trifluoromethyl group (e.g., aprepitant (EMEND®)). Besides conventional small organic compounds, Fig. 2L presents an United States Food and Drug Administration (FDA)-approved fluorine-containing polymer, patiromer (Veltassa®), as a drug for treating hyperkalemia [53]. In recent years, polymers have become a novel class of therapeutic compounds [54]. In pharmaceutical formulations, almost all pharmaceutical excipients lack fluorine atoms. However, there are some exceptions. For example, several

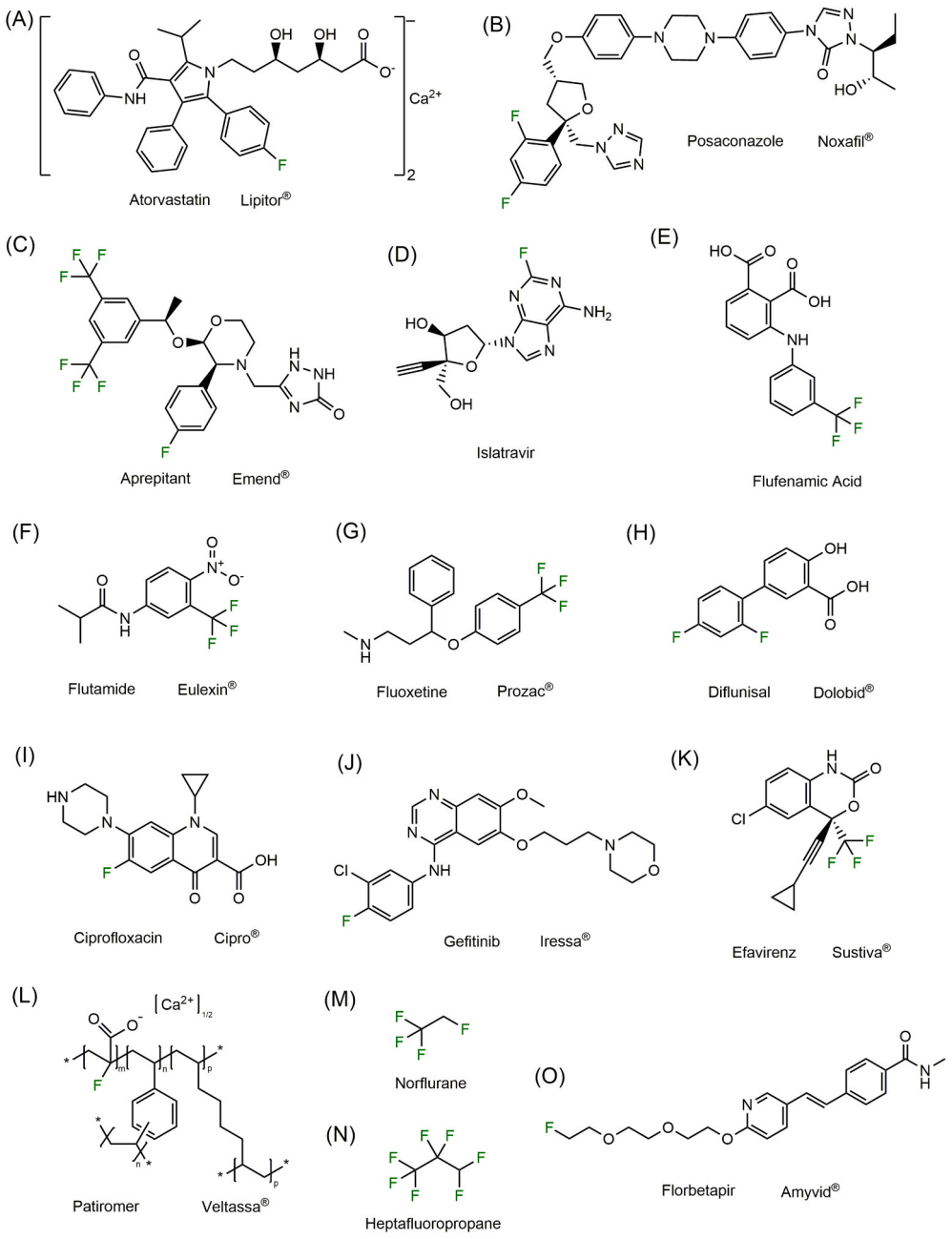


Fig. 2. Chemical structures of representative fluorine-containing small organic molecule drugs (A–K), polymers as the drug substance (L), excipients as the gas propellant in inhaler formulations (M–N), and imaging agent for PET. The API and brand name (labeled with registered trademark ®) of the drug and imaging agent are shown in the left and right, respectively.

fluorine-containing excipients are used as the gas propellant in the inhaler for pulmonary diseases [55], as shown by the two examples in Fig. 2M–N. In recent years, positron emission tomography (PET) has proven as an invaluable imaging tool to reveal the metabolic or biochemical function of tissue and organs [56–59]. Depending on the types of tracers, PET has been primarily utilized in various diseases, such as cancer, heart disease, brain disorders, etc. [60–62]. Fig. 2O presents an FDA-approved fluorinated PET imaging agent, florbetapir (Amyvid®), to detect amyloid plaques usually formed in Alzheimer's disease [63]. Such tracers permit PET to visualize amyloid plaques, largely aiding the diagnosis of many neurodegenerative diseases for clinicians. Overall, the successful development of fluorine-containing compounds provides excellent opportunities for ^{19}F ssNMR to characterize solid drug substances and drug products.

3. Stability analysis of drug substances and products

In drug development, the selection of optimal API may involve many solid forms, including crystal polymorphs, amorphous, hydrates, solvates, co-crystals, and salts [64–66]. For example, more than 60 solid forms of atorvastatin calcium have been patented [64,67]. Different solid forms can have distinct physicochemical properties, which directly impact the solubility, dissolution rate, stability, and therefore, bioavailability of the final drug product [64,68–70]. Undesired phase transformations of crystalline-to-crystalline and crystalline-to-amorphous inter-conversions can occur under various mechanical, thermal, and chemical stresses during manufacturing, shipping, and storage [71–73]. Therefore, API form purity is critical to ensure the stability of drug substances and drug products. Solid-state analytical techniques that can efficiently evaluate API forms are appreciated. As a high-resolution and sensitive technique, ^{19}F ssNMR has

been extensively employed to investigate API phase stability of fluorinated pharmaceuticals by detecting and quantifying phase changes, which provides invaluable guidance for formulation design and process development [26].

3.1. Identification of API polymorphism

Different intermolecular arrangements in the crystal lattice can substantially differ in physicochemical properties [74,75]. Thus, the phase conversion of crystalline drug substances to other polymorphs needs to be avoided. One example is the withdrawal of Ritonavir from the market due to the formation of a more thermodynamically stable crystalline polymorph [76,77]. ^{19}F ssNMR has been demonstrated as an orthogonal approach to differentiate various crystalline polymorphs when the results of other techniques are ambiguous [78]. For example, Fig. 3A shows a study by Skomski and coworkers in the API phase assessment of a fluorinated compound, islatravir [78,79]. A new anhydrate form IV was readily detected by ^{19}F direct polarization (DP) MAS ssNMR, where the spectrum of anhydrate form IV is distinct from other polymorphs. Similarly, Quinn et al. revealed the existence of two polymorphs of levofloxacin in two generic formulations by a series of 1D and 2D^{19}F MAS ssNMR experiments [52]. Moreover, Moseson et al. demonstrated that ^{19}F MAS ssNMR offers high sensitivity in determining the crystallinity of bicalutamide (BCL) produced by different recrystallization methods. As shown in Fig. 3B, no alternations of peak width and chemical shift were observed for BCL in different lots, suggesting a consistent formation of BCL form I by varied recrystallization processes [80].

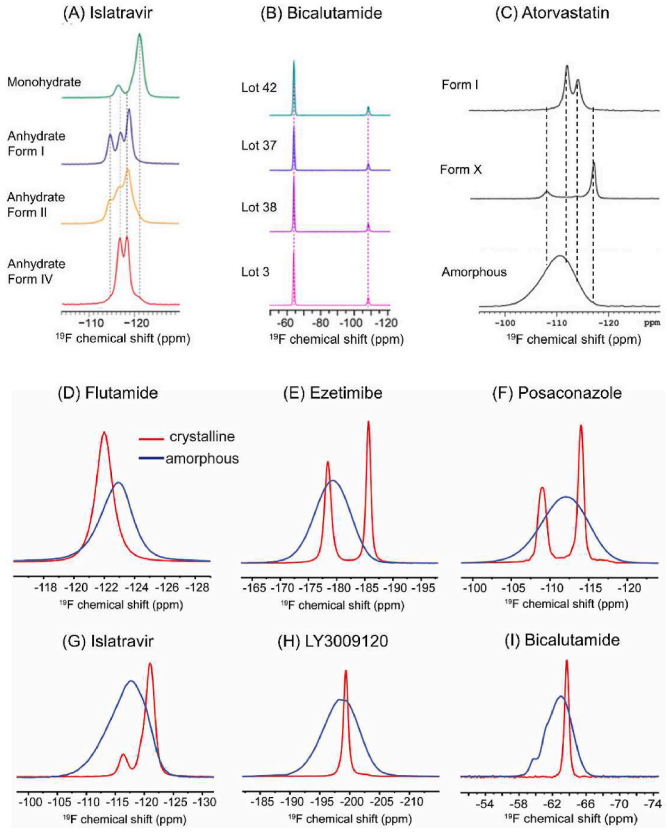


Fig. 3. ^{19}F ssNMR investigation of API crystalline and amorphous forms. (A) ^{19}F ssNMR spectra of islatravir reference crystalline forms and a new crystalline polymorph (i.e., anhydrate form IV) generated from hot melt extrusion under high shear forces [78]; (B) ^{19}F ssNMR spectra of bicalutamide crystalline form I of different lots prepared by different recrystallization methods [80]; (C) ^{19}F ssNMR spectra of crystalline (form I and X) and amorphous atorvastatin calcium [84]; Superimposed ^{19}F ssNMR spectra of crystalline (red traces) and amorphous (blue traces) of (D) flutamide [81], (E) ezetimibe [81], (F) posaconazole [82], (G) islatravir, (H) LY3009120 [83], and (I) bicalutamide. Figures were reproduced with permission from Elsevier and the American Chemical Society.

^{19}F ssNMR was also extensively employed to identify amorphous and crystalline forms in fluorinated drug substances and products, apart from crystalline polymorphs. Fig. 3C–I presents the ^{19}F ssNMR spectra of crystalline and amorphous forms of 7 fluorinated APIs [78,81–83]. The NMR peaks of crystalline and amorphous forms show different peak widths. The absence of long-range order in the amorphous state results in a much broader peak, as a characteristic spectral feature, compared to crystalline counterparts. Such a difference in spectral features allows the reliable and straightforward determination of API phases. As shown in Fig. 3C, Brus et al. coupled ^{19}F MAS ssNMR with chemometric analysis to quickly identify various crystalline and amorphous forms of atorvastatin calcium in both drug substances and low-dose tablet formulations [51]. The proposed method can exploit the subtle difference of ^{19}F MAS NMR spectra to identify an unknown form of atorvastatin in less than 1 h. Moreover, the phase conversion of Compound I, a selective M_3 neuronal receptor antagonist, in its tablet formulation, has been detected using ^{19}F ssNMR [47]. The NMR spectrum of the tablet dosed with 2% w/w crystalline form I is similar to that of 50%/50% w/w form I/amorphous mixture, indicating that a significant amount of crystalline form I in the tablet was converted to the amorphous form.

3.2. Quantification of crystalline and amorphous contents

NMR is an inherently quantitative technique [26,31,85,86]. Compared to other analytical methods such as powder XRD (PXRD) and DSC, quantification studies using ssNMR can proceed without needing a standard curve [87]. In general, most quantitative studies in ssNMR were accomplished by ^{13}C ssNMR. However, when the drug loading in the formulation is notably low, sufficient signal averaging is required to ensure the confidence of quantification, which often results in time-consuming ^{13}C acquisition. Moreover, the signal from pharmaceutical excipients can dominate the overall ^{13}C spectrum, resulting in peak overlaps [88]. ^{19}F ssNMR provides an alternative for the quantitative studies of fluorinated pharmaceuticals. Advantages include: (1) ^{19}F has much higher NMR receptivity than ^{13}C (~4900-fold higher), which enables rapid analysis of fluorine-containing drugs in a variety of formulations; (2) No signal interference from pharmaceutical excipients due to the absence of fluorine. So far, ^{19}F ssNMR quantitative studies include direct integration and reference-based methods. When NMR peaks are well-resolved, the compositions of components in the solid mixture can be obtained by calculating the relative ratios of integrated peak areas. Peak overlapping is inevitable in most situations since different solid forms of the same API usually exhibit similar peak positions. Therefore, peak deconvolution is required in the first place before extracting information of area integrals and can largely impact the quantification accuracy and confidence. Peak deconvolution is not applicable when different components lack substantial spectral features or the minor component in the mixture is at low concentrations. The reference-based method is usually utilized to retrieve the compositions in these situations [81–83]. Briefly, the NMR spectra of reference samples are first collected. The mixture compositions are obtained via spectral fitting, where the ratios of reference spectra are adjusted to match the experimental one. Besides, the relaxation filtration method exploits the difference in longitudinal relaxation time in the laboratory and the rotating frame (T_1 and $T_{1\rho}$) of the components in the mixture [89–91]. The NMR signal of a specific component in the mixture can be selectively excited while the signals of other components are filtered. This allows straightforward detection of the component of interest in the mixture. Moreover, multivariate chemometric analysis has also been demonstrated [92,93]. NMR spectra provide a wealth of information of the sample, and chemometric models can analyze the differences in the spectral feature to achieve quantification purposes [94].

It has been convinced that ^{19}F ssNMR is a robust technique to

quantify different crystalline API forms. For example, ^{19}F ssNMR was utilized to evaluate the polymorphic impurity of form III of Casopitant mesylate in API batches of form I [95]. In addition, it was also employed to quantify insoluble crystalline API in the semi-liquid and liquid formulations [88]. Farrer et al. demonstrated a linear correlation between ^{1}H–^{19}F cross polarization (CP) MAS peak area and mass of the analyte in the slurry suspension. ^{1}H–^{19}F CP MAS is able to detect and quantify very low levels (2 mg/g) of crystalline I (Sodium (2R)-7-{3-[2-chloro-4-(2,2,2-trifluoromethoxy)phenoxy]propoxy}-2-methyl-3,4-dihydro-2H-chromane-2-carboxylate) within the liquid vehicle [88].

Crystalline drug substances may also convert partly or entirely to the amorphous phase during pharmaceutical manufacturing [82,96,97]. Such an amorphization may present safety concerns for the final drug products due to the increased aqueous solubility and dissolution rate [26]. Besides detecting crystalline-to-crystalline conversion, ^{19}F ssNMR has been well recognized for detecting and quantifying crystalline-to-amorphous conversions. For example, as shown in Fig. 4A, Huang et al. utilized a reference-based method to study the extent of amorphization of crystalline posaconazole (POSA) during the compression processes. A detection limit of 1.7% w/w with a 95% confidence level was obtained via linear regression analysis. Higher content of amorphous POSA was seen with increasing axial stress. In combination with finite element analysis, it was found that apart from hydrostatic pressure, the shear stress also plays an essential role in the amorphization. Moreover, drug loading and excipients also significantly affect the phase conversion. The addition of excipients significantly amplified the amorphization compared to neat POSA. An 11.1% and 5.9% w/w increase of amorphization was observed using microcrystalline cellulose and dibasic calcium phosphate anhydrous as excipients, respectively. The discrepancy between the two excipients was attributed to the local interparticulate stress resulting from the different interparticulate friction and particle sizes [82]. Similarly, Petzoldt et al. demonstrated an example of how to quantify the fraction of amorphous API (SAR114137) in early pharmaceutical development. Different levels of amorphization were observed in tablets with different tableting forces, humidity, and polymer excipients [98]. The quantification of amorphization was conducted by several solid-state analytical techniques, including DSC, PXRD, and ^{19}F ssNMR and the latter was considered the most sensitive method. ^{19}F ssNMR was found able to quantify 0.5% w/w amorphous API in the tablet.

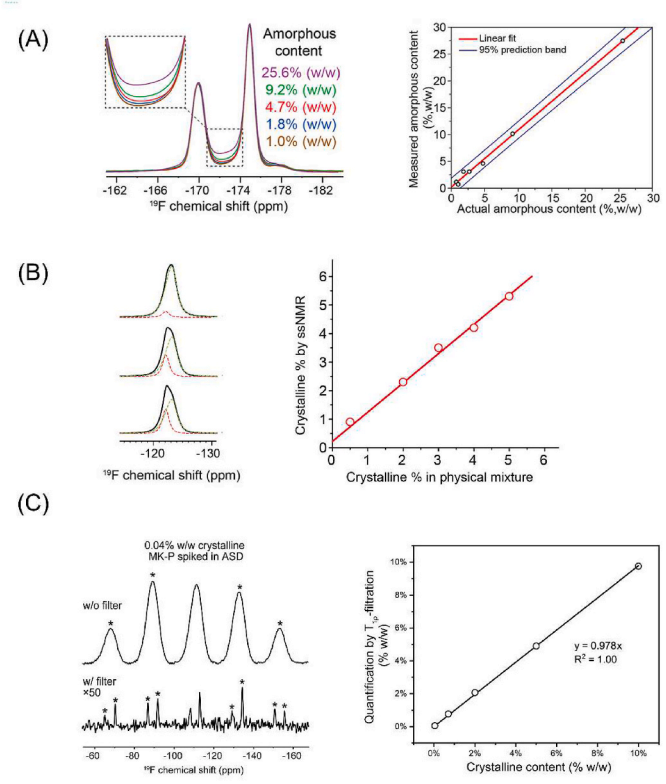


Fig. 4. ^{19}F ssNMR quantitation of crystalline and amorphous forms in drug substances and products. (A) ^{19}F DPMAS spectra (left) and calibration curve (right) for a series of crystalline and amorphous POSA mixtures with known amorphous weight fractions [82]; (B) Calibration curve correlating ssNMR results of fractions of crystalline flutamide with the actual weight fractions in the physical mixtures (left); Experimental, simulated, and deconvoluted ^{19}F DPMAS spectra of flutamide ASDs at different days of accelerated storage conditions (right) [81]; (C) ^{1}H–^{19}F CPMAS spectra of 0.04% w/w crystalline MK-P spiked ASD sample in the presence and absence of $T_{1\rho}$ filtration (left) and the calibration curve of ^{1}H–^{19}F $T_{1\rho}$-filtered quantification method (right) [109]; Figures were reproduced with permission from Elsevier and the American Chemical Society.

In the past two decades, ASD has become a popular formulation strategy for pharmaceutical compounds that are poorly water-soluble [17,99,100]. The amorphous form possesses a disordered structure and excessive Gibbs free energy than its crystalline counterparts, resulting in low physical stability [18,96,101]. The amorphous form tends to transform to a thermodynamically stable crystalline form, which can diminish the advantage of solubility and bioavailability enhancement. ^{19}F ssNMR has been demonstrated as an excellent technique to evaluate the stability of ASD formulations in stability testing at various conditions, e.g., light, temperature, and humidity. As shown in Fig. 4B, Taylor and coworkers applied ^{19}F DPMAS ssNMR to quantify <1% w/w crystalline flutamide in spray-dried ASDs. The reference-based method was exploited to extract the fractions of crystalline form, where 1%, 3.8%, and 4.6% recrystallization of amorphous flutamide were determined on 35, 39, and 48 days of storage at 75% relative humidity (RH) and 40 °C [81]. In a study evaluating the crystallinity of LY3009120, an Eli Lilly investigational drug, in the ASD formulation, ^{19}F ssNMR successfully distinguished 0.9%, 1.0%, and 1.2% crystallinity for sample 59–4 at time zero (T_0) and 4 months after the storage conditions of 25 °C/60% RH and 25 °C/75% RH, respectively [83]. Besides the reference-based method, multivariate chemometric analysis of ^{19}F ssNMR spectra was also performed to quantify crystallinity in ASDs [51,84]. For example, Brus et al. reported that 1% w/w of the crystalline form of atorvastatin can be accurately determined in the matrix of amorphous atorvastatin. Conversely, the limit of quantification for the amorphous form in the crystalline atorvastatin is only roughly 5%–10% due to the broadened linewidth of amorphous atorvastatin [51]. Crystalline and amorphous API usually possess sufficiently different T_1 and $T_{1\rho}$ values due to the difference in molecular mobility [102–108]. This allows applying relaxation-filtered experiments to detect and quantify form conversion in ASDs. In a study by Liu et al., the delay time in the inversion recovery experiments was purposely set when the crystalline signal vanishes to zero. However, at such a delay time, the amorphous signal already has a certain degree of magnetization build-up due to its fast relaxation rate. In such a scenario, the NMR signal of inversion recovery experiments is purely from the amorphous, and the crystallinity of the tablets can be simply calculated by direct peak integration [91]. Moreover, Asada et al. developed a relaxation-filtered method to quantify the crystalline content (form I) of atorvastatin calcium in the tablet where amorphous is the predominant form. By applying selective excitation, only the target component in the mixture (either amorphous or crystalline atorvastatin) can be detected. The level of crystalline that can be quantified in the study was shown as low as 0.5% w/w [90]. Fig. 4C presents a recent study by Su and coworkers, in which they have compared various methods of ^{19}F ssNMR to quantify the crystallinity of MK-P in ASD [109]. ^{19}F DPMAS and CPMAS can reliably quantify 0.1% w/w crystalline. Compared to DSC and PXRD, ^{19}F ssNMR demonstrated significant improvements in accuracy and precision. It is worth noting that in most ASDs, crystalline content can potentially be less than 0.1% w/w. The quantification of such low levels of crystalline remains challenging for most techniques due to the limitation of sensitivity. In the study, to further explore the boundary of quantification, a $T_{1\rho}$-filtered

^{1}H–^{19}F CPMAS experiment was performed. As shown in Fig. 4C, an extreme low, i.e., 0.04% w/w, crystalline MK-P can be plausibly quantified. This represents the lowest micromolar level quantification that has been achieved so far in the solid-state analysis of pharmaceutical materials.

Besides quantification of API forms, ^{19}F ssNMR was also utilized to determine impurity content in pharmaceutical formulations. For example, when other techniques such as high-performance liquid chromatography (HPLC), IR and Raman spectroscopy cannot give conclusive evidence of the contamination of polytetrafluoroethylene (PTFE) in a fluorinated API, Pham et al. successfully quantified the contamination level of PTFE as low as 0.02% w/w by ^{19}F ssNMR [110]. In another study by Stueber and Jehle, time-domain (TD) benchtop NMR and quantitate ^{19}F T_1 saturation recovery curves (qSRC) were utilized to determine the compositions of a two-component blend system. The qSRC method uses the weighted SRCs of the pure components to fit the SRCs for the mixture, where the weighting coefficients represent the compositions of each component. One of the inherent requirements of the qSRC method is that the T_1 relaxation times of pure ingredients are substantially different for the separation. In the study, the authors performed ^{19}F T_1 qSRC in two model systems: 2-trifluoromethyl cinnamic acid/6-trifluoromethyl uracil (2TFMCA/6TFMU), and 2-trifluoromethyl cinnamic acid/fluoxetine HCl (2TFMCA/FXT), where the T_1 relaxation times of the pure components differ significantly and by only 12%, respectively. The method predicted the blend compositions within 0.5% to the prepared mass percentages. For 2TFMCA/FXT blends with only a 12% difference in T_1 relaxation times, a high correlation coefficient of $R^2 = 0.9999$ was also obtained at the expense of long signal averaging. The method can potentially be extended to quantify the compositions of API polymorphs as long as the pure polymorphs have substantially different T_1 relaxation times [111].

4. Molecular structural investigations

Molecular understanding of drug substances can uncover mechanisms related to the physicochemical properties and stability of drugs. Traditionally, single crystal XRD (SCXRD) is the prevailing method in determining the atomic and molecular structure of crystals [112,113]. However, when the single crystal diffraction data is unavailable, the structure elucidation must be performed in an alternate route. ssNMR is a high-resolution technique able to probe a wealth of structural information, including the number of crystallographically inequivalent positions in the unit cell, molecular packing, direct measurement of through-space distances on the atomic scale, etc. Moreover, the sensitivity offered by ssNMR to the local environment of the nuclear spins can also provide profound details of molecular dynamics, local order, and molecular interactions [20,86,114,115]. In recent years, NMR crystallography, which utilizes the data from ssNMR primarily and other supplementary techniques such as density functional theory (DFT) and powder diffraction, has gained popularity as an alternative to elucidate the structure of solid materials [114,116,117]. It has been demonstrated to solve the structure of several small-molecule APIs in the last two decades [118–122]. For example, Emsley and coworkers present a protocol using ^{1}H ssNMR in combination with crystal structure prediction and DFT chemical shift calculations to determine an unknown crystal structure of an investigational drug [121]. Similarly, such integrated methods were also utilized by Luedeker et al. to investigate the structure of cocrystal formation of niclosamide with different co-formers [122].

Accurate internuclear distances are essential for structure elucidation in NMR crystallography. ssNMR is well-known and capable of measuring the internuclear distance between two spatially close nuclei via dipole-dipole couplings. The dipolar coupling strength is inversely proportional to the cubic of the internuclear distance. Such a relationship provides a direct way for distance measurement in ssNMR-based structure determination. It has been demonstrated that ssNMR can measure interatomic distances from angstroms to nanometers [123, 124]. MAS can reduce or remove the homo- and hetero-nuclear dipolar coupling. Therefore, to retrieve information on dipolar coupling in MAS experiments, several ssNMR dipolar recoupling methods have been designed and developed to probe the distance constraints in the organic compounds, peptides, and proteins [123,125–127].

Among these methods, radiofrequency-driven dipolar recoupling (RFDR) applies a single π pulse per rotor cycle for recoupling homonuclear dipolar coupling [128–130]. To quantify heteronuclear distances, rotational-echo double-resonance (REDOR) is routinely employed using rotor-synchronized π pulses to recover the heteronuclear dipolar interactions [131,132]. For these two sequences, numerical simulations are performed to fit RFDR buildup curves and REDOR dephasing curves to extract homonuclear and heteronuclear distances, respectively. The nuclear-spin dipole-dipole coupling is proportional to $\gamma_I\gamma_S$, where γ_I and γ_S are the gyromagnetic ratio of spin I and S. Therefore, for spin-1/2 nuclei with low γ values such as ^{13}C, ^{15}N, and ^{31}P, the dipolar interactions are relatively weak if the internuclear nuclear distance r, is kept the same. In other words, the range of the distance that can be measured by ssNMR-based dipolar recoupling experiments is relatively limited for spin-1/2 nuclei with low γ because of the reduced dipolar interaction. In this regard, ^{19}F is a nucleus that can increase the distance reach of ssNMR. ^{19}F has a 3.7-fold higher γ than ^{13}C, thus can lead to strong dipolar interactions and permitting the measurement of longer distances. For example, McDermott and coworkers have demonstrated the interatomic fluorine distance measurement up to 12 Å by RFDR in fluorinated organic compounds with a precision of 1 Å and 2 Å for short- and long-range distances, respectively [133]. Moreover, Roos et al. utilized ^{19}F spin-exchange NMR to measure the interatomic fluorine distance up to 16 Å, which provides valuable information on distance constraints in studying the structure of pharmaceutical and biological compounds [134]. In contrast, the maximum ^{13}C–^{13}C distance that RFDR can measure is only roughly 7 Å [135]. Besides RFDR, many studies have also utilized REDOR experiments to obtain distance restraints between fluorine and other nuclei. Most recently, Hong and colleagues used the ^{13}C–^{19}F REDOR method to measure intermolecular ^{13}C–^{19}F distances of a mixture of ^{13}C- and ^{19}F-labeled envelope protein E of the SARS-CoV-2 virus. A total of 35 interhelical ^{13}C–^{19}F distances was obtained, which provides substantial distance restraints for the structure elucidation of the envelope protein E [136].

4.1. Investigation of asymmetric unit and resonance assignment

Many reports have demonstrated ^{19}F ssNMR as a sensitive and high-resolution technique to probe the structural details of fluorine-containing pharmaceuticals [26,28,85]. ^{19}F ssNMR can investigate the number of API molecules in the asymmetric unit and facilitate resonance assignments for different nuclei. As shown in Fig. 5A, Vogt et al. demonstrated the spectral assignments for form I of ronacaleret HCl by 2D ssNMR and DFT calculations of chemical shielding. ^{19}F–^{19}F cross-polarization dipolar-assisted rotational resonance (CP-DARR) and ^{1}H–^{19}F–^{13}C double cross-polarization heteronuclear correlation (DCP-HETCOR) were utilized to assign the fluorine and carbon resonances [137]. Fig. 5B presents the study by Wang and coworkers, who applied ^{13}C, ^{19}F, and ^{15}N ssNMR to probe the crystal structure of form I of atorvastatin calcium [50]. The doubling of resonances for several carbon sites, fluorine sites, and the amide nitrogen site indicates two atorvastatin molecules in the asymmetric unit. Such an observation was further supported by the ^{19}F–^{13}C HETCOR spectrum, where two sets of ^{19}F–^{13}C correlations were detected for fluorine and several carbon sites of atorvastatin calcium. Fig. 5C presents the study by Guo et al., where the crystal structure of a fluorinated pharmaceutical compound, mefloquine, was investigated by ^{19}F MAS NMR in combination with DFT calculations [36]. The fluorines in CF_3 groups are usually of high rotational mobility, and thus a single resonance is often expected in the 1D ^{19}F spectrum. However, utilizing the 1D ^{19}F delays alternating with nutation for tailored excitation (DANTE) pulse sequence, two CF_3 groups

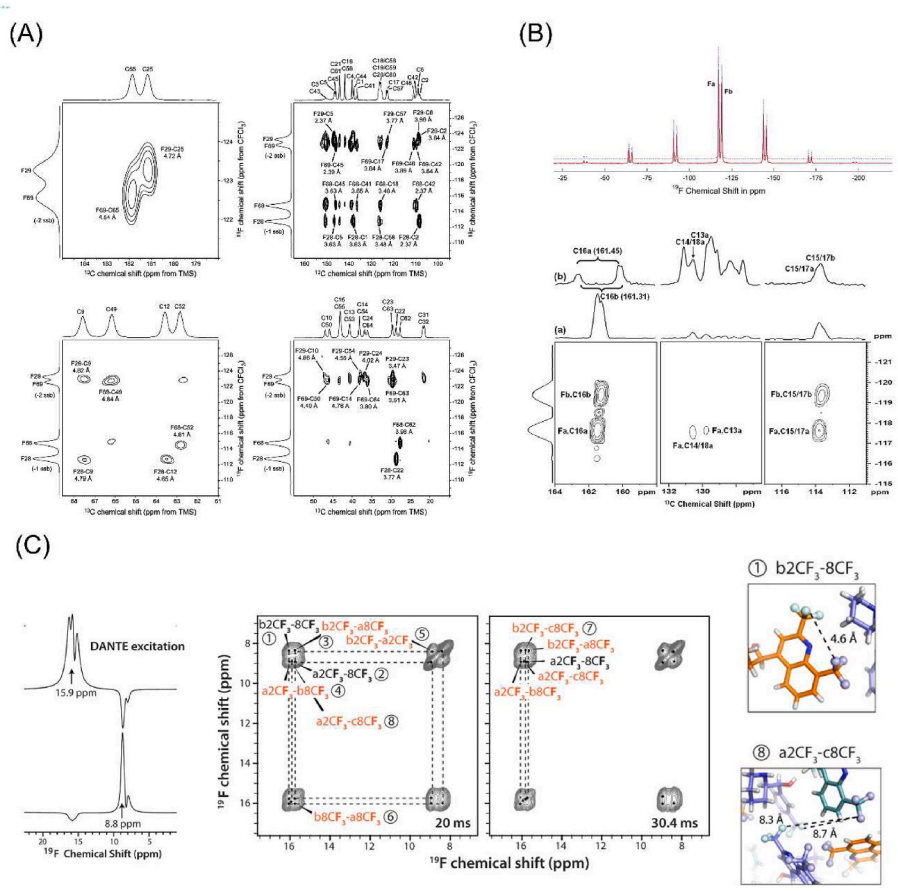


Fig. 5. ^{19}F NMR investigation of crystallographically inequivalent sites and resonance assignment. (A) ^{1}H–^{19}F–^{13}C DCP-HETCOR spectrum of form I of ronacaleret HCl obtained using a 2-ms ^{1}H–^{19}F contact time and a 6-ms ^{19}F–^{13}C contact time for 2D dipolar correlation between ^{19}F and ^{13}C spins [137]; (B) 1D ^{19}F CPMAS and ^{19}F–^{13}C HETCOR spectra of atorvastatin calcium form I showing two distinguishable fluorine resonances [50]; (C) 1D ^{19}F DANTE selective excitation of the $8CF_3$ resonance at 15.9 ppm and $2CF_3$ resonance at 8.8 ppm; 2D ^{19}F–^{19}F RFDR spectra with various mixing times, unraveling intramolecular and intermolecular ^{19}F–^{19}F correlations; Intra- and inter-molecular ^{19}F–^{19}F distances in the crystal structure of mefloquine. Figures are reproduced with permission from the American Chemical Society.

in mefloquine showed multiple resolved ^{19}F resonances. This provided strong evidence of inequivalent fluorine positions in the CF_3 group and the presence of three mefloquine molecules in the unit cell. To further measure the intra- and inter-molecular interatomic distances, the ^{19}F RFDR experiments were applied. A total of 8 different ^{19}F–^{19}F distances were obtained, and RFDR-measured distances are in close agreement with the data from the crystal structure of mefloquine.

4.2. Investigation of molecular interactions

Investigating molecular interactions can probe the molecular packing of drug substances and drug-drug and drug-polymer contacts in ASDs. These investigations can provide insights for rational selection of pharmaceutical excipients in formulation development [138–140]. Various analytical techniques, including vibrational spectroscopy, high-energy X-ray diffraction, and pair distribution function analysis, have been employed to study drug-drug and drug-polymer interactions [141–145]. However, none of these techniques can provide atomic-level details of molecular interactions. In contrast, ssNMR has many approaches to probing molecular and even atomic interactions. The chemical shift can be sensitive to the local structural changes due to molecular interactions [146,147]. If significant alternation of chemical shift in the 1D spectrum was observed, it provides strong evidence for molecular interaction. For example, in an investigation of efavirenz in a series of pharmaceutical cocrystals, the ^{19}F ssNMR chemical shift of the efavirenz trifluoromethyl group exhibited changes up to 3.6 ppm, which may indicate strong interactions between coformers as a result of the formation of cocrystals [148]. For scenarios where the interactions are too weak to induce chemical shift change or such detection is prohibited by significant peak overlap, 2D homonuclear and heteronuclear correlation experiments can be utilized to provide information of interaction, where the presence of a cross peak in the 2D spectrum is indicative of proximity. Furthermore, as discussed previously, ssNMR methods that measure the interatomic distances further offer a rigorous way to reflect molecular interactions by determining the spatial proximity. This section provides several examples of ^{19}F ssNMR as a high-resolution approach to probe atomic-level drug-drug and drug-polymer interactions.

4.2.1. Drug-drug interaction

The understanding of API-API interactions can elucidate the molecular packing details of API and uncover the molecular mechanism of phase conversions [149–151]. Su and coworkers have comprehensively studied the drug-drug molecular interactions using POSA as a model compound. Fig. 6A presents the results of ^{19}F–^{19}F homonuclear correlation and ^{19}F–^{1}H HETCOR experiments in crystalline and amorphous POSA. The para (F1) and ortho (F2) fluorine atoms in the POSA aromatic ring showed correlations with the aliphatic protons in crystalline and amorphous POSA at a long mixing time. These intermolecular interactions unravel the "head-to-tail" molecular packing between POSA molecules in both API forms [149]. Fig. 6B presents ^{13}C–^{19}F HETCOR and ^{19}F–^{13}C CPMAS experiments with short and long mixing times in crystalline and amorphous POSA. In the ^{19}F–^{13}C CPMAS spectra of crystalline POSA, the appearance of C23 and C49-51 peaks directly proves the close spatial proximity to the POSA fluorines, elucidating the "head-to-head" and "head-to-tail" molecular packing in the crystalline POSA. In contrast, no detectable C23 peak was observed in amorphous with long contact time. This suggests the absence of "head-to-head" packing in the amorphous form of POSA [149].

ssNMR can quantify the strength of molecular interactions from qualitative or quantitative distance measurements. CPMAS has been demonstrated as a semiquantitative method to probe the interatomic

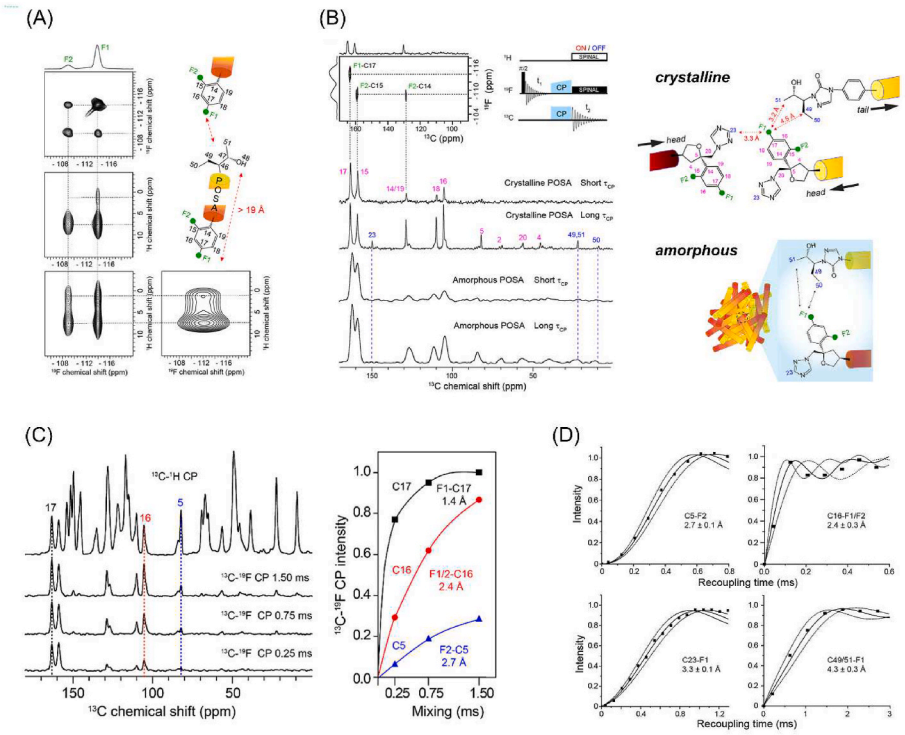


Fig. 6. Investigation of drug-drug interactions in crystalline and amorphous POSA using ^{19}F ssNMR. (A) 2D ^{1}H–^{1}H and ^{1}H–^{19}F correlation spectra of crystalline and amorphous POSA, revealing the "head-to-tail" molecular packing in both forms [149]; (B) Elucidation of intramolecular ^{13}C–^{19}F contacts by 2D ^{13}C–^{19}F HETCOR experiment with short contact time; 1D ^{19}F–^{13}C CP spectra of crystalline and amorphous POSA with the short and long contact time, revealing the missing "head-to-head" molecular packing mode in the amorphous form [149]; (C) Semiquantitative evaluation of ^{13}C–^{19}F distances in crystalline POSA from ^{13}C–^{19}F CP build-up curves [152]; (D) ^{13}C–^{19}F REDOR dephasing curves and simulations for measuring intramolecular (C5–F2 and C16–F) and intermolecular (C23–F1 and C49/51−F1) distances in crystalline POSA [152]. Figures are reproduced with permission from the American Chemical Society.

distances by observing the rate of CP build-up curves. The fast CP build-up rate represents strong dipolar coupling induced by the relatively short distance. For example, Fig. 6C presents a study by Lu et al. The ^{19}F–^{13}C CPMAS experiment with variable CP contact times was used to investigate the proximity of fluorines and carbons in crystalline POSA. The interatomic distances of F1–C17, F1/2−C16, and F2–C5 obtained from the CP build-up curve followed the same order as the distance measurements from the crystallography structure [152]. Apart from semiquantitative measurements, REDOR experiments, as discussed in the previous session, are a more rigorous approach to analyzing the distances between heteronuclear spins. Fig. 6D presents the quantitative distance measurement in crystalline POSA using ^{13}C–^{19}F REDOR. The derived intramolecular (C5–F2 and C16–F) and intermolecular (C23–F1 and C49/51−F1) distances of carbons and fluorines are in remarkable agreement with the results from crystallography data. The REDOR results also implied the existence of "head-to-head" and "head-to-tail" molecular packing in crystalline POSA [152].

Besides POSA, ^{19}F ssNMR was also employed to elucidate the atomic connectivities in many other fluorinated APIs. As shown in Fig. 7A, Guo et al. carried out 2D ^{19}F–^{13}C HETCOR experiments with different CP contact times to distinguish short- and long-range ^{19}F–^{13}C correlations in mefloquine [36]. The fluorine correlations with carbons in mefloquine separated within three bonds, and above three bonds were detected at CP contact times of 1 and 7 ms, respectively. Moreover, the ^{19}F–^{13}C correlations involving fluorine and the piperidine ring carbons such as C12 and C15-17 require a contact time of 9 ms or longer. Besides intramolecular correlations, the intermolecular ^{19}F–^{13}C distances <6 Å between mefloquine molecules were also uncovered. Overall, the ^{19}F–^{13}C HETCOR experiments can detect intra- and intermolecular distances of as long as 6.8 Å, and these distances are consistent with the crystal structure of mefloquine.

In another study, Quinn et al. performed a series of 1D and 2D experiments to elucidate the molecular structure of levofloxacin in the two formulations manufactured by two different manufacturers [52]. Two sets of fluorine resonances (peak I-II and III-IV) suggest the presence of two crystalline polymorphs of levofloxacin in these formulations. 1D ^{19}F DANTE-RFDR experiments revealed the ^{19}F–^{19}F distances between the two crystalline polymorphs. As shown by the RFDR magnetization exchange curves in Fig. 7B, distinct ^{19}F–^{19}F distances were observed. The simulated distances for the deshielded (I and II) and shielded (III and IV) fluorine were 2.9 and 10 Å, respectively. In addition, 2D ^{1}H–^{19}F and ^{1}H–^{13}C–^{19}F HETCOR experiments were further performed and different ^{1}H–^{19}F and ^{13}C–^{19}F intermolecular interactions were observed in the two crystalline polymorphs of levofloxacin.

4.2.2. *Drug-polymer interactions*

In ASD, API is dispersed in the polymer matrix at a molecular level, where the previous crystal lattice is disrupted along with the formation of a metastable amorphous state [18,154,155]. The polymer plays a crucial role in stabilizing the ASD products by preventing amorphous API recrystallization and minimizing the mobility of API molecules [156]. It has been well reported that drug-polymer interaction is important to stabilize the ASD products and improve their oral bioavailability [140,146,152,157–163]. In this regard, the investigation of API-polymer interactions is essential to provide valuable insights into the rational design of ASD formulations. ^{19}F ssNMR has been primarily demonstrated in probing various atomic-level interactions between drug and polymer, such as hydrogen bonding, π-π interaction, etc. [26,146,152,164].

For example, in Fig. 8A, Abraham and Crull applied ^{19}F–^{13}C HETCOR experiments to measure the carbon-fluorine distances between crystalline API, avagacestat, and polymer, hydroxypropyl methylcellulose-acetate succinate (HPMCAS) [164]. The correlation between carbonyl groups of the polymer HPMCAS and CF_3 group of API avagacestat suggests that the polymer may form a hydrogen bond with the NH_2 group of avagacestat, where the NH_2 is spatially close to the CF_3 group. Similarly, Lu et al. utilized ^{19}F–^{13}C CPMAS and ^{1}H–^{19}F HETCOR experiments to study the drug-polymer interactions in 30 wt% drug-loaded POS-A-HPMCAS ASD [146]. As shown in Fig. 8B, the peak of the carbon neighbored to a hydroxyl group (C_{OH}) in HPMCAS showed up in ASD at a long mixing time, which indicates the intermolecular contacts between POSA fluorine and HPMAS C_{OH}. Moreover, by comparing ^{1}H–^{19}F HETCOR spectra of amorphous POSA, HPMCAS, and POSA-HPMCAS dispersion, the appearance of the proton peak at ~4 ppm in ASD

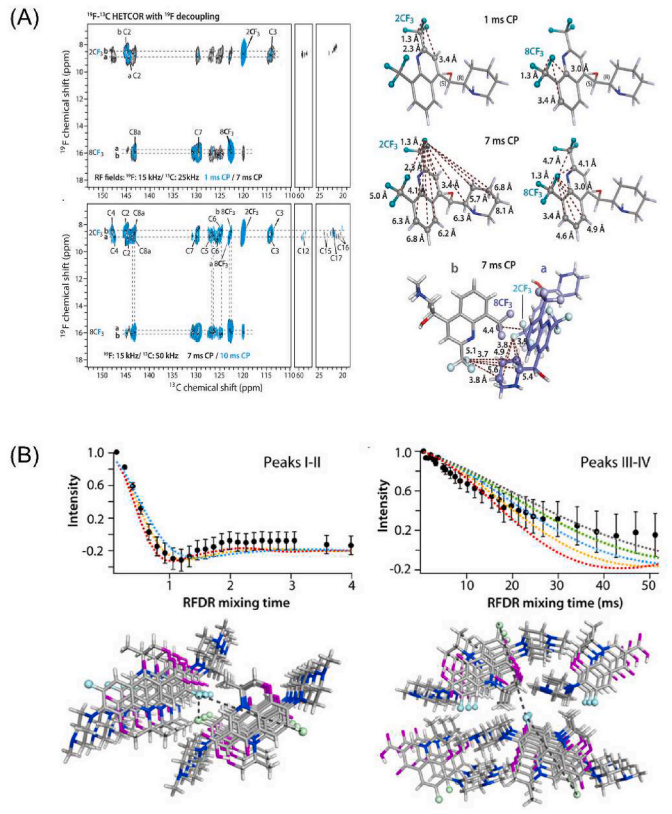


Fig. 7. Investigation of drug-drug interactions in mefloquine and levofloxacin using ^{19}F ssNMR. (A) ^{19}F–^{13}C HETCOR spectra of mefloquine acquired with various CP contact times with ^{19}F decoupling; Short- and long-range intra- and inter-molecular ^{19}F–^{13}C distances in the mefloquine crystal structure [36]; (B) Experimental and simulated ^{19}F DANTE-RFDR exchange curves for fluorine pairs I−II (left) and III-IV(right) in levofloxacin; X-ray structure of levofloxacin, depicting short-range ^{19}F–^{19}F interactions as observed in ^{19}F DANTE-RFDR spectra [52,153]; Figures reproduced with the permission from the American Chemical Society.

further suggested the interaction between POSA difluorophenyl group and polymer hydroxyl groups. This ^{1}H–^{19}F correlation provided direct evidence of the formation of hydrogen bond O–H ⋯ F–C between POSA and HPMCAS. In the same study, ^{19}F–^{13}C REDOR experiments were also performed to quantitatively measure the distances between the fluorines in POSA and C_{OH} in HPMCAS [152]. Two F–F–C configurations, straight-line and triangle, were proposed, and the simulations of the REDOR dephasing curve suggest the internuclear ^{13}C–^{19}F distances are 4.3 ± 0.2 Å and 4.5 ± 0.4 Å, respectively. Fig. 8C presents the two scenarios of the formation of hydrogen bonds in POSA-HPMCAS dispersion based on the ^{13}C–^{19}F distance constraints. In the first scenario, the formation of hydrogen bond O–H ⋯ F–C directly involves the fluorine from POSA. In contrast, in the second scenario, the hydrogen bond is formed between O−H ⋯ Ph (phenyl group of POSA, π acceptor). Utilizing mathematical geometric calculations, the range of the distances of H ⋯ F and H⋯ M (center of the phenyl group) in the two scenarios were derived respectively for the two F–F–C configurations.

4.3. Molecular miscibility and mobility of API in solid dispersions

In ASDs, the amorphous drug substances often undergo undesired amorphous-amorphous phase separation (AAPS), eventually recrystallization [165,166]. Therefore, AAPS promotes drug- and polymer-rich phases and an inhomogeneous and unstable formulation system. Such phase separation has a significant impact on the long-term stability of ASDs [165, 167]. Thus, the evaluation of mixing behaviors of API and polymer in ASD is of vital importance for understanding and predicting formulation stability [168,169]. DSC is commonly employed to qualitatively determine the miscibility of ASD formulations with the criteria that a single glass-transition temperature (T_g) in a DSC thermogram indicates good miscibility [170]. However, recently many reports have demonstrated that the presence of a single T_g can also occur in the phase-separated system [171–173]. In addition, DSC cannot characterize the phase separation on length scales smaller than 30 nm [35,174].

In contrast, ssNMR has been demonstrated as a high-resolution technique for evaluating the drug-polymer homogeneity at domain sizes of several to hundreds of nanometers [175–178]. Heteronuclear detected ^{1}H T_1 and $T_{1\rho}$ experiments are often utilized, where a single homogeneous ^{1}H T_1 and $T_{1\rho}$ usually suggests good miscibility with domain sizes of 20–100 and 1–20 nm, respectively [26,35,179]. Such ^{1}H spin diffusion NMR technique was initially introduced by Schmidt-Rhor and coworkers to evaluate the domain sizes in the mixing of heterogeneous polymers [180,181]. Later, the method was adopted by Aso et al. to assess the molecular mobility of amorphous drugs and, subsequently the miscibility of nifedipine and hydrophilic polymers [182,183]. The last two decades have witnessed the extensive utilization of ^{1}H spin-lattice relaxation measurement to determine the API-polymer miscibility [35,105,106,178,184,185]. For example, Schmidt-Rohr, Su, and coworkers have further pushed the boundary to establish a ^{1}H spin diffusion method to quantify the miscibility and homogeneity of API and polymer excipient at sub-100 nm scale [35]. Most recently, the relaxation method was further extended to study the miscibility of protein and excipient in solid biologics [179,186,187]. It is worth noting that most heteronuclear detected ^{1}H relaxation measurements are carried out by ^{13}C detection. This is mainly due to the ubiquitous presence of ^{13}C in all components in the drug formulations so that the T_1 or $T_{1\rho}$ values for API and excipients can be obtained at the same time.

However, when the drug loadings in ASDs are at considerably low levels, the ^{13}C detected experiments could not confidently measure the T_1 or $T_{1\rho}$ values. In such cases, multinuclear detected ^{1}H relaxation time analysis can be employed to assess the miscibility. For example, the ^{19}F detected ^{1}H relaxation analysis could be conducted for fluorinated APIs, while the analysis of pharmaceutical excipient can be accomplished by ^{13}C detection. If statistically similar ^{1}H relaxation values were obtained for multinuclear detection, this also provides strong evidence of good miscibility of the heterogeneous system. For example, Pham et al. reported the miscibility study of a ternary dispersion containing amorphous API voriconazole, polymer polyvinylpyrrolidone K-30 (PVP K30), and surfactant sodium lauryl sulfate (SLS) [105]. The ^{19}F- and ^{13}C-detected ^{1}H T_1 experiments were utilized to probe the ^{1}H T_1 values of fluorinated API voriconazole and polymer PVP K30, respectively. The same ^{1}H T_1 values from two experiments indicate good miscibility between voriconazole and PVP K30. However, in the same study, a deviated ^{1}H T_1 value obtained from ^{23}Na detection suggests the possible phase separation of surfactant SLS from voriconazole and PVP K30. Such relaxation measurements were further extended to study the miscibility and homogeneity of other multi-component systems, such as drug-cyclodextrin complexes and drug-silica materials composite. For example, Vogt and Strohmeier performed the miscibility analysis of a fluorinated API, diflunisal, confined in the β-cyclodextrin [188]. Because of the weak ^{13}C NMR intensity of diflunisal, the ^{1}H T_1 measurements of diflunisal were carried out with ^{19}F detection. Only 2 h of acquisition is required for ^{19}F-detected ^{1}H T_1 measurement for diflunisal, while 22 h is needed for ^{13}C detection of β-cyclodextrin [188]. Statistically different ^{1}H T_1 values were observed for diflunisal and β-cyclodextrin, indicating a certain degree of heterogeneity in such a drug delivery system. Furthermore, the ^{19}F-detected relaxation measurements were applied to examine the miscibility of ezetimibe confined in mesoporous silica materials. The ^{19}F- and ^{29}Si-detected ^{1}H T_1 experiments were able to probe the miscibility of amorphous ezetimibe and two mesoporous silica materials, SY350 and SY740 [189]. Similar ^{19}F-

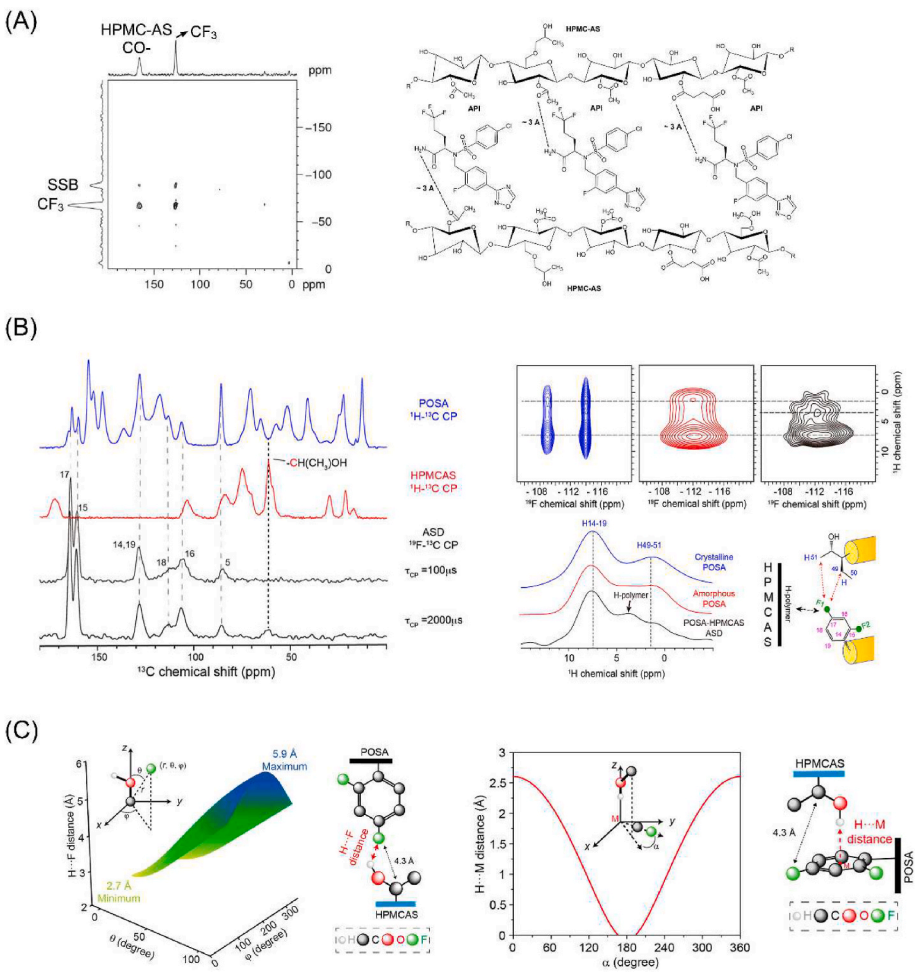


Fig. 8. Investigation of drug-polymer interactions using ^{19}F ssNMR. (A) 2D ^{19}F–^{13}C HETCOR spectrum of the avagacestat-HPMCAS dispersions with CP contact time of 2 ms [164]; (B) 1D ^{19}F–^{13}C CP spectra of amorphous POSA, HPMCAS, and 30 wt% POSA-HPMCAS dispersion, revealing the intermolecular interaction between POSA and HPMCAS [146]; 2D ^{1}H–^{19}F HETCOR spectra and 1D ^{1}H cross-sections of crystalline POSA, amorphous POSA, and POSA-HPMCAS dispersion, elucidating the formation of hydrogen bond between POSA fluorine and the hydroxyl group of HPMCAS [152]; (C) Two hypothetical hydrogen bonding complexes formed between POSA and HPMCAS, including the interaction between the polymer O–H group as an acceptor and POSA fluorine (left) or difluorophenyl ring (right) as a donor [152]. Figures are reproduced with permission from the American Chemical Society.

and ^{29}Si-detected ^{1}H T_1 values were obtained in ezetimibe-SY350 composite, indicating no phase separation in this drug-silica dispersion. In contrast, different ^{1}H T_1 values were observed in the ezetimibe-SY740 dispersion, which was tentatively attributed to the large silica surface area and stronger hydrogen bonding in the dispersion.

The stability enhancement of ASDs is partially due to the restriction of drug mobility in the polymer matrices [106,190,191]. ^{19}F ssNMR was reported able to probe the mobility of APIs in ASDs. For instance, Aso et al. measured ^{19}F T_1 values of flufenamic acid (FLF) in solid dispersions with two different polymer excipients, hydroxypropyl methylcellulose (HPMC) and PVP [192]. The correlation time, τ, derived from T_1 or $T_{1\rho}$, can represent the degree of rotational molecular mobility. It was found that the τ of FLF for solid dispersion containing 20% PVP was 2–3 times longer than that with 20% HPMC at 50 °C, indicating lower molecular mobility in the FLF-PVP dispersion. Monitoring the initial state of the drug when exposed to the aqueous environment can provide a mechanistic understanding of drug disintegration and dissolution. Dahlberg et al. demonstrated an *in situ* characterization of flutamide ASD tablets during disintegration and dissolution using a combination of localized NMR spectroscopic and NMR imaging techniques [193]. ^{19}F NMR relaxation was sensitive to the state and molecular mobility of flutamide in ASD. The ^{19}F T_1 of flutamide in ASD after the immediate mixing with water was only half of that for dry flutamide (crystalline form). This indicates that the initial state of the drug in ASD is either in the form of amorphous grains or is molecularly distributed in the polymer matrix, where the mobility of flutamide is significantly higher than in the bulk crystals. During the time of a few hours of mixing in a liquid environment, the T_1 of flutamide gradually increases and reaches the same level as the bulk flutamide crystal, suggesting the recrystallization of flutamide along with the decrease of molecular mobility. By combining results from ^{19}F T_1 measurement and calculations of transverse relaxation rate, the author speculated that the initial state of flutamide is small (3–4 nm) amorphous grains distributed homogeneously in the matrix upon the hydration. ^{19}F relaxation was also attempted to study the mobility of fluorinated drug molecules confined in porous materials. For example, Vogt et al. measured ^{19}F T_1 and $T_{1\rho}$ relaxation times of ezetimibe to analyze its mobility difference in SY350 and SY740 silica materials [189]. The shorter $T_{1\rho}$ time for ezetimibe in SY350 suggested a higher degree of mobility in the silica materials with larger pore sizes. Such assessment of local mobility by ^{19}F relaxation measurements provides mechanistic insights into stabilizing pharmaceutical amorphous materials imparted by either polymeric excipients or mesoporous silica nanoparticles. Besides relaxation measurements, ^{19}F chemical shift anisotropy (CSA) has also been utilized to reflect the molecular dynamics of functional groups in pharmaceutical compounds [149]. For example, Lu et al. compared the ^{19}F CSA between crystalline and amorphous POSA [149]. The *para*-fluorine (F1) of POSA in both forms showed smaller absolute CSA than *ortho*-fluorine (F2), indicating relatively high mobility of F1 because the motion of F1 is less restricted by other chemical groups. Moreover, their results suggest the CSA of the disordered amorphous form has a slightly smaller CSA than crystalline POSA. This interesting finding from CSA measurement is correlated to the difference of local molecular packing of crystalline and amorphous forms. The absence of a "head-to-head" packing pattern in amorphous POSA likely results in an increase of molecular mobility and thus smaller CSA values.

5. Characterization of drug delivery systems

The design of site-specific and stimuli-responsive drug delivery systems (DDSs) has attracted immense interest in recent years [194–196]. DDSs possess many advantages, such as targeted delivery, precisely controlled drug release, improved drug efficacy, and stability as well as reduced side effects [115,197,198]. Many drug carriers, for example, mesoporous silica nanoparticles, cyclodextrins, and polymer matrices, have been described as promising platforms for achieving drug delivery [199–202]. To better design intelligent DDSs, in-depth knowledge about the structural details of API and DDSs is essential. Solid-state NMR is a powerful technique for the investigations of API in DDSs [196,197,202]. It can probe structural information at a molecular level relevant to the structure and physicochemical properties such as API phase conversion, local structure, and molecular dynamics, intra- and inter-molecular connections, and API-DDS interactions. This section presents the application of ^{19}F ssNMR in characterizing three different DDSs, including mesoporous silica nanoparticles, cyclodextrins, and polymer matrices.

5.1. Drug loading in mesoporous materials

Recently, mesoporous silica nanoparticles have been described as promising nanocarriers for drug molecules [199,203,204]. These mesoporous materials can be specifically designed to achieve controlled drug release by using the tunable pore size and architecture and large surface areas [205]. Moreover, it has been reported that the confinement of drug molecules in the mesoporous pores can stabilize the metastable amorphous form API with the reduction of the tendency to recrystallize [189,206–208]. The stabilization of the amorphous API in mesoporous materials is attributed to the spatial constraints imposed by the nanometer-sized pores, where the crystal growth is significantly inhibited [189]. ^{19}F ssNMR was recently demonstrated as a powerful technique to investigate the behaviors of fluorinated APIs confined in mesoporous materials [115]. As shown in Fig. 9A, Vogt et al. utilized ^{19}F ssNMR to study the physical states of ezetimibe loaded in mesoporous silica materials [189]. The ^{19}F CPMAS spectra of ezetimibe with three different weight fractions displayed broad, amorphous NMR peaks in two silica materials, SY350 and SY740, with varying pore sizes. No crystalline ezetimibe was observed even at a longer acquisition time. This alternative stabilizes the amorphous APIs without introducing polymeric excipients to form solid dispersions. The interactions between ezetimibe and mesoporous silica materials were also probed by ^{19}F–^{29}Si, ^{1}H–^{19}F, and ^{1}H–^{29}Si heteronuclear correlation experiments. The ^{19}F–^{29}Si CPMAS spectrum of ezetimibe in SY740 is similar to that of ^{1}H–^{29}Si, which indicates proximity between all silicone sites (Q_x, x = 2, 3,4) to the fluorines in ezetimibe. In contrast, no such correlation was observed for ezetimibe in SY350.

Similarly, Khimyak and coworkers confined flufenamic acid (FFA) in three porous silica materials (MCM-41, SBA-15, and MCF). They systematically investigated the effect of pore size and drug loading on the phase of FFA by ^{19}F ssNMR [208]. Fig. 9B proposed the mechanisms of the crystalline phase formation at large pore sizes (~29 nm). Only FFA at the internal pore surfaces and high mobile species in the void were detected at lower drug loading. By gradually increasing the FFA content, the amorphous phase was observed until 20 wt%, and crystalline FFA started to show up at 25 wt%. In the study, variable-temperature ^{19}F

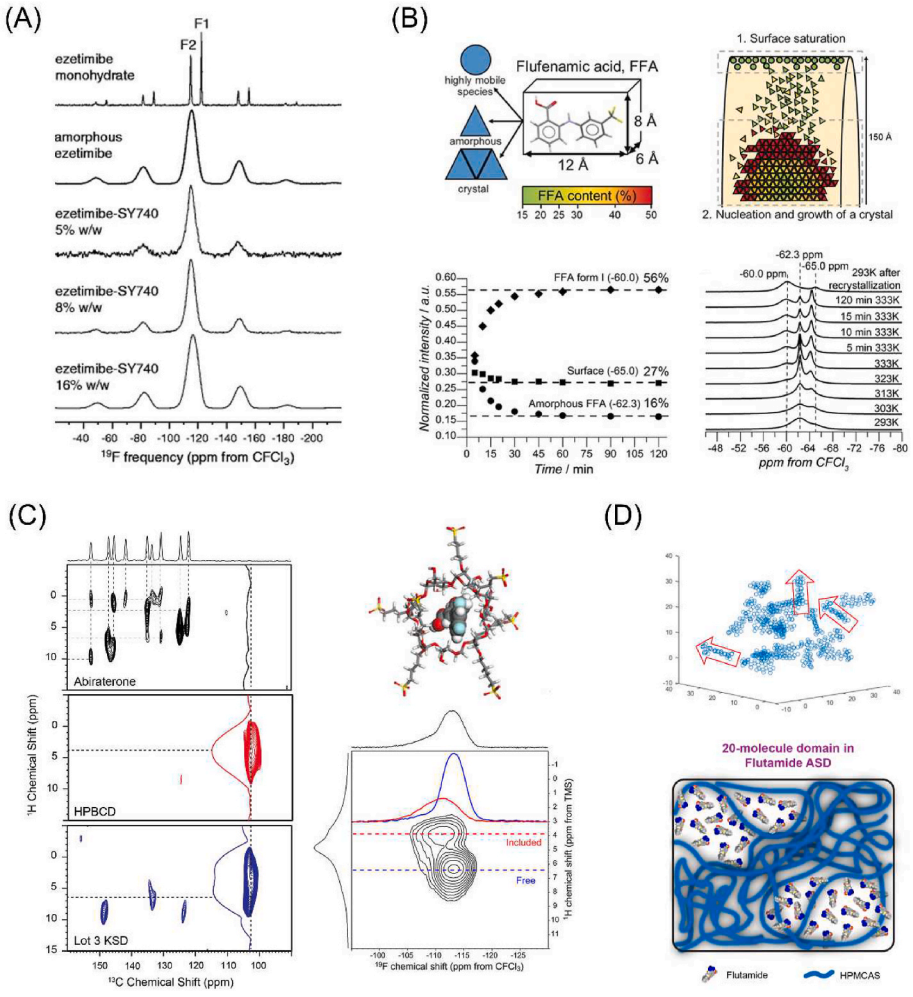


Fig. 9. Characterization of drug molecules in various drug delivery systems using ^{19}F ssNMR. (A) 1D ^{19}F CPMAS spectra of crystalline ezetimibe monohydrate, amorphous ezetimibe, and amorphous ezetimibe loaded in mesoporous material SY740 [189]; (B) Three different phases and average dimensions of flufenamic acid and proposed mechanism of the formation of crystalline flufenamic acid form I in MCF silica (top); Kinetics of crystalization of flufenamic acid confined in MCF at 333 K and variable-temperature ^{19}F ssNMR spectra (bottom) [208]; (C) 2D ^{13}C–^{1}H HETCOR spectra of crystalline abiraterone API, HPBCD, and the Lot 3 KSD (left) [218]; Inclusion of a drug molecule in the cavity of cyclodextrin and ^{1}H–^{19}F CP-HETCOR spectrum of a coground 1:2 molar ratio mixture of diflunisal and β-CD [188]; (D) Molecular packing of flutamide in ASD from ^{19}F CODEX; Orientations of flutamide molecule packed randomly (top); Flutamide-rich domain in HPMCAS polymer matrix (Bottom) [219]; Figures are reproduced with the permission of Springer, John Wiley & Sons, Elsevier, and the American Chemical Society.

ssNMR experiments were employed to investigate the kinetics of crystallization of amorphous FFA *in situ* in the MCF-FFA host-guest system. As shown in Fig. 9B, at 293 K, only highly mobile liquid-like (~65 ppm) and amorphous forms (~62.3 ppm) of FFA were observed. When the temperature increases, the confined amorphous FFA species gradually recrystallize to form crystalline FFA form I after 323 K. Meanwhile, the intensity of mobile species is not affected by the crystallization. The size of pore in different silica materials significantly impacted the recrystallization. No crystalline FFA was detected in the identical *in situ* analysis of SBA-FFA composite, indicating an effective stabilization of confined amorphous FFA with a much smaller pore size (7.1 nm of SBA vs. 29 nm of MCF).

5.2. Drug-cyclodextrin complex

Cyclodextrins (CDs) are widely utilized as excipients for more than 30 different pharmaceutical products on the market [209]. Bearing a hydrophilic exterior and hydrophobic interior, CDs can form host-guest complexes by incorporating the hydrophobic compounds in the cavity via hydrophobic effects and hydrogen bonds/ion-dipole bonds/electrostatic interactions [209,210]. Drug-CD complexes have been regarded as an efficient approach for *in vivo* drug delivery [211–213]. Moreover, such inclusion of drug molecules in CDs was reported to enhance the aqueous solubility and stability of drugs, and therefore their bioavailability [200,210]. ssNMR is an ideal approach to studying the inclusion of drug molecules in CDs, and most studies are proceeded using ^{13}C detection [188,214–218]. In these studies, 2D ssNMR is widely utilized to probe the drug-CD interactions via dipolar coupling by detecting the homonuclear and heteronuclear correlations. For example, Gala et al. employed ^{13}C ssNMR to investigate the molecular interaction between abiraterone and hydroxypropyl β-cyclodextrin (HPBCD) in a KinetiSol® processed solid dispersions (KSDs) [218]. Fig. 9C (left panel) presents the ^{1}H–^{13}C HETCOR spectra of crystalline abiraterone, HPBCD, and Lot 3 KSD. A new cross peak was observed in the spectrum of KSD and assigned as the correlation between the aromatic proton of abiraterone (~6.4 ppm) and anomeric carbons of HPBCD (~103 ppm). This provides direct evidence for the intermolecular interaction between abiraterone and HPBCD within KSDs. Apart from ^{13}C detection, ^{19}F ssNMR was also involved in the characterization of drug-CD complexes. In a study by Vogt et al., ^{1}H, ^{13}C, ^{19}F, and ^{31}P ssNMR were employed to study the inclusion of different drug molecules in a variety of CDs [188]. ^{1}H–^{19}F CP-HETCOR experiment was utilized to validate the inclusion of diflunisal, a fluorinated API, in the cavities of three different CDs, α-CD, β-CD, and SBE-β-CD. Since diflunisal lacks aliphatic protons, the peaks in the HECTOR spectrum that correlate fluorine atoms of diflunisal, and aliphatic protons of CDs can be exclusively assigned to short-range intermolecular interactions between diflunisal and CDs within 10 Å range. Among three CDs, β-CD, SBE-β-CD clearly showed such correlation peaks, suggesting successful inclusion of diflunisal within the cavity of these two macromolecules. In contrast, no such ^{1}H–^{19}F correlation was observed in α-CD and the inclusion of the drug in α-CD is likely inhibited due to the smaller cavity size. Moreover, as shown in Fig. 9C (right panel), the quantification of the levels of included and free drugs in a CD matrix was also demonstrated using ^{19}F ssNMR. ^{19}F DPMAS spectrum of the coground 1:2 molar ratio mixture of diflunisal with β-CD suggested 28% of the diflunisal formed the drug-CD complex. This was also proved by a strong correlation between aliphatic protons of β-CD and fluorine of diflunisal in the 2D ^{1}H–^{19}F CP-HETCOR experiment. The chemical shift of fluorine in the included diflunisal (−111 ppm) was more deshielded than that of free diflunisal.

5.3. Molecular packing of drugs in amorphous solid dispersion

Despite the broad utilization of ASDs as a major platform for delivering poorly water-soluble drugs, a fundamental understanding of drug stability and instability within the polymer matrix at the molecular level is largely unexplored. Specifically, the structural basis for rationalizing how polymer serves as a network that separates drug molecules to enhance the energy barrier of recrystallization is unclear. Besides, phase separation-induced drug-rich domain is often accused of promoting crystallization and lacks structural evidence. Therefore, drug-drug interaction in molecular packing within the porous polymer system offers critical information. Such molecular properties are highly challenging to elucidate by many high-resolution techniques, e.g., XRD, for its multicomponent and amorphous nature. Most recently, Phyo et al. have applied the ^{19}F centerband-only detection of exchange (CODEX) NMR method to probe the molecular packing of drugs in an amorphous formulation (Fig. 9D) [219]. CODEX experiment was initially designed to study slow molecular re-orientation [220] and well implemented to quantify protein oligomerization in the past years [45,221–225]. It utilizes spin diffusion and CSA to quantify the number of non-equivalent molecular orientations in an oligomer. The fast spin diffusion rate and large CSA of ^{19}F have benefited ^{19}F-CODEX as a powerful technique for spin counting. Xue et al. have utilized ^{19}F CODEX to elucidate the oligomerization of organic compounds in their crystalline forms [226]. This ^{19}F spin-exchange NMR method has recently been applied to study pharmaceutical compounds. For example, Roos et al. have investigated the structure of sitagliptin phosphate, a drug for type 2 diabetes [134]. In the study by Phyo et al., the authors have included flutamide-HPMCAS (15% w/w drug loading) and POSA-HPMCAS (25% w/w drug loading) as two examples of ASDs produced by spray drying. ^{19}F CODEX results have identified 20 flutamide and 10 POSA molecules in the nanometer domain. For the first time, their study has provided experimental data to quantify the number of drug molecules packed in the drug-rich domain within the polymer matrix. Taking flutamide-HPMCAS ASD, for example, ^{19}F CODEX shows a dephasing at 1/20. As illustrated in Fig. 9D, a randomized molecular packing model is utilized to fit the ^{19}F CODEX data. The findings of 20-molecule packing represent a cubic box or length of the drug-rich domain of ~2.8 nm, which is well within the range estimated from the ^{1}H $T_{1\rho}$ measurement. This method provides an opportunity to investigate the role of the drug-drug interaction in API recrystallization in amorphous pharmaceutical formulations to understand the underlying mechanism and predict drug product design's long-term stability.

6. Molecular mechanism of drug actions

Understanding the molecular mechanism of drug actions is critical for drug design. For example, antimicrobial molecules function by disrupting the lipid membrane [227]. ssNMR has been extensively utilized to investigate antimicrobial drugs (AMDs) and peptides (AMPs), and various models have been proposed, including Barrel stave transmembrane model, toroidal pore model, carpet model, and in-plane diffusion or partial-insertion model [228–230]. However, isotopic labeling is often necessary for ^{13}C NMR methods in these studies. ^{19}F ssNMR provides a unique opportunity to investigate the dug action without isotopic labeling. For example, Su et al. studied the orientation, dynamics, and lipid interaction of an antimicrobial acrylamide, PMX30016, using ^{31}P and ^{19}F ssNMR. As shown in Fig. 10A, the ^{19}F–^{19}F dipolar coupling in the trifluoromethyl group was measured by ^{19}F CSA and 2D dipolar chemical-shift (DIPSHIFT) correlation experiment under static conditions. Such information of ^{19}F–^{19}F dipolar couplings was utilized to derive the orientation of PMX30016 in the lipid bilayers, where a 20° and 30° tilt angle of PMX30016 molecular plane to the bilayer normal was obtained for neutral and negatively charged lipid bilayers.

Besides the investigation of fluorinated small molecular drugs, ^{19}F ssNMR has been widely utilized to investigate the mechanism of AMPs. Fig. 10B shows a study by Toke et al., which used ^{19}F ssNMR to examine the mode of action of $(KIAGKIA)_3$ peptides (K3). The fast dephasing of ^{13}C–^{19}F REDOR suggests the formation of K3 dimers. Based on all the distance and orientation information obtained from REDOR, a toroidal pore model was proposed for K3 peptides [231,232]. Apart from

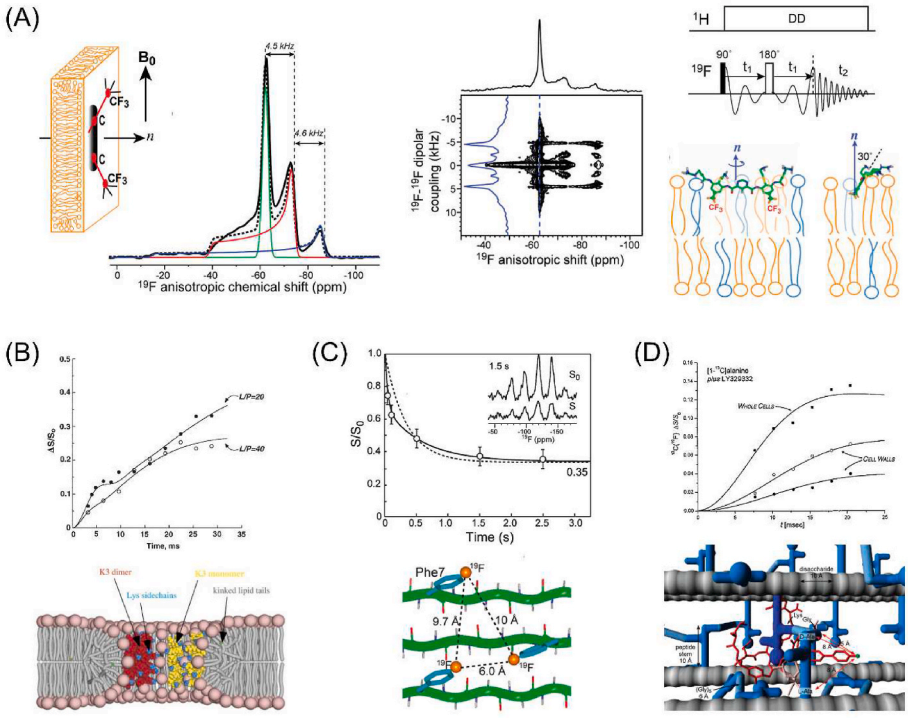


Fig. 10. Molecular mechanism of drug actions. (A) The geometry of magnetically oriented bicelles containing PMX30016 and measurements of ^{19}F CSA of trifluoromethyl group in PMX30016; 2D ^{19}F homonuclear DIPSHIFT spectrum and pulse sequence of PMX30016 in aligned DMPC/6-O-PC bicelles, where the obtained dipolar coupling was utilized to generate the best-fit for the orientation of PMX30016 in lipid membranes [240]; (B) ^{13}C–^{19}F REDOR dephasing curves of K3 peptides in lipid bilayers at a lipid-to-peptide molar ratio (L/P) of 20 and 40 and cross-section view of the cartoons of the K3 pore model [231,232]; (C) Normalized CODEX intensities as a function of mixing time for 4-^{19}F-Phe$_7$ penetratin in the lipid membrane and the three-spin geometry with unequal distances used to obtain the solid-line best-fit curve [225]; (D) ^{13}C–^{19}F REDOR dephasing curves as a function of dipolar evolution time for complexes of [^{19}F]oritavancin with whole cells and cell walls of *Staphylococcus aureus* and the model of [^{19}F]oritavancin binding to the peptidoglycans in cell walls [238]. Figures are reproduced with permission from the American Chemical Society and Elsevier.

REDOR, CODEX experiments were also able to provide information on the interaction between AMP and lipid membranes. For example, Buffy et al. presented a^{19}F CODEX study to determine the oligomeric structures of an AMP, protegrin-1, bound to the lipid bilayer at different peptide-to-lipid ratios [233]. Similarly, Salnikov et al. reported using ^{19}F CODEX to define the size of the aggregates of alamethicins and the relative arrangement of the helices [222].

Moreover, the design of cell-penetrating peptides (CPPs), a promising drug delivery system, can benefit from the structural basis responsible for its membrane permeation [234]. Su et al. utilized a ^{19}F CODEX experiment to determine the oligomeric number and intermolecular distances of penetratin, a CPP, in lipid bilayers [225]. As shown in Fig. 10C, the ^{19}F CODEX intensities of 4–^{19}F-Phe$_7$ penetratin decay to an equilibrium value of 0.35, suggesting a formation of penetratin trimer in the lipid membrane. Furthermore, the CODEX decay trajectory was then fitted to a triangular geometry representing the penetratin trimer. A triangle with a side length of 6, 9.7, and 10.2 Å displays the best fit to the experimental data. In recent years, in-cell ssNMR is an emerging technique that can probe *in situ* structural and functional information in cellular systems at an atomic level [235–237]. By applying ^{19}F REDOR internuclear distance measurements, Kim et al. studied the binding site of the peptidoglycans to [^{19}F]oritavancin, an Eli Lilly compound for the treatment of serious Gram-positive bacterial infection, in both isolated cell walls and the cell walls of *Staphylococcus aureus* [232,238]. Fig. 10D presents the model of [^{19}F]oritavancin binding to the cell walls based on all the ^{19}F–^{13}C and ^{19}F–^{15}N distance constraints obtained from REDOR experiments. Apart from drugs and peptides, another category of fluorinated compounds utilized in clinics is the imaging agents such as ^{18}F-containing positron emission tomography (PET) tracers. A recent study by Duan et al. demonstrated the capability of using ^{19}F and ^{13}C ssNMR to probe the binding sites of flutemetamo, a PET imaging agent, to an Alzheimer's β-amyloid peptide (Aβ40) [239]. Compared to the interaction between amyloid fibrils and small molecules, the flutemetamo was found to bind preferentially with polar, charged, and aromatic amino acid residues on the β-sheet surface in Aβ40. Such a study provides invaluable insights for the rational design of PET tracers with high affinity and specificity for various amyloid fibrils presented in neurodegenerative diseases.

7. Sensitivity enhancement of ^{19}F MAS NMR

Strong homonuclear ^{19}F–^{19}F and heteronuclear ^{19}F–^{1}H dipolar couplings resulting in broad NMR lines can hinder its application in the solid-state analysis of fluorinated compounds [26,36,241]. In this regard, techniques and methods that can reduce or eliminate the strong dipolar couplings can further enhance the utilization of ^{19}F ssNMR. Moreover, as ASD becomes increasingly popular in formulation development, the broad spectra feature and low peak intensity present challenges for ^{19}F ssNMR in the characterizations of amorphous pharmaceuticals [26]. Additionally, the sensitivity can also be an issue for ^{19}F ssNMR when the solid formulation has extremely low drug loadings. In such a case, the advanced spectroscopic methods such as multidimensional experiments are likely restricted due to the low sensitivity. Therefore, even though ^{19}F is the second-highest sensitive nucleus (among typical nuclei), techniques that can improve the spectral resolution and sensitivity are still desired. In this section, two state-of-the-art techniques, ultrafast MAS (UFMAS) and dynamic nuclear polarization (DNP), are presented to demonstrate how the sensitivity enhancement advances the pharmaceutical applications in ^{19}F ssNMR.

7.1. Fast and ultrafast MAS

Strong spin interactions can be troublesome for ^{19}F ssNMR in the pharmaceutical analysis of fluorinated compounds. Generally, high-power homo- and heteronuclear ^{1}H, ^{19}F, and ^{13}C decoupling are often required in ^{19}F ssNMR to improve the spectral quality [36,71,242]. Apart from achieving decoupling by specialized hardware, another way to improve spectral quality is by increasing the MAS frequencies. Many reports have demonstrated significant improvements in sensitivity and resolution of the ^{19}F spectra when the MAS rate is increased substantially [36,52,71,123,124,134,243–247]. The narrowed NMR lines and enhanced resolution by fast MAS experiments can ease the peak assignment in ^{19}F ssNMR spectra. For example, by spinning the crystalline and ASD samples of voriconazole at 35 kHz, the peak assignment of fluorines becomes straightforward without interference from spinning sidebands [105].

In the past decade, fast MAS representing the sample-spinning rate at $V_R \geq 60$ kHz has further averaged the dipolar couplings to a greater extent. The remarkable gain of sensitivity and resolution has further advanced ^{19}F ssNMR in many pharmaceutical applications, including structural elucidation, quantification, and investigation of molecular interactions. It is worth noting that the sample masses packed into rotors decrease considerably for smaller rotors. For example, only ~4 mg sample is required for packing a 1.3 mm rotor capable of rotating up to ~65 kHz while a typical 4 mm rotor can contain 60–120 mg of sample. However, improving spectral quality at higher MAS still practically overcomes the sensitivity limitations resulting from the reduced sample mass. For example, in Fig. 11A, Lu et al. quantitatively studied the effect of fast MAS in spectral quality by spinning the crystalline API aprepitant at a series of MAS frequencies from 8 to 65 kHz [71]. The signal intensity of trifluoromethyl fluorine (F1,2) increases by five times at the rate of 65 kHz compared to 8 kHz, and a 25-fold intensity gain was obtained for the fluorophenyl fluorine (F3). Consistent with intensity change, the linewidth narrowing effect leads to significantly improved spectral resolution. The improved spectral quality at 60 kHz enabled the two 3D ^{19}F–^{1}H–^{1}H and ^{19}F–^{19}F–^{1}H correlation experiments to analyze the structural difference between the aprepitant API and its nanoparticulate formulation, EMEND®. As shown in Fig. 11A, the 2D ^{1}H–^{19}F planes are greatly similar, indicating no structural alternation between API and its commercial drug product. Most drugs in solid dosage formulations are in crystalline forms, where the long-range order can result in a long longitudinal relaxation time (T_1). This situation is even worse for ^{19}F ssNMR considering the relatively long $T_{1,F}$ than $T_{1,H}$, leading to time-consuming spectral acquisition. Paramagnetic relaxation enhancement (PRE) has been described as a practical approach to reducing T_1, and therefore, the signal intensity can be improved with efficient signal averaging [248–250]. Fig. 11B presents the first application of PRE in the investigation of pharmaceutical solids [245]. By doping the crystalline POSA with Cu (II) ions, the $T_{1,F}$ of POSA was shortened by 3-fold at no expense of structural change, enabling a 3-fold faster ^{19}F acquisition. Moreover, in the same study, the PRE was coupled with UFMAS experiments at 60 kHz to elucidate the molecular packing of crystalline POSA. The vastly improved resolution in ^{1}H–^{19}F HETCOR experiments offers the opportunity to extract rich information on intra- and intermolecular interactions in POSA, resulting in the revealing of the "head-to-head" and "head-to-tail" packing structures [245].

Recently, UFMAS ^{19}F ssNMR with a rotation rate at ≥100 kHz has been further applied in the characterization of fluorinated pharmaceutical materials [52,245]. Fig. 11C presents a study by Quinn et al. utilizing the UFMAS at V_r = 60–111 kHz to investigate the two generic formulations of atorvastatin calcium [52]. The linewidth narrowing in ^{19}F spectra was systematically evaluated for MAS frequencies ranging from 60 to 111 kHz in the presence and absence of ^{1}H decoupling. The linewidth was decreased by ca. 1.3-fold when increasing the MAS rate from 60 to 111 kHz without ^{1}H decoupling. Moreover, in their study, the ^{1}H–^{19}F HETCOR spectra with a high signal-to-noise ratio (S/N) for two atorvastatin samples containing only 6–9% w/w API were collected in just a few hours, attributed to the sensitivity enhancement resulting from UFMAS. In addition to HETCOR experiments, the ^{19}F–^{19}F REDOR experiments at UFMAS frequencies also enabled the high-resolution structural analysis of atorvastatin samples, where four different fluorine atom environments were revealed for the two groups of fluorine resonances. Most recently, GalPorat-Dahlerbruch et al. have probed structures of atorvastatin calcium and mefloquine by measuring ^{19}F

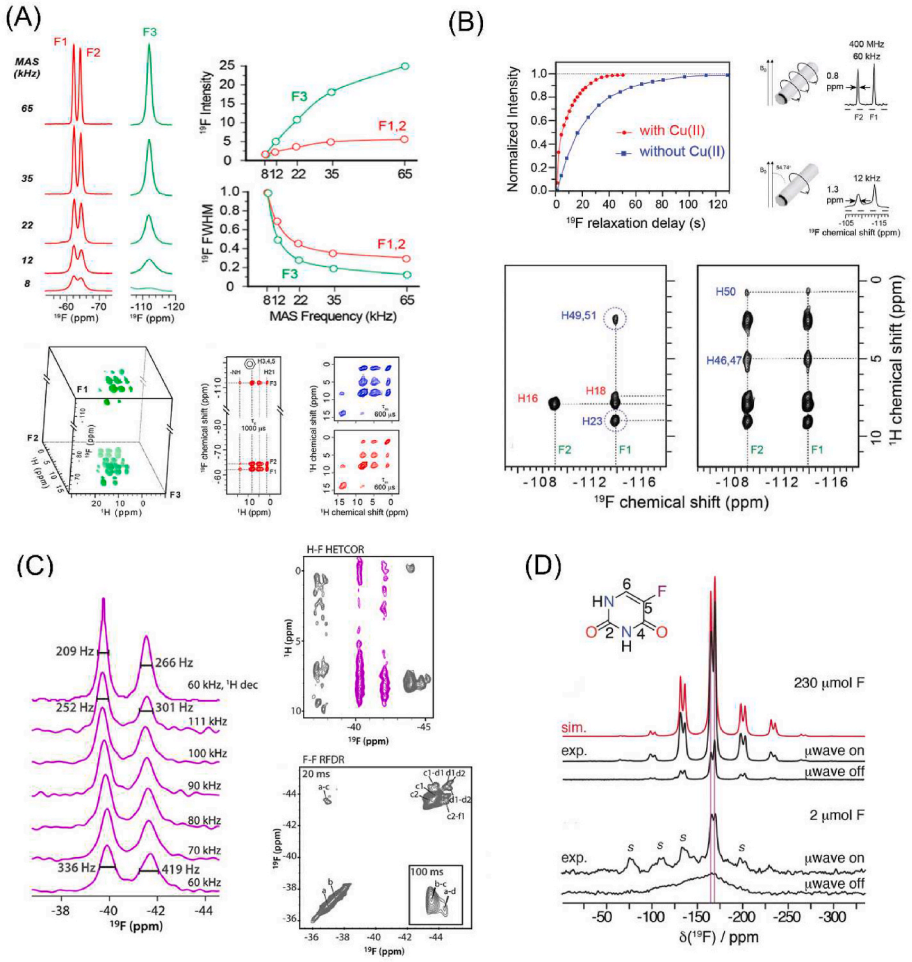


Fig. 11. ^{19}F ssNMR spectral improvement using fast MAS and DNP in pharmaceutical applications. (A) The sensitivity and resolution enhancement of ^{19}F 1D spectra of crystalline aprepitant at different MAS frequencies ranging from 8 to 65 kHz (top); 3D spectra of ^{19}F–^{1}H–^{1}H correlation experiments of nanoparticulate formulation of aprepitant and the extraction of 2D ^{1}H–^{19}F planes of crystalline aprepitant and its nanoparticulate formulation (bottom) [71]; (B) ^{19}F magnetization build-up curves of crystalline POSA with and without the doping of Cu (II) and ^{19}F 1D spectra collected under spinning rate of 12 and 60 kHz (top); 2D ^{1}H–^{19}F HETCOR spectra acquired with short (50 us) and long (1000 us) contact time at MAS of 60 kHz (bottom) [245]; (C) ^{19}F 1D spectra of atorvastatin sample 1 acquired at MAS frequencies ranging from 60 to 111 kHz (left); ^{1}H–^{19}F HETCOR spectra of atorvastatin sample 1 (magenta) and 2 (grey) and ^{19}F–^{19}F RFDR spectra of sample 2 collected under UFMAS (right) [52]; (D) ^{19}F Hahn echo spectra of 5-fluorouracil with and without DNP enhancements for two different concentrations of fluorine, 230 (top) and 2 μmol (bottom) [260]. Figures reproduced with permission from the American Chemical Society, Royal Society of Chemistry, and John Wiley & Sons.

chemical shift tensors at the MAS frequencies of 60–100 kHz [251]. The above studies demonstrated the usefulness of fast and ultrafast MAS ^{19}F ssNMR in the characterizations of fluorine-containing drug substances and drug products. It can be anticipated that future advancements in MAS with more effective averaging of dipolar couplings will further enhance spectral sensitivity and resolution.

7.2. Dynamic nuclear polarization

DNP is a technique that can boost the sensitivity of NMR by transferring the polarization of unpaired electrons to the nearby nuclei via microwave irradiation of electron-nuclear transitions. It exploits the significant difference in the gyromagnetic ratio between electrons and nuclei, and theoretically, the enhancement factor for ^{1}H is ~660 [26,252–254]. The development of the polarizing radicals, cryogenic MAS probe, and high-frequency and high-power microwave sources has led to the advancements of DNP to a great extent. In recent years, DNP has been prosperously applied to many nuclei, such as ^{13}C, ^{15}N, ^{35}Cl, etc., to characterize various pharmaceutical APIs and formulations [255–258]. Typically, one to two orders of magnitude signal enhancement can be achieved [252,259]. This has enabled multidimensional experiments to analyze the pharmaceutical materials at their natural abundances. For example, Ni et al. have demonstrated a 32-fold ^{15}N signal enhancement by DNP, which allows the complete chemical shift assignments of ^{15}N in the POSA-deuterated vinyl acetate ASD [255].

Nevertheless, the use of DNP-enhanced ^{19}F ssNMR remains scarce in pharmaceutical applications. Fig. 11D presents the ^{19}F ssNMR DNP study for an API, 5-fluorouracil, by Viger-Gravel et al. using the incipient wetness impregnation (IWI) method [260]. A roughly 25-fold enhancement was reported. Moreover, a signal enhancement factor of 10 was also obtained for ^{13}C when transferring the fluorine polarization to carbon by ^{19}F–^{13}C CPMAS. In the study, besides the sample with a high concentration (230 μmol of fluorine), a low concentration sample (2 μmol of fluorine) was also prepared by mixing 5-fluorouracil with cellulose, an excipient to mimic the pharmaceutical drug product. As shown in Fig. 11D, DNP significantly amplified the signal intensity while detecting a few micromoles of fluorine was not applicable in the routine MAS experiments [260]. Furthermore, Polenova and coworkers have achieved a remarkably high ^{19}F signal enhancement (~100-fold) using DNP in combination with fast MAS at $>$ 20 kHz in the study on HIV-1 capsid protein assemblies [261]. The improved sensitivity allowed the collection of ^{19}F–^{13}C HETCOR spectra, providing a wealth of information on distance constraints for the protein structural analysis. These two examples demonstrate that ^{19}F MAS ssNMR coupled with DNP is a powerful tool in characterizing drug products and biologic materials even with low fluorine concentrations.

Recently, Emsley et al. discussed the possibility of applying MAS DNP experiments for quantitative studies [262]. Coupling with multiple-contact CP, ^{13}C MAS DNP was demonstrated as an efficient and robust method for absolute quantification of an analyte with errors less than 10% [262]. The uniform DNP enhancements for the analyte of interest and the internal standard aided the quantification. In the study, the authors also proposed that the quantification by DNP MAS NMR in a more complex system is likely still applicable if signal intensities are normalized to their steady-state enhancements. Such DNP-enhanced experiments can be extended to ^{19}F ssNMR. The sensitivity enhancement offered by DNP and ^{19}F can further leverage the efficiency for the quantification studies of fluorinated pharmaceuticals.

8. Conclusion and Outlook

Fluorinated drugs represent a considerably large share of the pharmaceutical market. Given the high NMR receptivity and the absence of fluorine in most pharmaceutical excipients, ^{19}F ssNMR has become an efficient analytical technique to characterize fluorine-containing drug substances and drug products. As a versatile and high-resolution technique, ^{19}F ssNMR is widely utilized to identify and quantify different API forms, unravel structural details and molecular interactions, and provide a mechanistic understanding of API phase conversion, molecular packing, and drug actions. The rational design of next-generation drug delivery systems demands in-depth structural knowledge of the API and drug carriers. ^{19}F ssNMR is an indispensable tool in characterizing novel drug delivery systems to extract information on molecular connectivity, local molecular dynamics, homogeneity of fluorinated drugs and carriers, etc. Cutting-edge techniques such as UFMAS and DNP further expand the utilization of ^{19}F ssNMR by significantly improving the spectral resolution and sensitivity, which enables the characterization of fluorinated drug substances even at notably low drug loadings. Besides, ^{19}F ssNMR has a high potential to be implemented as an automatic and high-throughput method for pharmaceutical analysis. Moreover, we foresee that many ^{19}F methods in the studies of NMR crystallography will be utilized to investigate the structure-function relationship of amorphous pharmaceuticals.

Declaration of competing interest

The authors declare that they have no known competing financial interests or personal relationships that could have appeared to influence the work reported in this paper.

Acknowledgments

Y. D. is grateful to MRL Postdoctoral Research Program.

References

[1] K.J. Bittorf, T. Sanghvi, J.P. Katstra, Design of solid dosage formulations, Chem. Eng. Pharm. Ind. (2019) 19–52, https://doi.org/10.1002/9781119600800.CH52.
[2] S.S. Bharate, R.A. Vishwakarma, Impact of preformulation on drug development, 10, http://doi.org/10.1517/17425247.2013.783563, 2013, 1239–1257.
[3] L.X. Yu, G. Amidon, M.A. Khan, S.W. Hoag, J. Polli, G.K. Raju, J. Woodcock, Understanding pharmaceutical quality by design, AAPS J. 16 (2014) 771–783, https://doi.org/10.1208/S12248-014-9598-3/TABLES/2.
[4] M. Kar, Y. Chourasiya, R. Maheshwari, R.K. Tekade, Current developments in excipient science: implication of quantitative selection of each excipient in product development, Basic Fundam. Drug Deliv. (2019) 29–83, https://doi.org/10.1016/B978-0-12-817909-3.00002-9.
[5] Q.T. Zhou, T. Li, Formulation and manufacturing of solid dosage forms, Pharm. Res. 2018 361 (36) (2018) 1–3, https://doi.org/10.1007/S11095-018-2547-6.
[6] M.P. Lodaya, Oral solid dosage forms, Martin's Phys. Pharm. Pharm. Sci. Phys. Chem. Biopharm. Princ. Pharm. Sci. Sixth Ed. (2011) 563–593, https://doi.org/10.1201/B14413-17/ORAL-SOLID-DOSAGE-FORMS-PETER-DAVIES.
[7] N.A. Meanwell, Improving drug candidates by design: a focus on physicochemical properties as a means of improving compound disposition and safety, Chem. Res. Toxicol. 24 (2011) 1420–1456, https://doi.org/10.1021/TX200211V.
[8] B.-J. Lee, Pharmaceutical preformulation: physicochemical properties of excipients and powders and tablet characterization, Pharm. Sci. Encycl. (2010) 1–54, https://doi.org/10.1002/9780470571224.PSE362.
[9] S. Lohani, H. Cooper, X. Jin, B.P. Nissley, K. Manser, L.H. Rakes, J.J. Cummings, S.E. Fauty, A. Bak, Physicochemical properties, form, and formulation selection strategy for a biopharmaceutical classification system class II preclinical drug candidate, J. Pharm. Sci. 103 (2014) 3007–3021, https://doi.org/10.1002/JPS.24088.
[10] A. Charalabidis, M. Sfouni, C. Bergström, P. Macheras, The Biopharmaceutics classification system (BCS) and the Biopharmaceutics drug disposition classification system (BDDCS): beyond guidelines, Int. J. Pharm. 566 (2019) 264–281, https://doi.org/10.1016/J.IJPHARM.2019.05.041.
[11] L.Z. Benet, Predicting drug disposition via application of a Biopharmaceutics drug disposition classification system, Basic Clin. Pharmacol. Toxicol. 106 (2010) 162–167, https://doi.org/10.1111/J.1742-7843.2009.00498.X.
[12] L. Yu, S.M. Reutzel, G.A. Stephenson, Physical characterization of polymorphic drugs: an integrated characterization strategy, Pharmaceut. Sci. Technol. Today 1 (1998) 118–127, https://doi.org/10.1016/S1461-5347(98)00031-5.
[13] H.G. Brittain, Effects of mechanical processing on phase composition, J. Pharm. Sci. 91 (2002) 1573–1580, https://doi.org/10.1002/JPS.10115.
[14] S.R. Vippagunta, H.G. Brittain, D.J.W. Grant, Crystalline solids, Adv. Drug Deliv. Rev. 48 (2001) 3–26, https://doi.org/10.1016/S0169-409X(01)00097-7.
[15] S.V. Bhujbal, B. Mitra, U. Jain, Y. Gong, A. Agrawal, S. Karki, L.S. Taylor, S. Kumar, Q. Tony, Zhou, Pharmaceutical amorphous solid dispersion: a review of manufacturing strategies, Acta Pharm. Sin. B. 11 (2021) 2505–2536, https://doi.org/10.1016/J.APSB.2021.05.014.

[16] X. Ma, R.O. Williams, Characterization of amorphous solid dispersions: an update, J. Drug Deliv. Sci. Technol. 50 (2019) 113–124, https://doi.org/10.1016/J.JDDST.2019.01.017.
[17] G. Van Den Mooter, The use of amorphous solid dispersions: a formulation strategy to overcome poor solubility and dissolution rate, Drug Discov. Today Technol. 9 (2012) e79–e85, https://doi.org/10.1016/J.DDTEC.2011.10.002.
[18] P. Pandi, R. Bulusu, N. Kommineni, W. Khan, M. Singh, Amorphous solid dispersions: an update for preparation, characterization, mechanism on bioavailability, stability, regulatory considerations and marketed products, Int. J. Pharm. 586 (2020) 119560, https://doi.org/10.1016/J.IJPHARM.2020.119560.
[19] P. Kanaujia, P. Poovizhi, W.K. Ng, R.B.H. Tan, Amorphous formulations for dissolution and bioavailability enhancement of poorly soluble APIs, Powder Technol. 285 (2015) 2–15, https://doi.org/10.1016/J.POWTEC.2015.05.012.
[20] M. Geppi, G. Mollica, S. Borsacchi, C.A. Veracini, Solid-state NMR studies of pharmaceutical systems, 202–302, http://doi.org/10.1080/05704920801944338. 43, 2008.
[21] S. Ram, K. Vaka, M. Bommana, D. Desai, J. Djordjevic, W. Phuapradit, N. Shah, Excipients for amorphous solid dispersions, 123–161, https://doi.org/10.1007/978-1-4939-1598-9_4, 2014.
[22] N. Mendonsa, B. Almutairy, V.R. Kallakunta, S. Sarabu, P. Thipsay, S. Bandari, M. A. Repka, Manufacturing strategies to develop amorphous solid dispersions: an overview, J. Drug Deliv. Sci. Technol. 55 (2020) 101459, https://doi.org/10.1016/J.JDDST.2019.101459.
[23] A.W. Newman, S.R. Byrn, Solid-state analysis of the active pharmaceutical ingredient in drug products, Drug Discov. Today 8 (2003) 898–905, https://doi.org/10.1016/S1359-6446(03)02832-0.
[24] D.E. Bugay, Characterization of the solid-state: spectroscopic techniques, Adv. Drug Deliv. Rev. 48 (2001) 43–65, https://doi.org/10.1016/S0169-409X(01)00101-6.
[25] E. Pindelska, A. Sokal, W. Kolodziejski, Pharmaceutical cocrystals, salts and polymorphs: advanced characterization techniques, Adv. Drug Deliv. Rev. 117 (2017) 111–146, https://doi.org/10.1016/J.ADDR.2017.09.014.
[26] M. Li, W. Xu, Y. Su, Solid-state NMR spectroscopy in pharmaceutical sciences, TrAC Trends Anal. Chem. (Reference Ed.) 135 (2021) 116152, https://doi.org/10.1016/j.trac.2020.116152.
[27] B. Reif, S.E. Ashbrook, L. Emsley, M. Hong, Solid-state NMR spectroscopy, Nat. Rev. Methods Prim. 2021 11 (1) (2021) 1–23, https://doi.org/10.1038/s43586-020-00002-1.
[28] F.G. Vogt, Evolution of solid-state NMR in pharmaceutical analysis, Http://Dx.Doi.Org/10.4155/Fmc.10.200. 2, 915–921, https://doi.org/10.4155/FMC.10.200, 2010.
[29] D.E. Bugay, Solid-state nuclear magnetic resonance spectroscopy: theory and pharmaceutical applications, Pharm. Res. 1993 103 (10) (1993) 317–327, https://doi.org/10.1023/A:1018967717781.
[30] P.A. Tishmack, D.E. Bugay, S.R. Byrn, Solid-state nuclear magnetic resonance spectroscopy-pharmaceutical applications, J. Pharm. Sci. 92 (2003) 441–474, https://doi.org/10.1002/JPS.10307.
[31] F. Ziarelli, S. Caldarelli, Solid-state NMR as an analytical tool: quantitative aspects, Solid State Nucl. Magn. Reson. 29 (2006) 214–218, https://doi.org/10.1016/J.SSNMR.2005.08.013.
[32] I. Wawer, qNMR in solid state, NMR spectrosc, Pharm. Anal. (2008) 63–82, https://doi.org/10.1016/B978-0-444-53173-5.00003-2.
[33] K. Schmidt-Rohr, J. Clauss, B. Blümich, H.W. Spiess, Miscibility of polymer blends investigated by 1H spin diffusion and 13C NMR detection, Magn. Reson. Chem. 28 (1990) S3–S9, https://doi.org/10.1002/MRC.1260281304.
[34] K. Sarpal, S. Delaney, G.G.Z. Zhang, E.J. Munson, Phase behavior of amorphous solid dispersions of felodipine: homogeneity and drug-polymer interactions, Mol. Pharm. 16 (2019) 4836–4851, https://doi.org/10.1021/ACS.MOLPHARMACEUT.9B00731.
[35] P. Duan, M.S. Lamm, F. Yang, W. Xu, D. Skomski, Y. Su, K. Schmidt-Rohr, Quantifying molecular mixing and heterogeneity in pharmaceutical dispersions at sub-100 nm resolution by spin diffusion NMR, Mol. Pharm. 17 (2020) 3567–3580, https://doi.org/10.1021/ACS.MOLPHARMACEUT.0C00592.
[36] C. Guo, M.P. Fritz, J. Struppe, S. Wegner, J. Stringer, I.V. Sergeyev, C.M. Quinn, A.M. Gronenborn, T. Polenova, Fast 19F magic angle spinning NMR crystallography for structural characterization of fluorine-containing pharmaceutical compounds, Anal. Chem. 93 (2021) 8210–8218, https://doi.org/10.1021/ACS.ANALCHEM.1C00784.
[37] J.T. Gerig, Fluorine NMR. https://www.princess-day.com/Portals/0/BPSAssets/Articles/gerig.pdf, 2001. May 15th, 2022.
[38] Y.G. Gakh, A.A. Gakh, A.M. Gronenborn, Fluorine as an NMR probe for structural studies of chemical and biological systems †, Magn. Reson. Chem. Magn. Reson. Chem. 38 (2000) 551–558, https://doi.org/10.1002/1097-458X.
[39] J. Wang, M. Sánchez-Roselló, J.L. Aceña, C. Del Pozo, A.E. Sorochinsky, S. Fustero, V.A. Soloshonok, H. Liu, Fluorine in pharmaceutical industry: fluorine-containing drugs introduced to the market in the last decade (2001–2011), Chem. Rev. 114 (2013) 2432–2506, https://doi.org/10.1021/CR4002879.
[40] Y. Zhou, J. Wang, Z. Gu, S. Wang, W. Zhu, J.L. Aceña, V.A. Soloshonok, K. Izawa, H. Liu, Next generation of fluorine-containing pharmaceuticals, compounds currently in phase II–III clinical trials of major pharmaceutical companies: new structural trends and therapeutic areas, Chem. Rev. 116 (2016) 422–518, https://doi.org/10.1021/ACS.CHEMREV.5B00392.
[41] O. Chen, K. Schmidt-Rohr, Backbone dynamics of the nafion ionomer studied by 19F-13C solid-state NMR, Macromol. Chem. Phys. 208 (2007) 2189–2203, https://doi.org/10.1002/MACP.200700200.
[42] P.K. Mikhailiuk, S. Afonin, A.N. Chernega, E.B. Rusanov, M.O. Platonov, G. G. Dubinina, M. Berditsch, A.S. Ulrich, I.V. Komarov, Conformationally rigid trifluoromethyl-substituted α-amino acid designed for peptide structure analysis by solid-state 19F NMR spectroscopy, Angew. Chem. Int. Ed. 45 (2006) 5659–5661, https://doi.org/10.1002/ANIE.200600346.
[43] A.M. Gronenborn, Small, but powerful and attractive: 19F in biomolecular NMR, Structure 30 (2022) 6–14, https://doi.org/10.1016/J.STR.2021.09.009.
[44] Q. Chen, K. Schmidt-Rohr, 13C NMR signal assignment and analysis in a perfluorinated ionomer (nafion) by two-dimensional solid-state NMR, Macromolecules 37 (2004) 5995–6003, https://doi.org/10.1021/MA049759B, 19F.
[45] W. Luo, R. Mani, M. Hong, Side-chain conformation of the M2 transmembrane peptide proton channel of influenza a virus from19F solid-state NMR, J. Phys. Chem. B. 111 (2007) 10825–10832, https://doi.org/10.1021/JP073823K.
[46] S. Wi, N. Sinha, M. Hong, Long-range 1H-19F distance measurement in peptides by solid-state NMR, J. Am. Chem. Soc. 126 (2004) 12754–12755, https://doi.org/10.1021/JA0462732.
[47] R.M. Wenslow, 19F solid-state NMR spectroscopic investigation of crystalline and amorphous forms of a selective muscarinic M3 receptor antagonist, in: Both Bulk and Pharmaceutical Dosage Form Samples, 2002, pp. 555–561, https://doi.org/10.1081/DDC-120003451. 28.
[48] P. Shah, A.D. Westwell, The role of fluorine in medicinal chemistry, Http://Dx.Doi.Org/10.1080/14756360701425014, 527–540, https://doi.org/10.1080/14756360701425014, 2008, 22.
[49] D. O'Hagan, Fluorine in health care: organofluorine containing blockbuster drugs, J. Fluor. Chem. 131 (2010) 1071–1081, https://doi.org/10.1016/J.JFLUCHEM.2010.03.003.
[50] W.D. Wang, X. Gao, M. Strohmeier, W. Wang, S. Bai, C. Dybowski, Solid-state NMR studies of form I of atorvastatin calcium, J. Phys. Chem. B. 116 (2012) 3641–3649, https://doi.org/10.1021/JP212074A.
[51] J. Brus, M. Urbanova, I. Sedenkova, H. Brusova, New perspectives of 19F MAS NMR in the characterization of amorphous forms of atorvastatin in dosage formulations, Int. J. Pharm. 409 (2011) 62–74, https://doi.org/10.1016/J.IJPHARM.2011.02.030.
[52] C.M. Quinn, R. Zadorozhnyi, J. Struppe, I.V. Sergeyev, A.M. Gronenborn, T. Polenova, Fast19F magic-angle spinning nuclear magnetic resonance for the structural characterization of active pharmaceutical ingredients in blockbuster drugs, Anal. Chem. 93 (2021) 13029–13037, https://doi.org/10.1021/ACS.ANALCHEM.1C02917.
[53] T.W. Jarrells, D. Zhang, S. Li, E.J. Munson, Quantification of monomer units in insoluble polymeric active pharmaceutical ingredients using solid-state NMR spectroscopy I: patiromer, AAPS PharmSciTech 213 (21) (2020) 1–14, https://doi.org/10.1208/S12249-020-01654-8, 2020.
[54] E.F. Connor, I. Lees, D. Maclean, Polymers as drugs—advances in therapeutic applications of polymer binding agents, J. Polym. Sci. Part A Polym. Chem. 55 (2017) 3146–3157, https://doi.org/10.1002/POLA.28703.
[55] G. Pilcer, K. Amighi, Formulation strategy and use of excipients in pulmonary drug delivery, Int. J. Pharm. 392 (2010) 1–19, https://doi.org/10.1016/J.IJPHARM.2010.03.017.
[56] G. Muehllehner, J.S. Karp, Positron emission tomography, Phys. Med. Biol. 51 (2006) R117, https://doi.org/10.1088/0031-9155/51/13/R08.
[57] D.W. Townsend, Positron emission tomography/computed tomography, Semin. Nucl. Med. 38 (2008) 152–166, https://doi.org/10.1053/J.SEMNUCLMED.2008.01.003.
[58] M.E. Phelps, Positron emission tomography provides molecular imaging of biological processes, Proc. Natl. Acad. Sci. Unit. States Am. 97 (2000) 9226–9233, https://doi.org/10.1073/PNAS.97.16.9226.
[59] H.T. Chugani, M.E. Phelps, J.C. Mazziotta, Positron emission tomography study of human brain functional development, Ann. Neurol. 22 (1987) 487–497, https://doi.org/10.1002/ANA.410220408.
[60] S. Pauls, A.K. Buck, K. Hohl, G. Halter, M. Hetzel, N.M. Blumstein, F.M. Mottaghy, G. Glatting, S. Krüger, L. Sunder-Plassmann, P. Möller, V. Hombach, H.J. Brambs, S.N. Reske, Improved non-invasive T-Staging in non-small cell lung cancer by integrated 18F-FDG PET/CT, Nuklearmedizin 46 (2007) 9–14, https://doi.org/10.1055/S-0037-1616618/ID/JR6618-29.
[61] K. Anand, M. Sabbagh, Amyloid imaging: poised for integration into medical practice, Neurotherapeutics 14 (2017) 54, https://doi.org/10.1007/S13311-016-0474-Y.
[62] F.M. Bengel, T. Higuchi, M.S. Javadi, R. Lautamäki, Cardiac positron emission tomography, J. Am. Coll. Cardiol. 54 (2009) 1–15, https://doi.org/10.1016/J.JACC.2009.02.065.
[63] C.M. Clark, J.A. Schneider, B.J. Bedell, T.G. Beach, W.B. Bilker, M.A. Mintun, M. J. Pontecorvo, F. Hefti, A.P. Carpenter, M.L. Flitter, M.J. Krautkramer, H.F. Kung, R.E. Coleman, P.M. Doraiswamy, A.S. Fleisher, M.N. Sabbagh, C.H. Sadowsky, P. E.M. Reiman, S.P. Zehntner, D.M. Skovronsky, Use of florbetapir-PET for imaging β-amyloid pathology, JAMA 305 (2011) 275–283, https://doi.org/10.1001/JAMA.2010.2008.
[64] B. Kratochvíl, Solid forms of pharmaceutical molecules, 129–140, https://doi.org/10.1007/978-90-481-2882-2_8, 2011.
[65] S.X. Yin, J.A. Grosso, Selecting and controlling API crystal form for pharmaceutical development–strategies and processes, Curr. Opin. Drug Discov. Dev 11 (2008) 771–777. https://europepmc.org/article/med/18946842. March 4th, 2022.
[66] M.Y. Gokhale, R.V. Mantri, API solid-form screening and selection, Dev. Solid Oral Dos. Forms Pharm. Theory Pract (2017) 85–112, https://doi.org/10.1016/B978-0-12-802447-8.00004-2. Second Ed.

[67] Y.S. Jin, J. Ulrich, New crystalline solvates of atorvastatin calcium, Chem. Eng. Technol. 33 (2010) 839–844, https://doi.org/10.1002/CEAT.200900571.
[68] A.M. Healy, Z.A. Worku, D. Kumar, A.M. Madi, Pharmaceutical solvates, hydrates and amorphous forms: a special emphasis on cocrystals, Adv. Drug Deliv. Rev. 117 (2017) 25–46, https://doi.org/10.1016/J.ADDR.2017.03.002.
[69] H.G. Brittain, D.J.R. Grant, P.B. Myrdal, Effects of polymorphism and solid-state solvation on solubility and dissolution rate, Polymorph. Pharm. Solids (2016) 436–480, https://doi.org/10.3109/9781420073225-15/Effects-Polymorphism-Solid-State-Solvation-Solubility-Dissolution-Rate-Harry-Brittain-David-Grant-Paul-Myrdal, second ed.
[70] R. Censi, P. Di Martino, Polymorph impact on the bioavailability and stability of poorly soluble drugs, Molecules 20 (2015) 18759, https://doi.org/10.3390/MOLECULES201018759.
[71] X. Lu, D. Skomski, K.C. Thompson, M.J. McNevin, W. Xu, Y. Su, Three-dimensional NMR spectroscopy of fluorinated pharmaceutical solids under ultrafast magic angle spinning, Anal. Chem. 91 (2019) 6217–6224, https://doi.org/10.1021/acs.analchem.9b00884.
[72] G.G.Z. Zhang, D. Law, E.A. Schmitt, Y. Qiu, Phase transformation considerations during process development and manufacture of solid oral dosage forms, Adv. Drug Deliv. Rev. 56 (2004) 371–390, https://doi.org/10.1016/J.ADDR.2003.10.009.
[73] S. Thakral, R. Govindarajan, R. Suryanarayanan, Processing-induced phase transformations and their implications on pharmaceutical product quality, Polymorph. Pharm. Ind. (2018) 329–380, https://doi.org/10.1002/9783527697847.CH12.
[74] A.Y. Lee, D. Erdemir, A.S. Myerson, Crystal polymorphism in chemical process development. http://doi.org/10.1146/Annurev-Chembioeng-061010-114224. 2, 2011, 259-280.
[75] A.J. Cruz-Cabeza, J. Bernstein, Conformational polymorphism, Chem. Rev. 114 (2013) 2170–2191, https://doi.org/10.1021/CR400249D.
[76] J. Bauer, S. Spanton, R. Henry, J. Quick, W. Dziki, W. Porter, J. Morris, Ritonavir, An extraordinary example of conformational polymorphism, Pharm. Res. (N. Y.) 186 (18) (2001) 859–866, https://doi.org/10.1023/A:1011052932607, 2001.
[77] S.R. Chemburkar, J. Bauer, K. Deming, H. Spiwek, K. Patel, J. Morris, R. Henry, S. Spanton, W. Dziki, W. Porter, J. Quick, P. Bauer, J. Donaubauer, B. A. Narayanan, M. Soldani, D. Riley, K. McFarland, Dealing with the impact of Ritonavir polymorphs on the late stages of bulk drug process development, Org. Process Res. Dev. 4 (2000) 413–417, https://doi.org/10.1021/OP000023Y.
[78] D. Skomski, R.J. Varsolona, Y. Su, J. Zhang, R. Teller, S.P. Forster, S.E. Barrett, W. Xu, Islatravir case study for enhanced screening of thermodynamically stable crystalline anhydrate phases in pharmaceutical process development by hot melt extrusion, Mol. Pharm. 17 (2020) 2874–2881, https://doi.org/10.1021/ACS.MOLPHARMACEUT.0C00316.
[79] D. Skomski, Y. Su, W. Xu, M. Cubrovic, Novel Crystalline Forms of an Nrtti Compound, vol. 20220056067, 2019.
[80] D.E. Moseson, A. Eren, K.J. Altman, I.D. Corum, M. Li, Y. Su, Z.K. Nagy, L. S. Taylor, Optimization of amorphization kinetics during hot melt extrusion by particle engineering: an experimental and computational study, Cryst. Growth Des. 22 (2022) 821–841, https://doi.org/10.1021/ACS.CGD.1C01306.
[81] C. Correa-Soto, N.S. Trasi, P.D. Schmitt, Y. Su, Z. Liu, E. Miller, N. Variankaval, P. J. Marsac, G.J. Simpson, L.S. Taylor, Second harmonic generation microscopy as a tool for the early detection of crystallization in spray dried dispersions, J. Pharm. Biomed. Anal. 146 (2017) 86–95, https://doi.org/10.1016/J.JPBA.2017.07.066.
[82] C. Huang, G. Klinzing, A. Procopio, F. Yang, J. Ren, R. Burlage, L. Zhu, Y. Su, Understanding compression-induced amorphization of crystalline posaconazole, Mol. Pharm. 16 (2018) 825–833, https://doi.org/10.1021/ACS.MOLPHARMACEUT.8B01122.
[83] D.A. Davis, D.A. Miller, S. Santitewagun, J.A. Zeitler, Y. Su, R.O. Williams, Formulating a heat- and shear-labile drug in an amorphous solid dispersion: balancing drug degradation and crystallinity, Int. J. Pharm. X. 3 (2021) 100092, https://doi.org/10.1016/J.IJPX.2021.100092.
[84] M. Urbanova, J. Brus, I. Sedenkova, O. Policianova, L. Kobera, Characterization of solid polymer dispersions of active pharmaceutical ingredients by 19F MAS NMR and factor analysis, Spectrochim. Acta Part A Mol. Biomol. Spectrosc. 100 (2013) 59–66, https://doi.org/10.1016/J.SAA.2012.02.057.
[85] K. Paradowska, I. Wawer, Solid-state NMR in the analysis of drugs and naturally occurring materials, J. Pharm. Biomed. Anal. 93 (2014) 27–42, https://doi.org/10.1016/J.JPBA.2013.09.032.
[86] R.T. Berendt, D.M. Sperger, E.J. Munson, P.K. Isbester, Solid-state NMR spectroscopy in pharmaceutical research and analysis, TrAC Trends Anal. Chem. (Reference Ed.) 25 (2006) 977–984, https://doi.org/10.1016/J.TRAC.2006.07.006.
[87] Z. Rahman, A. Mohammad, S. Akhtar, A. Siddiqui, M. Korang-Yeboah, M.A. Khan, Chemometric model development and comparison of Raman and 13C solid-state nuclear magnetic resonance–chemometric methods for quantification of crystalline/amorphous warfarin sodium fraction in the formulations, J. Pharm. Sci. 104 (2015) 2550–2558, https://doi.org/10.1002/JPS.24524.
[88] B.T. Farrer, A. Peresypkin, R.M. Wenslow, Quantitation of crystalline material within a liquid vehicle using 1H/19F CP/MAS NMR, J. Pharm. Sci. 96 (2007) 264–267, https://doi.org/10.1002/JPS.20759.
[89] M. Asada, T. Nemoto, H. Mimura, K. Sako, Advanced new relaxation filter-selective signal excitation methods for 13C solid-state nuclear magnetic resonance, Anal. Chem. 86 (2014) 10091–10098, https://doi.org/10.1021/AC501367J.
[90] M.N. Asada, T. Nemoto, H. Mimura, Pharmaceutical applications of relaxation filter-selective signal excitation methods for 19F solid-state nuclear magnetic resonance: case study with atorvastatin in dosage formulation, J. Pharm. Sci. 105 (2016) 1233–1238, https://doi.org/10.1016/J.XPHS.2015.12.023.
[91] J. Liu, K. Nagapudi, Y.-H. Kiang, E. Martinez, J. Jona, Quantification of compaction-induced crystallinity reduction of a pharmaceutical solid using 19F solid-state NMR and powder X-ray diffraction, 969–975, http://doi.org/10.1080/03639040902729424. 35, 2009.
[92] K. Héberger, Chemoinformatics—multivariate mathematical–statistical methods for data evaluation, Med. Appl. Mass Spectrom. (2008) 141–169, https://doi.org/10.1016/B978-044451980-1.50009-4.
[93] J. Djuris, S. Ibric, Z. Djuric, Chemometric methods application in pharmaceutical products and processes analysis and control, Comput. Appl. Pharm. Technol. (2013) 57–90, https://doi.org/10.1533/9781908818324.57.
[94] P. Ebrahimi, N. Viereck, R. Bro, S.B. Engelsen, Chemometric analysis of NMR spectra, Mod. Magn. Reson. (2017) 1–20, https://doi.org/10.1007/978-3-319-28275-6_20-1.
[95] S.J. Barry, T.N. Pham, P.J. Borman, A.J. Edwards, S.A. Watson, A risk-based statistical investigation of the quantification of polymorphic purity of a pharmaceutical candidate by solid-state 19F NMR, Anal. Chim. Acta 712 (2012) 30–36, https://doi.org/10.1016/J.ACA.2011.10.064.
[96] Y. Guo, E. Shalaev, S. Smith, Physical stability of pharmaceutical formulations: solid-state characterization of amorphous dispersions, TrAC Trends Anal. Chem. (Reference Ed.) 49 (2013) 137–144, https://doi.org/10.1016/J.TRAC.2013.06.002.
[97] A. Heinz, C.J. Strachan, K.C. Gordon, T. Rades, Analysis of solid-state transformations of pharmaceutical compounds using vibrational spectroscopy, J. Pharm. Pharmacol. 61 (2010) 971–988, https://doi.org/10.1211/JPP.61.08.0001.
[98] C. Petzoldt, O. Bley, S.J. Byard, D. Andert, B. Baumgartner, N. Nagel, C. Tappertzhofen, M.P. Feth, An example of how to handle amorphous fractions in API during early pharmaceutical development: SAR114137 – a successful approach, Eur. J. Pharm. Biopharm. 86 (2014) 337–350, https://doi.org/10.1016/J.EJPB.2013.09.015.
[99] J. Liu, D.R. Rigsbee, C. Stotz, M.J. Pikal, Dynamics of pharmaceutical amorphous solids: the study of enthalpy relaxation by isothermal microcalorimetry, J. Pharm. Sci. 91 (2002) 1853–1862, https://doi.org/10.1002/JPS.10181.
[100] S.V. Jermain, C. Brough, R.O. Williams, Amorphous solid dispersions and nanocrystal technologies for poorly water-soluble drug delivery – an update, Int. J. Pharm. 535 (2018) 379–392, https://doi.org/10.1016/J.IJPHARM.2017.10.051.
[101] A.M. Abdul-Fattah, V. Truong-Le, L. Yee, L. Nguyen, D.S. Kalonia, M.T. Cicerone, M.J. Pikal, Drying-induced variations in physico-chemical properties of amorphous pharmaceuticals and their impact on stability (I): stability of a monoclonal antibody, J. Pharm. Sci. 96 (2007) 1983–2008, https://doi.org/10.1002/JPS.20859.
[102] S. Wairkar, R. Gaud, Co-amorphous combination of nateglinide-metformin hydrochloride for dissolution enhancement, AAPS PharmSciTech 17 (2016) 673–681, https://doi.org/10.1208/S12249-015-0371-4.
[103] J.F. Willart, M. Descamps, Solid state amorphization of pharmaceuticals, Mol. Pharm. 5 (2008) 905–920, https://doi.org/10.1021/MP800092T.
[104] A. Johansson, J. Tegenfeldt, NMR study of crystalline and amorphous poly (ethylene oxide), Macromolecules 25 (2002) 4712–4715, https://doi.org/10.1021/MA00044A036.
[105] T.N. Pham, S.A. Watson, A.J. Edwards, M. Chavda, J.S. Clawson, M. Strohmeier, F.G. Vogt, Analysis of amorphous solid dispersions using 2D solid-state NMR and 1H T1 relaxation measurements, Mol. Pharm. 7 (2010) 1667–1691, https://doi.org/10.1021/MP100205G.
[106] X. Yuan, D. Sperger, E.J. Munson, Investigating miscibility and molecular mobility of nifedipine-PVP amorphous solid dispersions using solid-state NMR spectroscopy, Mol. Pharm. 11 (2013) 329–337, https://doi.org/10.1021/MP400498N.
[107] J.W. Lubach, D. Xu, B.E. Segmuller, E.J. Munson, Investigation of the effects of pharmaceutical processing upon solid-state NMR relaxation times and implications to solid-state formulation stability, J. Pharm. Sci. 96 (2007) 777–787, https://doi.org/10.1002/JPS.20684.
[108] T.J. Offerdahl, J.S. Salsbury, Z. Dong, D.J.W. Grant, S.A. Schroeder, I. Prakash, E. M. Gorman, D.H. Barich, E.J. Munson, Quantitation of crystalline and amorphous forms of anhydrous neotame using 13C CPMAS NMR spectroscopy, J. Pharm. Sci. 94 (2005) 2591–2605, https://doi.org/10.1002/JPS.20469.
[109] Y. Du, P. Phyo, M. Li, B. Sorman, M. McNevin, W. Xu, Y. Liu, Y. Su, Quantifying Micromolar Crystallinity in Pharmaceutical Materials Utilizing 19F Solid-State NMR, (in press).
[110] T.N. Pham, C.J. Day, A.J. Edwards, H.R. Wood, I.R. Lynch, S.A. Watson, A.S. Z. Bretonnet, F.G. Vogt, Detection of low-level PTFE contamination: an application of solid-state NMR to structure elucidation in the pharmaceutical industry, J. Pharm. Biomed. Anal. 54 (2011) 401–405, https://doi.org/10.1016/J.JPBA.2010.08.027.
[111] D. Stueber, S. Jehle, Quantitative component analysis of solid mixtures by analyzing time domain 1H and 19F T1 saturation recovery curves (qSRC), J. Pharm. Sci. 106 (2017) 1828–1838, https://doi.org/10.1016/J.XPHS.2017.03.034.
[112] A.D. Bond, Single-crystal X-ray diffraction, 315–337, https://doi.org/10.1007/978-1-4939-4029-5_9, 2016.
[113] A.L. Albright, J.M. White, Determination of absolute configuration using single crystal X-ray diffraction, Methods Mol. Biol. 1055 (2013) 149–162, https://doi.org/10.1007/978-1-62703-577-4_11.

[114] C. Martineau, J. Senker, F. Taulelle, NMR crystallography, Annu. Rep. NMR Spectrosc. 82 (2014) 1–57, https://doi.org/10.1016/B978-0-12-800184-4.00001-1.
[115] E. Skorupska, A. Jeziorna, S. Kazmierski, M.J. Potrzebowski, Recent progress in solid-state NMR studies of drugs confined within drug delivery systems, Solid State Nucl. Magn. Reson. 57–58 (2014) 2–16, https://doi.org/10.1016/J.SSNMR.2013.12.001.
[116] J.A. Ripmeester, R.E. Wasylishen, NMR crystallography, CrystEngComm 15 (2013) 8598, https://doi.org/10.1039/C3CE90151C.
[117] P. Hodgkinson, NMR crystallography of molecular organics, Prog. Nucl. Magn. Reson. Spectrosc. 118–119 (2020) 10–53, https://doi.org/10.1016/J.PNMRS.2020.03.001.
[118] E. Salager, G.M. Day, R.S. Stein, C.J. Pickard, B. Elena, L. Emsley, Powder crystallography by combined crystal structure prediction and high-resolution1H solid-state NMR spectroscopy, J. Am. Chem. Soc. 132 (2010) 2564–2566, https://doi.org/10.1021/JA909449K/SUPPL_FILE/JA909449K_SI_002.CIF.
[119] E. Salager, R.S. Stein, C.J. Pickard, B. Elena, L. Emsley, Powder NMR crystallography of thymol, Phys. Chem. Chem. Phys. 11 (2009) 2610–2621, https://doi.org/10.1039/B821018G.
[120] J.A. Fernandes, M. Sardo, L. Mafra, D. Choquesillo-Lazarte, N. Masciocchi, X-ray and NMR crystallography studies of novel theophylline cocrystals prepared by liquid assisted grinding, Cryst. Growth Des. 15 (2015) 3674–3683, https://doi.org/10.1021/ACS.CGD.5B00279.
[121] M. Baias, J.N. Dumez, P.H. Svensson, S. Schantz, G.M. Day, L. Emsley, De novo determination of the crystal structure of a large drug molecule by crystal structure prediction-based powder NMR crystallography, J. Am. Chem. Soc. 135 (2013) 17501–17507, https://doi.org/10.1021/JA4088874.
[122] D. Luedeker, R. Gossmann, K. Langer, G. Brunklaus, Crystal engineering of pharmaceutical Co-crystals: "nMR crystallography" of niclosamide Co-crystals, Cryst. Growth Des. 16 (2016) 3087–3100, https://doi.org/10.1021/ACS.CGD.5B01619.
[123] A.A. Shcherbakov, J. Medeiros-Silva, N. Tran, M.D. Gelenter, M. Hong, From angstroms to nanometers: measuring interatomic distances by solid-state NMR, Chem. Rev. (2021), https://doi.org/10.1021/ACS.CHEMREV.1C00662 acs.chemrev.1c00662.
[124] M. Fritz, J. Kraus, C.M. Quinn, G.P.A. Yap, J. Struppe, I.V. Sergeyev, A. M. Gronenborn, T. Polenova, Measurement of accurate interfluorine distances in crystalline organic solis: a high-frequency magic angle spinning NMR approach, J. Phys. Chem. B. 123 (2019) 10680–10690, https://doi.org/10.1021/ACS.JPCB.9B08919.
[125] G. De Pape, Dipolar recoupling in magic angle spinning solid-state nuclear magnetic resonance, Http://Dx.Doi.Org/10.1146/Annurev-Physchem-032511-143726. 63, 661–684, https://doi.org/10.1146/ANNUREV-PHYSCHEM-032511-143726, 2012.
[126] Y. Ji, L. Liang, X. Bao, G. Hou, Recent progress in dipolar recoupling techniques under fast MAS in solid-state NMR spectroscopy, Solid State Nucl. Magn. Reson. 112 (2021) 101711, https://doi.org/10.1016/J.SSNMR.2020.101711.
[127] R.G. Griffin, Dipolar recoupling in MAS spectra of biological solids, Nat. Struct. Biol. 57 (5) (1998) 508–512, https://doi.org/10.1038/749, 1998.
[128] M. Roos, V.S. Mandala, M. Hong, Determination of long-range distances by fast magic-angle-spinning radiofrequency-driven 19F-19F dipolar recoupling NMR, J. Phys. Chem. B. 122 (2018) 9302–9313, https://doi.org/10.1021/ACS.JPCB.8B06878/SUPPL_FILE/JP8B06878_SI_001.PDF.
[129] A.E. Bennett, C.M. Rienstra, J.M. Griffiths, W. Zhen, P.T. Lansbury, R.G. Griffin, Homonuclear radio frequency-driven recoupling in rotating solids, J. Chem. Phys. 108 (1998) 9463, https://doi.org/10.1063/1.476420.
[130] E. Nimerovsky, K. Xue, K.T. Movellan, L.B. Andreas, Heteronuclear and homonuclear radio-frequency-driven recoupling, Magnes. Res. 2 (2021) 343–353, https://doi.org/10.5194/MR-2-343-2021.
[131] T. Gullion, Introduction to rotational-echo, Double Reson. NMR 10 (1998) 277289, https://doi.org/10.1002/(SICI)1099-0534, 10:5, 1998.
[132] T. Gullion, Rotational-echo, double-resonance NMR, Mod. Magn. Reson. (2008) 713–718, https://doi.org/10.1007/1-4020-3910-7_89.
[133] M.L. Gilchrist, K. Monde, Y. Tomita, T. Iwashita, K. Nakanishi, A.E. McDermott, Measurement of interfluorine distances in solids, J. Magn. Reson. 152 (2001) 1–6, https://doi.org/10.1006/JMRE.2001.2351.
[134] M. Roos, T. Wang, A.A. Shcherbakov, M. Hong, Fast magic-angle-spinning 19F spin exchange NMR for determining nanometer 19F–19F distances in proteins and pharmaceutical compounds, J. Phys. Chem. B. 122 (2018) 2900–2911, https://doi.org/10.1021/ACS.JPCB.8B00310.
[135] O.B. Peersen, S. Yoshimura, H. Hojo, S. Aimoto, S.O. Smith, Rotational resonance NMR measurements of internuclear distances in an α-helical peptide, J. Am. Chem. Soc. 114 (1992) 4332–4335, https://doi.org/10.1021/JA00037A044.
[136] V.S. Mandala, M.J. McKay, A.A. Shcherbakov, A.J. Dregni, A. Kolocouris, M. Hong, Structure and drug binding of the SARS-CoV-2 envelope protein transmembrane domain in lipid bilayers, Nat. Struct. Mol. Biol. 2712 (27) (2020) 1202–1208, https://doi.org/10.1038/s41594-020-00536-8, 2020.
[137] F.G. Vogt, G.R. Williams, M. Strohmeier, M.N. Johnson, R.C.B. Copley, Solid-state NMR analysis of a complex crystalline phase of ronacaleret hydrochloride, J. Phys. Chem. B. 118 (2014) 10266–10284, https://doi.org/10.1021/JP505061J.
[138] P. Mistry, R. Suryanarayanan, Strength of drug-polymer interactions: implications for crystallization in dispersions, Cryst. Growth Des. 16 (2016) 5141–5149, https://doi.org/10.1021/ACS.CGD.6B00714.
[139] P. Gupta, R. Thilagavathi, A.K. Chakraborti, A.K. Bansal, Role of molecular interaction in stability of Celecoxib−PVP amorphous systems, Mol. Pharm. 2 (2005) 384–391, https://doi.org/10.1021/MP050004G.
[140] K. Kothari, V. Ragoonanan, R. Suryanarayanan, The role of drug-polymer hydrogen bonding interactions on the molecular mobility and physical stability of nifedipine solid dispersions, Mol. Pharm. 12 (2015) 162–170, https://doi.org/10.1021/MP5005146.
[141] L.A.E. Batista De Carvalho, M.P.M. Marques, J. Tomkinson, Drug–excipient interactions in ketoprofen: a vibrational spectroscopy study, Biopolymers 82 (2006) 420–424, https://doi.org/10.1002/BIP.20517.
[142] A. Heinz, C.J. Strachan, K.C. Gordon, T. Rades, Analysis of solid-state transformations of pharmaceutical compounds using vibrational spectroscopy, J. Pharm. Pharmacol. 61 (2010) 971–988, https://doi.org/10.1211/JPP.61.08.0001.
[143] G.L.B. De Araujo, C.J. Benmore, S.R. Byrn, Local structure of ion pair interaction in lapatinib amorphous dispersions characterized by synchrotron X-ray diffraction and pair distribution function analysis, Sci. Reports 2017 71 (7) (2017) 1–10, https://doi.org/10.1038/srep46367.
[144] L. Mafra, S.M. Santos, R. Siegel, I. Alves, F.A. Almeida Paz, D. Dudenko, H. W. Spiess, Packing interactions in hydrated and anhydrous forms of the antibiotic ciprofloxacin: a solid-state NMR, X-ray diffraction, and computer simulation study, J. Am. Chem. Soc. 134 (2012) 71–74, https://doi.org/10.1021/JA208647N.
[145] V.D.N. Bezzon, F.F. Ferreira, P. Smith, C.J. Benmore, S.R. Byrn, G.L.B. de Araujo, Amorphous dispersions of flubendazole in hydroxypropyl methylcellulose: formulation stability assisted by pair distribution function analysis, Int. J. Pharm. 600 (2021) 120500, https://doi.org/10.1016/J.IJPHARM.2021.120500.
[146] X. Lu, C. Huang, M.B. Lowinger, F. Yang, W. Xu, C.D. Brown, D. Hesk, A. Koynov, L. Schenck, Y. Su, Molecular interactions in posaconazole amorphous solid dispersions from two-dimensional solid-state NMR spectroscopy, Mol. Pharm. 16 (2019) 2579–2589, https://doi.org/10.1021/ACS.MOLPHARMACEUT.9B00174.
[147] M. Zilka, S. Sturniolo, S.P. Brown, J.R. Yates, Visualising crystal packing interactions in solid-state NMR: concepts and applications, J. Chem. Phys. 147 (2017) 144203, https://doi.org/10.1063/1.4996750.
[148] P.M.J. Szell, J.R. Lewandowski, Helen Blade, L.P. Hughes, S.O.N. Lill, S.P. Brown, Taming the dynamics in a pharmaceutical by cocrystallization: investigating the impact of the coformer by solid-state NMR, CrystEngComm 23 (2021) 6859–6870, https://doi.org/10.1039/D1CE01084K.
[149] X. Lu, C. Huang, M. Li, D. Skomski, W. Xu, L. Yu, S.R. Byrn, A.C. Templeton, Y. Su, Molecular mechanism of crystalline-to-amorphous conversion of pharmaceutical solids from 19F magic angle spinning NMR, J. Phys. Chem. B. 124 (2020) 5271–5283, https://doi.org/10.1021/acs.jpcb.0c02131.
[150] P. Kafle, R. Sanghavi, A. Khasbaatar, S. Punjani, D.W. Davies, Y. Diao, Drastic modulation of molecular packing and intrinsic dissolution rates by meniscus-guided coating of extremely confined pharmaceutical thin films, ACS Appl. Mater. Interfaces. 13 (2021) 56519–56529, https://doi.org/10.1021/ACSAMI.1C08398.
[151] L. Jia, S. Zhang, W. Yang, Y. Bao, B. Hou, L. Zhou, Q. Yin, Insights into intermolecular interactions of spironolactone solvates, Cryst. Growth Des. 21 (2021) 3677–3688, https://doi.org/10.1021/ACS.CGD.0C01654.
[152] X. Lu, M. Li, C. Huang, M.B. Lowinger, W. Xu, L. Yu, S.R. Byrn, A.C. Templeton, Y. Su, Atomic-level drug substance and polymer interaction in posaconazole amorphous solid dispersion from solid-state NMR, Mol. Pharm. 17 (2020) 2585–2598, https://doi.org/10.1021/acs.molpharmaceut.0c00268.
[153] E.M. Gorman, B. Samas, E.J. Munson, Understanding the dehydration of levofloxacin hemihydrate, J. Pharm. Sci. 101 (2012) 3319–3330, https://doi.org/10.1002/JPS.23200.
[154] S. Dedroog, T. Pas, B. Vergauwen, C. Huygens, G. Van den Mooter, Solid-state analysis of amorphous solid dispersions: why DSC and XRPD may not be regarded as stand-alone techniques, J. Pharm. Biomed. Anal. 178 (2020) 112937, https://doi.org/10.1016/J.JPBA.2019.112937.
[155] S. Dedroog, C. Huygens, G. Van den Mooter, Chemically identical but physically different: a comparison of spray drying, hot melt extrusion and cryo-milling for the formulation of high drug loaded amorphous solid dispersions of naproxen, Eur. J. Pharm. Biopharm. 135 (2019) 1–12, https://doi.org/10.1016/J.EJPB.2018.12.002.
[156] V. Sihorkar, T. Dürig, The role of polymers and excipients in developing amorphous solid dispersions: an industrial perspective, Drug Deliv. Asp. (2020) 79–113, https://doi.org/10.1016/B978-0-12-821222-6.00005-1.
[157] C. Que, X. Lou, D.Y. Zemlyanov, H. Mo, A.S. Indulkar, Y. Gao, G.G.Z. Zhang, L. S. Taylor, Insights into the dissolution behavior of ledipasvir-copovidone amorphous solid dispersions: role of drug loading and intermolecular interactions, Mol. Pharm. 16 (2019) 5054–5067, https://doi.org/10.1021/ACS.MOLPHARMACEUT.9B01025.
[158] S. Saboo, U.S. Kestur, D.P. Flaherty, L.S. Taylor, Congruent release of drug and polymer from amorphous solid dispersions: insights into the role of drug-polymer hydrogen bonding, surface crystallization, and glass transition, Mol. Pharm. 17 (2020) 1261–1275, https://doi.org/10.1021/ACS.MOLPHARMACEUT.9B01272.
[159] P. Mistry, S. Mohapatra, T. Gopinath, F.G. Vogt, R. Suryanarayanan, Role of the strength of drug-polymer interactions on the molecular mobility and crystallization inhibition in ketoconazole solid dispersions, Mol. Pharm. 12 (2015) 3339–3350, https://doi.org/10.1021/ACS.MOLPHARMACEUT.5B00333.
[160] H. Nie, Y. Su, M. Zhang, Y. Song, A. Leone, L.S. Taylor, P.J. Marsac, T. Li, S. R. Byrn, Solid-state spectroscopic investigation of molecular interactions between clofazimine and hypromellose phthalate in amorphous solid dispersions, Mol. Pharm. 13 (2016) 3964–3975, https://doi.org/10.1021/ACS.MOLPHARMACEUT.6B00740.

[161] Y. Song, X. Yang, X. Chen, H. Nie, S. Byrn, J.W. Lubach, Investigation of drug–excipient interactions in lapatinib amorphous solid dispersions using solid-state NMR spectroscopy, Mol. Pharm. 12 (2015) 857–866, https://doi.org/10.1021/MP500692A.
[162] P. Kolhe, E. Amend, S.K. Singh, Impact of freezing on pH of buffered solutions and consequences for monoclonal antibody aggregation, Biotechnol. Prog. 26 (2010) 727–733, https://doi.org/10.1002/BTPR.377.
[163] Y. Yani, P. Kanaujia, P.S. Chow, R.B.H. Tan, Effect of API-polymer miscibility and interaction on the stabilization of amorphous solid dispersion: a molecular simulation study, Ind. Eng. Chem. Res. 56 (2017) 12698–12707, https://doi.org/10.1021/ACS.IECR.7B03187.
[164] A. Abraham, G. Crull, Understanding API–polymer proximities in amorphous stabilized composite drug products using fluorine–carbon 2D HETCOR solid-state NMR, Mol. Pharm. 11 (2014) 3754–3759, https://doi.org/10.1021/MP400629J.
[165] C. Luebbert, F. Huxoll, G. Sadowski, G. Van Den Mooter, H. Grohganz, Amorphous-amorphous phase separation in API/polymer formulations, Mol 22 (2017) 296, https://doi.org/10.3390/MOLECULES22020296, 22 (2017) 296.
[166] H.S. Purohit, L.S. Taylor, Phase separation kinetics in amorphous solid dispersions upon exposure to water, Mol. Pharm. 12 (2015) 1623–1635, https://doi.org/10.1021/ACS.MOLPHARMACEUT.5B00041.
[167] S. Baghel, H. Cathcart, N.J. O'Reilly, Polymeric amorphous solid dispersions: a review of amorphization, crystallization, stabilization, solid-state characterization, and aqueous solubilization of biopharmaceutical classification system class II drugs, J. Pharm. Sci. 105 (2016) 2527–2544, https://doi.org/10.1016/J.XPHS.2015.10.008.
[168] F. Qian, J. Huang, M.A. Hussain, Drug–polymer solubility and miscibility: stability consideration and practical challenges in amorphous solid dispersion development, J. Pharm. Sci. 99 (2010) 2941–2947, https://doi.org/10.1002/JPS.22074.
[169] P.J. Marsac, S.L. Shamblin, L.S. Taylor, Theoretical and practical approaches for prediction of drug-polymer miscibility and solubility, Pharm. Res. (N. Y.) 23 (2006) 2417–2426, https://doi.org/10.1007/S11095-006-9063-9/TABLES/2.
[170] D. Lin, Y. Huang, A thermal analysis method to predict the complete phase diagram of drug-polymer solid dispersions, Int. J. Pharm. 399 (2010) 109–115, https://doi.org/10.1016/J.IJPHARM.2010.08.013.
[171] F. Qian, J. Huang, Q. Zhu, R. Haddadin, J. Gawel, R. Garmise, M. Hussain, Is a distinctive single Tg a reliable indicator for the homogeneity of amorphous solid dispersion? Int. J. Pharm. 395 (2010) 232–235, https://doi.org/10.1016/J.IJPHARM.2010.05.033.
[172] A.C.F. Rumondor, I. Ivanisevic, S. Bates, D.E. Alonzo, L.S. Taylor, Evaluation of drug-polymer miscibility in amorphous solid dispersion systems, Pharm. Res. (N. Y.) 26 (2009) 2523–2534, https://doi.org/10.1007/S11095-009-9970-7.
[173] A. Newman, D. Engers, S. Bates, I. Ivanisevic, R.C. Kelly, G. Zografi, Characterization of amorphous API:Polymer mixtures using X-ray powder diffraction, J. Pharm. Sci. 97 (2008) 4840–4856, https://doi.org/10.1002/JPS.21352.
[174] D. Klempner, K.C. Frisch, Polymer Alloys : Blends, Blocks, Grafts, and Interpenetrating Networks, 1978.
[175] K. Sarpal, E.J. Munson, Amorphous solid dispersions of felodipine and nifedipine with Soluplus®: drug-polymer miscibility and intermolecular interactions, J. Pharm. Sci. 110 (2021) 1457–1469, https://doi.org/10.1016/J.XPHS.2020.12.022.
[176] F. Yang, Y. Su, J. Zhang, J. Dinunzio, A. Leone, C. Huang, C.D. Brown, Rheology guided rational selection of processing temperature to prepare copovidone-nifedipine amorphous solid dispersions via hot melt extrusion (HME), Mol. Pharm. 13 (2016) 3494–3505, https://doi.org/10.1021/ACS.MOLPHARMACEUT.6B00516.
[177] O. Policianova, J. Brus, M. Hruby, M. Urbanova, A. Zhigunov, J. Kredatusova, L. Kobera, Structural diversity of solid dispersions of acetylsalicylic acid as seen by solid-state NMR, Mol. Pharm. 11 (2014) 516–530, https://doi.org/10.1021/MP400495H.
[178] H.S. Purohit, J.D. Ormes, S. Saboo, Y. Su, M.S. Lamm, A.K.P. Mann, L.S. Taylor, Insights into nano- and micron-scale phase separation in amorphous solid dispersions using fluorescence-based techniques in combination with solid state nuclear magnetic resonance spectroscopy, Pharm. Res. (N. Y.) 34 (2017) 1364–1377, https://doi.org/10.1007/S11095-017-2145-Z.
[179] Y. Chen, J. Ling, M. Li, Y. Su, K.S. Arte, T.T. Mutukuri, L.S. Taylor, E.J. Munson, E. M. Topp, Q.T. Zhou, Understanding the impact of protein-excipient interactions on physical stability of spray-dried protein solids, Mol. Pharm. 18 (2021) 2657–2668, https://doi.org/10.1021/ACS.MOLPHARMACEUT.1C00189.
[180] J. Clauss, K. Schmidt-Rohr, H.W. Spiess, Determination of domain sizes in heterogeneous polymers by solid-state NMR, Acta Polym. 44 (1993) 1–17, https://doi.org/10.1002/ACTP.1993.010440101.
[181] S. Spiegel, K. Schmidt-Rohr, C. Boeffel, H.W. Spiess, 1H spin diffusion coefficients of highly mobile polymers, Polymer 34 (1993) 4566–4569, https://doi.org/10.1016/0032-3861(93)90166-8.
[182] Y. Aso, S. Yoshioka, S. Kojima, Relationship between the crystallization rates of amorphous nifedipine, phenobarbital, and flopropione, and their molecular mobility as measured by their enthalpy relaxation and 1H NMR relaxation times, J. Pharm. Sci. 89 (2000) 408–416, https://doi.org/10.1002/(sici)1520-6017(200003)89:3<408::aid-jps11>3.0.co;2-#.
[183] Y. Aso, S. Yoshioka, T. Miyazaki, T. Kawanishi, K. Tanaka, S. Kitamura, A. Takakura, T. Hayashi, N. Muranushi, Miscibility of nifedipine and hydrophilic polymers as measured by (1)H-NMR spin-lattice relaxation, Chem. Pharm. Bull. (Tokyo) 55 (2007) 1227–1231, https://doi.org/10.1248/CPB.55.1227.
[184] J.L. Calahan, S.C. Azali, E.J. Munson, K. Nagapudi, Investigation of phase mixing in amorphous solid dispersions of AMG 517 in HPMC-AS using DSC, solid-state NMR, and solution calorimetry, Mol. Pharm. 12 (2015) 4115–4123, https://doi.org/10.1021/ACS.MOLPHARMACEUT.5B00556.
[185] B. Tian, X. Tang, L.S. Taylor, Investigating the correlation between miscibility and physical stability of amorphous solid dispersions using fluorescence-based techniques, Mol. Pharm. 13 (2016) 3988–4000, https://doi.org/10.1021/ACS.MOLPHARMACEUT.6B00803.
[186] E.J. Suihko, R.T. Forbes, D.C. Apperley, A solid-state NMR study of molecular mobility and phase separation in co-spray-dried protein–sugar particles, Eur. J. Pharmaceut. Sci. 25 (2005) 105–112, https://doi.org/10.1016/J.EJPS.2005.02.002.
[187] M.A. Mensink, M.J. Nethercott, W.L.J. Hinrichs, K. van der Voort Maarschalk, H. W. Frijlink, E.J. Munson, M.J. Pikal, Influence of miscibility of protein-sugar lyophilizates on their storage stability, AAPS J. 18 (2016) 1225–1232, https://doi.org/10.1208/S12248-016-9937-7.
[188] F.G. Vogt, M. Strohmeier, 2D solid-state NMR analysis of inclusion in drug-cyclodextrin complexes, Mol. Pharm. 9 (2012) 3357–3374, https://doi.org/10.1021/MP300416W.
[189] F.G. Vogt, K. Roberts-Skilton, S.A. Kennedy-Gabb, A solid-state NMR study of amorphous ezetimibe dispersions in mesoporous silica, Pharm. Res. 2013 309 (30) (2013) 2315–2331, https://doi.org/10.1007/S11095-013-1075-7.
[190] M. Brunsteiner, J. Khinast, A. Paudel, Relative contributions of solubility and mobility to the stability of amorphous solid dispersions of poorly soluble drugs: a molecular dynamics simulation study, Pharm. Times 10 (2018) 101, https://doi.org/10.3390/PHARMACEUTICS10030101, 10 (2018) 101.
[191] Y. Aso, S. Yoshioka, S. Kojima, Molecular mobility-based estimation of the crystallization rates of amorphous nifedipine and phenobarbital in poly (vinylpyrrolidone) solid dispersions, J. Pharm. Sci. 93 (2004) 384–391, https://doi.org/10.1002/JPS.10526.
[192] A. Y, Y. S, M. T, K. T, Feasibility of 19F-NMR for assessing the molecular mobility of flufenamic acid in solid dispersions, Chem. Pharm. Bull. (Tokyo) 57 (2009) 61–64, https://doi.org/10.1248/CPB.57.61.
[193] C. Dahlberg, S.V. Dvinskikh, M. Schuleit, I. Furó, Polymer swelling, drug mobilization and drug recrystallization in hydrating solid dispersion tablets studied by multinuclear NMR microimaging and spectroscopy, Mol. Pharm. 8 (2011) 1247–1256, https://doi.org/10.1021/MP200051E.
[194] S. Mura, J. Nicolas, P. Couvreur, Stimuli-responsive nanocarriers for drug delivery, Nat. Mater. 1211 (12) (2013) 991–1003, https://doi.org/10.1038/nmat3776, 2013.
[195] T. Shukla, N. Upmanyu, S.P. Pandey, M.S. Sudheesh, Site-specific drug delivery, targeting, and gene therapy, Nanoarchitectonics Biomed. (2019) 473–505, https://doi.org/10.1016/B978-0-12-816200-2.00013-X.
[196] P. Phyo, X. Zhao, A.C. Templeton, W. Xu, J.K. Cheung, Y. Su, Understanding molecular mechanisms of biologics drug delivery and stability from NMR spectroscopy, Adv. Drug Deliv. Rev. 174 (2021) 1–29, https://doi.org/10.1016/J.ADDR.2021.02.007.
[197] A. Marchetti, J. Yin, Y. Su, X. Kong, Solid-state NMR in the field of drug delivery: state of the art and new perspectives, Magn. Reson. Lett. (2021) 100003, https://doi.org/10.1016/J.MRL.2021.100003.
[198] G. Tiwari, R. Tiwari, B. Sriwastawa, L. Bhati, S. Pandey, P. Pandey, S. K. Bannerjee, Drug delivery systems: an updated review, Int. J. Pharm. Investig. 2 (2012) 2, https://doi.org/10.4103/2230-973X.96920.
[199] M. Vallet-Regi, A. Rámila, R.P. Del Real, J. Pérez-Pariente, A new property of MCM-41: drug delivery system, Chem. Mater. 13 (2000) 308–311, https://doi.org/10.1021/CM0011559.
[200] R. Challa, A. Ahuja, J. Ali, R.K. Khar, Cyclodextrins in drug delivery: an updated review, AAPS PharmSciTech 62 (6) (2005) E329–E357, https://doi.org/10.1208/PT060243, 2005.
[201] D.K. Mishra, V. Dhote, A. Bhargava, D.K. Jain, P.K. Mishra, Amorphous solid dispersion technique for improved drug delivery: basics to clinical applications, Drug Deliv. Transl. Res. 5 (2015) 552–565, https://doi.org/10.1007/S13346-015-0256-9/TABLES/3.
[202] M. Porcino, X. Li, R. Gref, C. Martineau-corcos, Solid-state NMR spectroscopy: a key tool to unravel the supramolecular structure of drug delivery systems, Mol 26 (2021) 4142, https://doi.org/10.3390/MOLECULES26144142, 26 (2021) 4142.
[203] M. Vallet-Regí, F. Balas, D. Arcos, Mesoporous materials for drug delivery, Angew. Chem. Int. Ed. 46 (2007) 7548–7558, https://doi.org/10.1002/ANIE.200604488.
[204] S. Giret, M. Wong Chi Man, C. Carcel, Mesoporous-silica-functionalized nanoparticles for drug delivery, Chem. Eur J. 21 (2015) 13850–13865, https://doi.org/10.1002/CHEM.201500578.
[205] S. Wang, Ordered mesoporous materials for drug delivery, Microporous Mesoporous Mater. 117 (2009) 1–9, https://doi.org/10.1016/J.MICROMESO.2008.07.002.
[206] R. Mellaerts, C.A. Aerts, J. Van Humbeeck, P. Augustijns, G. Van Den Mooter, J. A. Martens, Enhanced release of itraconazole from ordered mesoporous SBA-15 silica materials, Chem. Commun. (2007) 1375–1377, https://doi.org/10.1039/B616746B.
[207] M. Van Speybroeck, V. Barillaro, T. Do Thi, R. Mellaerts, J. Martens, J. Van Humbeeck, J. Vermant, P. Annaert, G. Van Den Mooter, P. Augustijns, Ordered mesoporous silica material SBA-15: a broad-spectrum formulation platform for poorly soluble drugs, J. Pharm. Sci. 98 (2009) 2648–2658, https://doi.org/10.1002/JPS.21638.
[208] K.P. Nartowski, D. Malhotra, L.E. Hawarden, J. Sibik, D. Iuga, J.A. Zeitler, L. Fábián, Y.Z. Khimyak, 19F NMR spectroscopy as a highly sensitive method for

the direct monitoring of confined crystallization within nanoporous materials, Angew. Chem. 128 (2016) 9050–9054, https://doi.org/10.1002/ANGE.201602936.
[209] A. Gu, N.J. Wheate, Macrocycles as drug-enhancing excipients in pharmaceutical formulations, J. Inclusion Phenom. Macrocycl. Chem. 1001 (100) (2021) 55–69, https://doi.org/10.1007/S10847-021-01055-9, 2021.
[210] T. Loftsson, P. Jarho, M. Másson, T. Järvinen, Cyclodextrins in drug delivery, Expet Opin. Drug Deliv. 2 (2005) 335–351, https://doi.org/10.1517/17425247.2.1.335.
[211] K. Uekama, Design and evaluation of cyclodextrin-based drug formulation, Chem. Pharm. Bull. (Tokyo) 52 (2004) 900–915, https://doi.org/10.1248/CPB.52.900.
[212] R.A. Rajewski, V.J. Stella, Pharmaceutical applications of cyclodextrins. 2. In vivo drug delivery, J. Pharm. Sci. 85 (1996) 1142–1169, https://doi.org/10.1021/JS960075U.
[213] V.J. Stella, R.A. Rajewski, Cyclodextrins: their future in drug formulation and delivery, Pharm. Res. (N. Y.) 145 (14) (1997) 556–567, https://doi.org/10.1023/A:1012136608249, 1997.
[214] A. Morales, J. Struppe, E. Meléndez, Host-guest interactions between niobocene dichloride and α-, β-, and γ-cyclodextrins: preparation and characterization, J. Inclusion Phenom. Macrocycl. Chem. 60 (2008) 263–270, https://doi.org/10.1007/S10847-007-9374-4.
[215] E. Redenti, M. Zanol, P. Ventura, G. Fronza, A. Comotti, P. Taddei, A. Bertoluzza, Raman and solid state 13 C-NMR investigation of the structure of the 1 : 1 amorphous piroxicam :-Cyclodextrin inclusion compound. https://doi.org/10.1002/(SICI)1520-6343(1999)5:4, 1999.
[216] K. Higashi, S. Ideura, H. Waraya, K. Moribe, K. Yamamoto, Incorporation of salicylic acid molecules into the intermolecular spaces of γ-cyclodextrin-polypseudorotaxane, Cryst. Growth Des. 9 (2009) 4243–4246, https://doi.org/10.1021/CG900573W.
[217] M. Wulff, M. Aldén, J. Tegenfeldt, Solid-state NMR investigation of Indomethacin−Cyclodextrin complexes in PEG 6000 carrier, Bioconjugate Chem. 13 (2002) 240–248, https://doi.org/10.1021/BC000156O.
[218] U.H. Gala, D.A. Miller, Y. Su, A. Spangenberg, R.O. Bill Williams, The effect of drug loading on the properties of abiraterone–hydroxypropyl beta cyclodextrin solid dispersions processed by solvent free KinetiSol® technology, Eur. J. Pharm. Biopharm. 165 (2021) 52–65, https://doi.org/10.1016/J.EJPB.2021.05.001.
[219] Y. Phyo, Pyae; Xu, Wei; Frank, Derek; Li, Tonglei; Su, Probing molecular packing of drug substances in nanometer domains in pharmaceutical formulations using 19F magic angle spinning NMR, J. Phys. Chem. C. (in press).
[220] E.R. DeAzevedo, W.G. Hu, T.J. Bonagamba, K. Schmidt-Rohr, Centerband-only detection of exchange: efficient analysis of dynamics in solids by NMR, J. Am. Chem. Soc. 121 (1999) 8411–8412, https://doi.org/10.1021/JA992022V.
[221] W. L, M. Hong*, Determination of the oligomeric number and intermolecular distances of membrane protein assemblies by anisotropic 1H-driven spin diffusion NMR spectroscopy, J. Am. Chem. Soc. 128 (2006) 7242–7251, https://doi.org/10.1021/JA0603406.
[222] E.S. Salnikov, J. Raya, M. De Zotti, E. Zaitseva, C. Peggion, G. Ballano, C. Toniolo, J. Raap, B. Bechinger, Alamethicin supramolecular organization in lipid membranes from 19F solid-state NMR, Biophys. J. 111 (2016) 2450–2459, https://doi.org/10.1016/J.BPJ.2016.09.048.
[223] V.S. Mandala, S.Y. Liao, B. Kwon, M. Hong, Structural basis for asymmetric conductance of the influenza M2 proton channel investigated by solid-state NMR spectroscopy, J. Mol. Biol. 429 (2017) 2192–2210, https://doi.org/10.1016/J.JMB.2017.05.015.
[224] J.K. Williams, Y. Zhang, K. Schmidt-Rohr, M. Hong, pH-dependent conformation, dynamics, and aromatic interaction of the gating tryptophan residue of the influenza M2 proton channel from solid-state NMR, Biophys. J. 104 (2013) 1698–1708, https://doi.org/10.1016/J.BPJ.2013.02.054.
[225] Y. Su, T. Doherty, A.J. Waring, P. Ruchala, M. Hong, Roles of arginine and lysine residues in the translocation of a cell-penetrating peptide from 13C, 31P, and 19F solid-state NMR, Biochemistry 48 (2009) 4587–4595, https://doi.org/10.1021/BI900080D.
[226] K. Xue, R. Dervisoglu, H. Sowa, L.B. Andreas, Centerband-only detection of exchange NMR with natural-abundance correction reveals an expanded unit cell in phenylalanine crystals, ChemPhysChem 21 (2020) 1622–1626, https://doi.org/10.1002/CPHC.202000517.
[227] T.J. Franklin, G.A. Snow, Biochemistry and molecular biology of antimicrobial drug action, Biochem. Mol. Biol. Antimicrob. Drug Action (2005) 1–182, https://doi.org/10.1007/0-387-27566-5.
[228] Y. Su, S. Li, M. Hong, Cationic membrane peptides: atomic-level insight of structure–activity relationships from solid-state NMR, Amino Acids 443 (44) (2012) 821–833, https://doi.org/10.1007/S00726-012-1421-9, 2012.
[229] M. Hong, Y. Su, Structure and dynamics of cationic membrane peptides and proteins: insights from solid-state NMR, Protein Sci. 20 (2011) 641–655, https://doi.org/10.1002/PRO.600.
[230] R. Han, S. Wang, Mechanisms of antimicrobial peptides as characterized by solid-state NMR, Magn. Reson. Lett. 2 (2) (2022) 119–129, https://doi.org/10.1016/J.MRL.2021.09.004.
[231] O. Toke, R.D. O'Connor, T.K. Weldeghiorghis, W.L. Maloy, R.W. Glaser, A. S. Ulrich, J. Schaefer, Structure of (KIAGKIA)3 aggregates in phospholipid bilayers by solid-state NMR, Biophys. J. 87 (2004) 675, https://doi.org/10.1529/BIOPHYSJ.103.032714.
[232] O. Toke, L. Cegelski, J. Schaefer, Peptide antibiotics in action: investigation of polypeptide chains in insoluble environments by rotational-echo double resonance, Biochim. Biophys. Acta Biomembr. 1758 (2006) 1314–1329, https://doi.org/10.1016/J.BBAMEM.2006.02.031.
[233] J.J. Buffy, A.J. Waring, M. Hong, Determination of peptide oligomerization in lipid bilayers using 19F spin diffusion NMR, J. Am. Chem. Soc. 127 (2005) 4477–4483, https://doi.org/10.1021/JA043621R/SUPPL_FILE/JA043621RSI20050102_020700.PDF.
[234] M. Lindgren, M. Hällbrink, A. Prochiantz, Ü. Langel, Cell-penetrating peptides, Trends Pharmacol. Sci. 21 (2000) 99–103, https://doi.org/10.1016/S0165-6147(00)01447-4.
[235] F. Separovic, D.W. Keizer, M.-A. Sani, In-cell solid-state NMR studies of antimicrobial peptides, Front. Med. Technol. (2020) 22, https://doi.org/10.3389/FMEDT.2020.610203, 0.
[236] J.A.H. Romaniuk, L. Cegelski, Bacterial cell wall composition and the influence of antibiotics by cell-wall and whole-cell NMR, Philos. Trans. R. Soc. B Biol. Sci. 370 (2015), https://doi.org/10.1098/RSTB.2015.0024.
[237] E. Luchinat, L. Banci, A unique tool for cellular structural biology: in-cell NMR, J. Biol. Chem. 291 (2016) 3776–3784, https://doi.org/10.1074/JBC.R115.643247.
[238] S.J. Kim, L. Cegelski, D.R. Studelska, R.D. O'Connor, A.K. Mehta, J. Schaefer, Rotational-echo double resonance characterization of vancomycin binding sites in Staphylococcus aureus, Biochemistry 41 (2002) 6967–6977, https://doi.org/10.1021/BI0121407.
[239] P. Duan, K.J. Chen, G. Wijegunawardena, A.J. Dregni, H.K. Wang, H. Wu, M. Hong, Binding sites of a positron emission tomography imaging agent in Alzheimer's β-amyloid fibrils studied using 19F solid-state NMR, J. Am. Chem. Soc. 144 (2022) 1416–1430, https://doi.org/10.1021/JACS.1C12056.
[240] Y. Su, W.F. DeGrado, M. Hong, Orientation, dynamics, and lipid interaction of an antimicrobial arylamide investigated by 19F and 31P solid-state NMR spectroscopy, J. Am. Chem. Soc. 132 (2010) 9197–9205, https://doi.org/10.1021/JA103658H.
[241] Asif Equbal, N. Kristoffer Basse, Chr. Nielsen, Highly efficient 19 F heteronuclear decoupling in solid-state NMR spectroscopy using supercycled refocused-CW irradiation, Phys. Chem. Chem. Phys. 18 (2016) 30990–30997, https://doi.org/10.1039/C6CP06574K.
[242] G.A. Montix, R.K. Harris, Fluorine-19 and studies of MAS 1H Ç 19F CP/MAS NMR ýuoropolymers viton, Magn. Reson. Chem. Magn. Reson. Chem. 36 (1998) 892–900, https://doi.org/10.1002/(SICI)1097-458X(199812)36:12.
[243] A.A. Shcherbakov, M. Hong, Rapid measurement of long-range distances in proteins by multidimensional 13C–19F REDOR NMR under fast magic-angle spinning, J. Biomol. NMR 71 (2018) 31–43, https://doi.org/10.1007/S10858-018-0187-0.
[244] A.A. Shcherbakov, V.S. Mandala, M. Hong, High-sensitivity detection of nanometer 1H–19F distances for protein structure determination by 1H-detected fast MAS NMR, J. Phys. Chem. B. 123 (2019) 4387–4391, https://doi.org/10.1021/ACS.JPCB.9B03812.
[245] Xingyu Lu, Tsutsumi Yu, Chengbin Huang, Wei Xu, S.R. Byrn, A.C. Templeton, A. V. Buevich, Jean-Paul Amoureux, Yongchao Su, Molecular packing of pharmaceuticals analyzed with paramagnetic relaxation enhancement and ultrafast magic angle pinning NMR, Phys. Chem. Chem. Phys. 22 (2020) 13160–13170, https://doi.org/10.1039/D0CP02049D.
[246] M. Lu, S. Sarkar, M. Wang, J. Kraus, M. Fritz, C.M. Quinn, S. Bai, S.T. Holmes, C. Dybowski, G.P.A. Yap, J. Struppe, I.V. Sergeyev, W. Maas, A.M. Gronenborn, T. Polenova, 19F magic angle spinning NMR spectroscopy and density functional theory calculations of fluorosubstituted tryptophans: integrating experiment and theory for accurate determination of chemical shift tensors, J. Phys. Chem. B. 122 (2018) 6148–6155, https://doi.org/10.1021/ACS.JPCB.8B00377.
[247] M. Wang, M. Lu, M.P. Fritz, C.M. Quinn, I.J.L. Byeon, C.H. Byeon, J. Struppe, W. Maas, A.M. Gronenborn, T. Polenova, Fast magic-angle spinning 19F NMR spectroscopy of HIV-1 capsid protein assemblies, Angew. Chem. Int. Ed. 57 (2018) 16375–16379, https://doi.org/10.1002/anie.201809060.
[248] M. Tang, D.A. Berthold, C.M. Rienstra, Solid-state NMR of a large membrane protein by paramagnetic relaxation enhancement, J. Phys. Chem. Lett. 2 (2011) 1836–1841, https://doi.org/10.1021/JZ200768R.
[249] I. Sengupta, P.S. Nadaud, C.P. Jaroniec, Protein structure determination with paramagnetic solid-state NMR spectroscopy, Acc. Chem. Res. 46 (2013) 2117–2126, https://doi.org/10.1021/AR300360Q.
[250] N.P. Wickramasinghe, M. Kotecha, A. Samoson, J. Past, Y. Ishii, Sensitivity enhancement in (13)C solid-state NMR of protein microcrystals by use of paramagnetic metal ions for optimizing (1)H T(1) relaxation, J. Magn. Reson. 184 (2007) 350–356, https://doi.org/10.1016/J.JMR.2006.10.012.
[251] G. Porat-Dahlerbruch, J. Struppe, C.M. Quinn, A.M. Gronenborn, T. Polenova, Determination of accurate 19F chemical shift tensors with R-symmetry recoupling at high MAS frequencies (60–100 kHz), J. Magn. Reson. 340 (2022) 107227, https://doi.org/10.1016/J.JMR.2022.107227.
[252] Y. Su, L. Andreas, R.G. Griffin, Magic angle spinning NMR of proteins: high-frequency dynamic nuclear polarization and 1H detection, Http://Dx.Doi.Org/10.1146/Annurev-Biochem-060614-034206. 84, 465–497, https://doi.org/10.1146/ANNUREV-BIOCHEM-060614-034206, 2015.
[253] T.F. Prisner, Dynamic nuclear polarization, NMR Biomol. Towar. Mech. Syst. Biol. (2012) 419–431, https://doi.org/10.1002/9783527644506.CH25.

[254] A. Henstra, T.S. Lin, J. Schmidt, W.T. Wenckebach, High dynamic nuclear polarization at room temperature, Chem. Phys. Lett. 165 (1990) 6–10, https://doi.org/10.1016/0009-2614(90)87002-9.
[255] Q.Z. Ni, F. Yang, T.V. Can, I.V. Sergeyev, S.M. D'Addio, S.K. Jawla, Y. Li, M. P. Lipert, W. Xu, R.T. Williamson, A. Leone, R.G. Griffin, Y. Su, In situ characterization of pharmaceutical formulations by dynamic nuclear polarization enhanced MAS NMR, J. Phys. Chem. B. 121 (2017) 8132–8141, https://doi.org/10.1021/ACS.JPCB.7B07213.
[256] D.A. Hirsh, A.J. Rossini, L. Emsley, R.W. Schurko, 35Cl dynamic nuclear polarization solid-state NMR of active pharmaceutical ingredients, Phys. Chem. Chem. Phys. 18 (2016) 25893–25904, https://doi.org/10.1039/C6CP04353D.
[257] L. Zhao, M.P. Hanrahan, P. Chakravarty, A.G. Dipasquale, L.E. Sirois, K. Nagapudi, J.W. Lubach, A.J. Rossini, Characterization of pharmaceutical cocrystals and salts by dynamic nuclear polarization-enhanced solid-state NMR spectroscopy, Cryst. Growth Des. 18 (2018) 2588–2601, https://doi.org/10.1021/ACS.CGD.8B00203.
[258] A.J. Rossini, C.M. Widdifield, A. Zagdoun, M. Lelli, M. Schwarzwälder, C. Copéret, A. Lesage, L. Emsley, Dynamic nuclear polarization enhanced NMR spectroscopy for pharmaceutical formulations, J. Am. Chem. Soc. 136 (2014) 2324–2334, https://doi.org/10.1021/JA4092038.
[259] G. Mollica, M. Dekhil, F. Ziarelli, P. Thureau, S. Viel, Quantitative structural constraints for organic powders at natural isotopic abundance using dynamic nuclear polarization solid-state NMR spectroscopy, Angew. Chem. Int. Ed. 54 (2015) 6028–6031, https://doi.org/10.1002/ANIE.201501172.
[260] J. Viger-Gravel, C.E. Avalos, D.J. Kubicki, D. Gajan, M. Lelli, O. Ouari, A. Lesage, L. Emsley, 19F magic angle spinning dynamic nuclear polarization enhanced NMR spectroscopy, Angew. Chem. Int. Ed. 58 (2019) 7249–7253, https://doi.org/10.1002/ANIE.201814416.
[261] M. Lu, M. Wang, I.V. Sergeyev, C.M. Quinn, J. Struppe, M. Rosay, W. Maas, A. M. Gronenborn, T. Polenova, Dynamic nuclear polarization at fast magic angle spinning for NMR of HIV-1 capsid protein assemblies, J. Am. Chem. Soc. 141 (2019) 5681–5691, https://doi.org/10.1021/JACS.8B09216, 19F.
[262] A. Bertarello, P. Berruyer, U. Skantze, S. Sardana, M. Sardana, C.S. Elmore, M. Schade, E. Chiarparin, S. Schantz, L. Emsley, Quantification of magic angle spinning dynamic nuclear polarization NMR spectra, J. Magn. Reson. 329 (2021) 107030, https://doi.org/10.1016/J.JMR.2021.107030.

ISSN: 2641-2020
DOI: 10.33552/APPR.2019.02.000543
Archives of
Pharmacy & Pharmacology Research
Iris Publishers

Mini Review

Copyright © All rights are reserved by Rosane Aguiar da Silva San Gil

^{13}C Solid State Nuclear Magnetic Resonance as a Tool for Studying Polymorphism in Pharmaceuticals

Eduardo Gomes Rodrigues de Sousa[1] and Rosane Aguiar da Silva San Gil[2,3]*

[1]*Fundação Oswaldo Cruz, FIOCRUZ/Instituto de Tecnologia em Fármacos, Brazil*

[2]*Universidade Federal do Rio de Janeiro, Instituto de Química, Brazil*

[3]*Universidade Federal do Rio de Janeiro, Instituto de Pesquisas de Produtos Naturais, Brazil*

***Corresponding author:** Rosane Aguiar da Silva San Gil, Universidade Federal do Rio de Janeiro, Instituto de Química, , Brazil, e-mail: rsangil@iq.ufrj.br

Received Date: December 09, 2019

Published Date: December 19, 2019

Abstract

The predisposition of pharmaceutical solids to crystallize in various forms can lead to differences in their physical and chemical properties. The study of polymorphism is an important step in drug development because it causes a relevant physical and chemical characteristic in both the API and the formulated drug. NMR is one of the most versatile techniques for structural characterization. In addition, Solid State NMR is important for the study of organic and inorganic compounds, both for structural determination and for the use of samples, bonding types and geometry, as well as for analytical studies and their applications in a wide range of areas, including drug studies, such as pure API or pharmaceutical formulations and excipients. In this mini review, there are some examples about its use for studying polymorphism in pharmaceuticals.

Keywords: Solid state NMR; ^{13}C CPMAS; Polymorphism; Pharmaceuticals

Mini Review

NMR is one of the most versatile techniques for structural characterization. In addition, NMR is important for the study of organic and inorganic compounds, both for structural determination and for the use of samples, bonding types and geometry, as well as for analytical studies and their applications in a wide range of areas, including drug studies, such as pure IFA or pharmaceutical formulations and excipients. All types of solid material can be studied by NMR, including crystals and powders, amorphous materials such as glass and rubber, superconductors and metals [1]. The Hamiltonian that describes the interactions present in a sample containing nuclear spin nuclei (I), consists of a sum of Hamiltonians related to the magnetic and electrical properties of the sample being analyzed [2], as shown EQUATION 1:

$$H_{RMN} = H_Z + H_{RF} + H_J + H_D + H_{DQ} + H_Q \qquad \text{Equation 1}$$

Where Hz is Zeeman Hamiltonian, HRF radiofrequency Hamiltonian, HJ scalar Hamiltonian, HD dipolar Hamiltonian, HDQ chemical shift Hamiltonian and HQ quadrupolar Hamiltonian. Zeeman's interaction between nuclear spin and the applied magnetic field induces the precession in the Larmor frequency ωo, which is defined by the nucleus and the external field strength. Magnetic fields as high as 21 T are in use, producing 900 MHz Larmor frequencies for hydrogen. Internal interactions observed include those of chemical shift, and scalar couplings. In addition, solid state NMR [1,2] can detect chemical shift anisotropies, magnetic dipole and electric quadrupole interactions, which are only observed indirectly in solution NMR. The most remarkable difference between the spectra obtained in solid NMR and in solution NMR is that in solid form the spectra show very broad signals. This difference is a function of the strong dipolar coupling interactions and the solid-state chemical shift anisotropy, which in the liquid state is averaged to its isotropic value or eliminated by molecular motion. Both dipolar coupling and chemical shift anisotropy are geometry dependent phenomena. The first gives relative orientation between two dipolar nuclei under study, while the second is a function of the orientation of the nucleus in relation to the static magnetic field [3].

The development of the techniques of magic angle rotation - MAS [4], high-power decoupling [5] and cross-polarization - CP [6] allowed obtaining high-resolution NMR spectra in solid

This work is licensed under Creative Commons Attribution 4.0 License

form. The implementation of several pulse sequences, such as TOSS (Total Suppression of Sidebands) that suppresses sideband signals [7], the dipolar dephasing technique (DD) for signaling non-proton carbons [8], and two-dimensional experiments such as PASS-adjusted spinning sidebands [9], allowed solid state NMR to be applied more broadly. The Figure 1 illustrates the solid state NMR spectrum, where the molecular orientation dependent interactions were eliminated by positioning and rotating around the magic angle (MAS) and the spectrum becomes similar to an NMR spectrum in the Figure 1, where dipolar and quadrupolar anisotropic interactions are maintained [1]. The most important technique for improving the resolution of solid-state NMR spectra is the sample positioning at 54.74° and the rotation at velocities of the order of magnitude of dipolar interactions and chemical shift anisotropies. Typically, for nuclei like ^{13}C, ^{31}P and ^{29}Si that have narrow chemical shift ranges, rotational speeds between 5 and 10 KHz, are sufficient to nullify dominant anisotropic interactions, as can be seen in Figure 2 [1,2]. On the other hand, the MAS technique significantly improves the resolution of spectra when coupled with the CP technique, and an improvement in sensitivity can be achieved. In the CPMAS technique, first magnetization of abundant species (1H) is done and then this magnetization is transferred to less abundant species, such as ^{13}C and ^{15}N, by dipolar interaction. The least abundant species are detected while uncoupling the most abundant species. The theoretical sensitivity gain is the ratio of the Larmor frequencies of the two spins, e.g. up to 4 to the ^{1}H-^{13}C [1,2] (Figure 1,2).

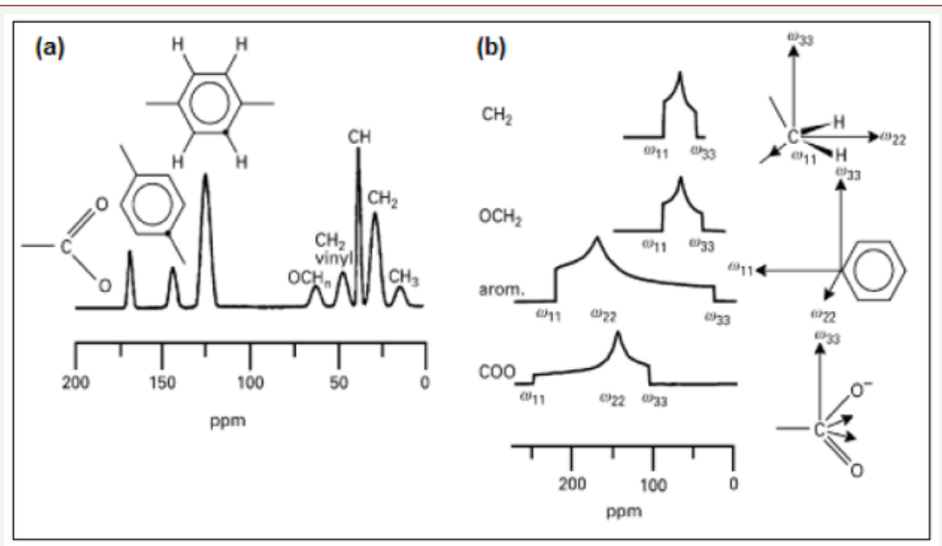


Figure 1: (a) ^{13}C solid-state NMR chemical shifts in different functional groups; (b) ^{13}C solid-state NMR chemical shifts in the same functional groups as (a) but illustrating anisotropic interactions [1].

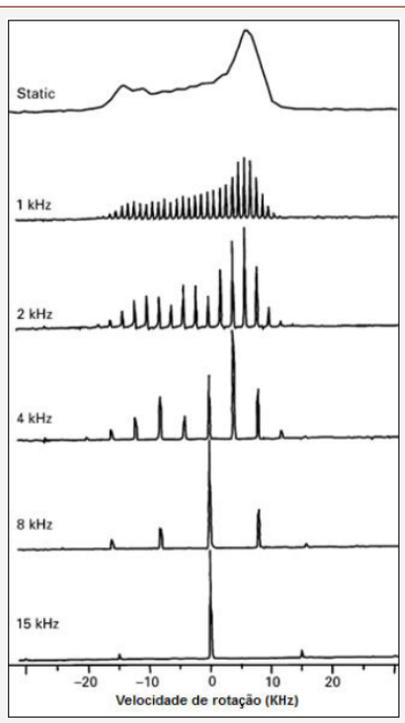


Figure 2: ^{31}P solid-state NMR spectra obtained for $Na_4P_2O_7.10H_2O$ as a function of rotational speed [1].

Solid-state NMR has been widely used in the identification of API polymorphs and in the characterization of pharmaceutical formulations, as well as in stability evaluation and drug-excipient interaction. In 2015, PINDELSKA and colleagues [10] used solid-state NMR for the analysis of clopidogrel hydrogensulfate polymorphs (HSCL), the antiplatelet agent, and the world's second-best selling drug. The solid dosage forms of the drug were evaluated, and the methodology was used to identify which polymorph was present in the commercial formulation. HSCL exists in different polymorphic forms, but only one of the two may be present in the final formulation, the HSCL1 polymorph or HSCL2. The standard spectra of the two polymorphs were obtained and compared with the ^{13}C CPMAS spectra of the different formulated products. Polymorphic forms were easily identified in pharmaceutical formulations by comparing the ^{13}C solid-state NMR spectra (Figure 3). AGUIAR et al. (2016) have used a combination of ^{13}C solid state NMR and GIPAW-DFT computed isotropic calculation to solve ambiguities in ^{13}C chemical shifts of 6-aminopenicilanic acid (6-APA). This is an intermediate in the industrial preparation of beta-lactam penicillin's [11]. SKOTNICKI et al. (2016) characterized two forms of valsartan IFA, an antihypertensive drug, by solid-state NMR [12]. From the ^{13}C CPMAS NMR spectra it was

possible to distinguish between the AR form (as received from the manufacturer with low crystallinity) and the AM form (completely amorphous), observing the region between 40 and 70 ppm that was distinct for the two forms analyzed (Figure 4). REZENDE et al. (2016), who studied polymorphs from carvedilol API (CAR), an antihypertensive, reported another recent work about solid-state NMR polymorphism identification [13] (Figure 3,4).

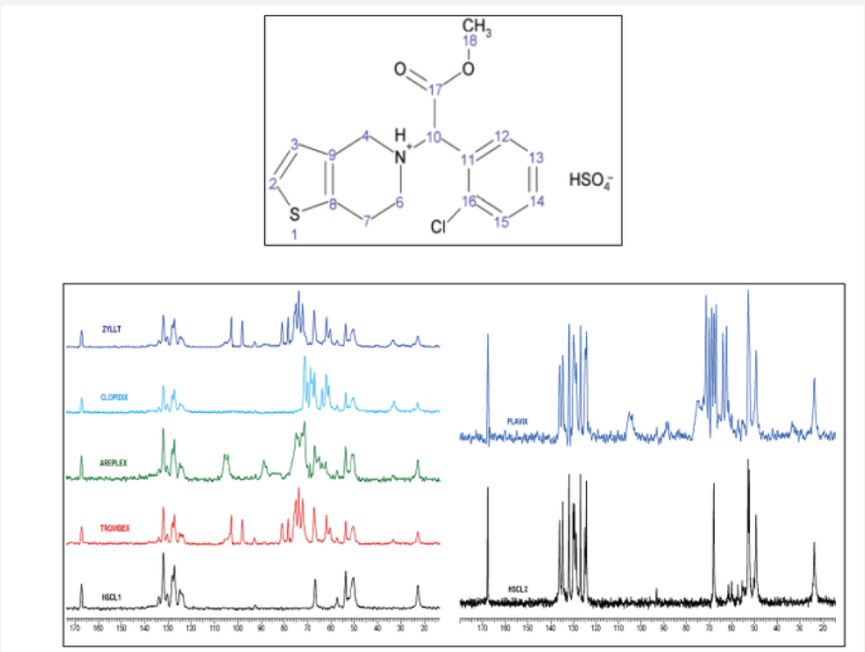


Figure 3: ^{13}C CPMAS NMR Spectrum: (a) Formulated products containing HSCL1 polymorph and (b) Formulated product containing HSCL2 polymorph [10].

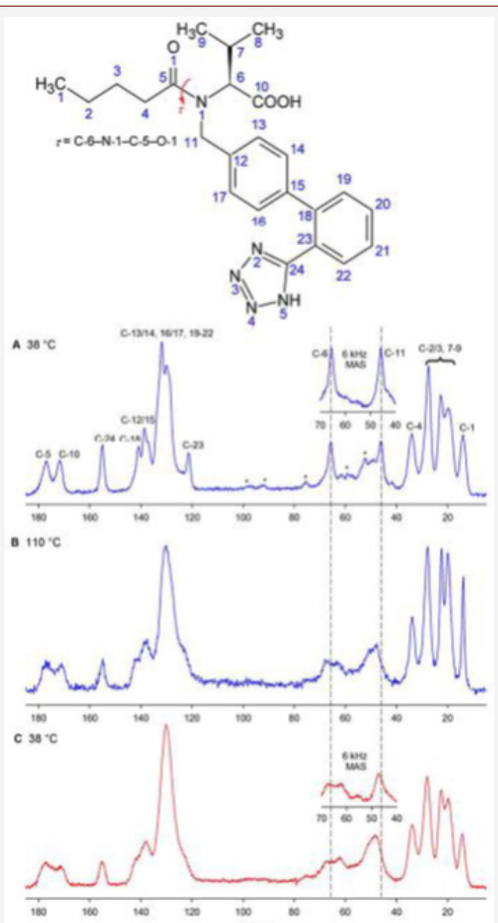


Figure 4:^{13}C CPMAS NMR spectra: (a) AR form at 38 °C, (b) AR form above glass transition temperature - 110 °C and (c) AM form at 38 °C [12].

It was possible to characterize by ^{13}C CPMAS NMR three polymorphic forms of the drug: form II, III and hydrate Figure 5. Solid-state NMR spectra signals were performed by the combination of NMR techniques and ab initio calculation.In the same year (2016), Sousa and coworkers studied polymorphism in efavirenz (EFZ), an antiretroviral drug [14]. In this study, the authors could be found, by solid-state NMR, the difference between EFZ used in the medicine formulations and the polymorphic form obtained by EFZ crystallization in heptane solvent. ^{13}C CPMAS NMR spectra Figure 6 of the EFZ/MIC and EFZ/HEPT showed 2 spectral regions, which present clear differences like signals multiplicity and intensity ratios of the signals. The first region of comparison is 60-100 ppm, and the second region of interest is the cyclopropyl group between -2.0 and 10 ppm (Figure 5,6).

Recently Solid-state NMR has been used combined with DFT calculations, to study polymorphism in dexamethasone acetate, by SILVA et al. in 2018 [15], inpharmacy samples of melxican [16] by ROMANI et al. (2018) and for evaluation of piracetam by Szeleszczuk et al. (2019). Piracetam is a popular nootropic drug, widely used in the treatment of age-associated mental decline and disorders of the nervous system such as Alzheimer's disease and dementia exists under normal pressure in three polymorphic forms (P1, P2 and P3) of different stability. The authors studied the relative stability of piracetam polymorphs depending on the temperature by using the solid-state NMR spectroscopy combined with ab initio DFT calculations. The results showed that DFT calculations can be used not only to obtain the NMR parameters but also to predict the influence of the temperature on the stability

order of the polymorphic forms of molecular crystals [17]. From the examples given it can be said that solid-state NMR offers a range of relevant information to basic scientific research or industry specific requirements unparalleled by any other technique.

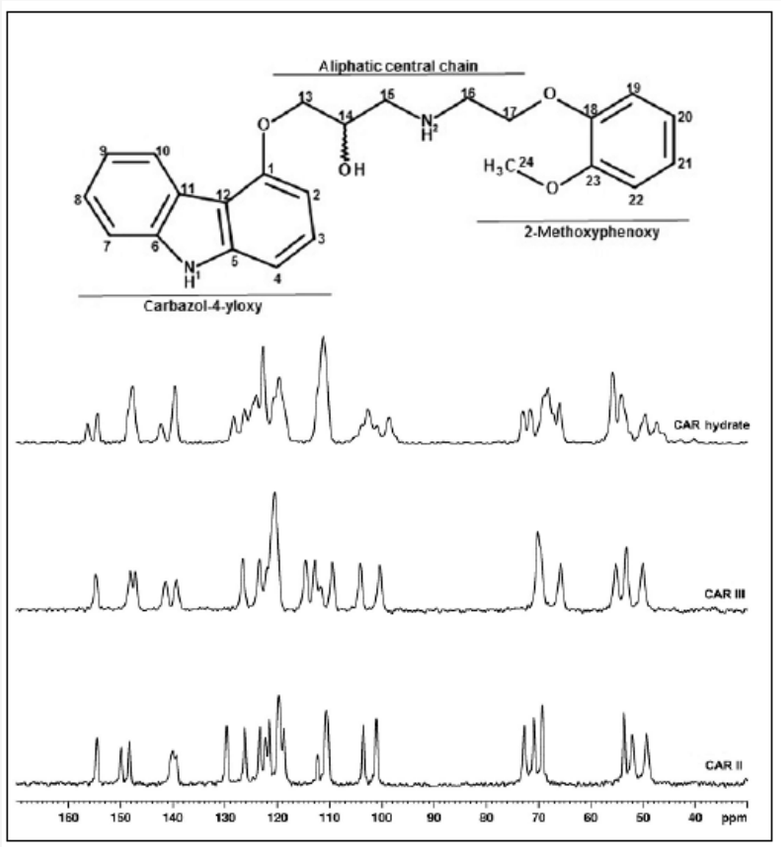


Figure 5: ^{13}C CPMAS NMR spectra of forms II, III and carvedilol hydrate [13].

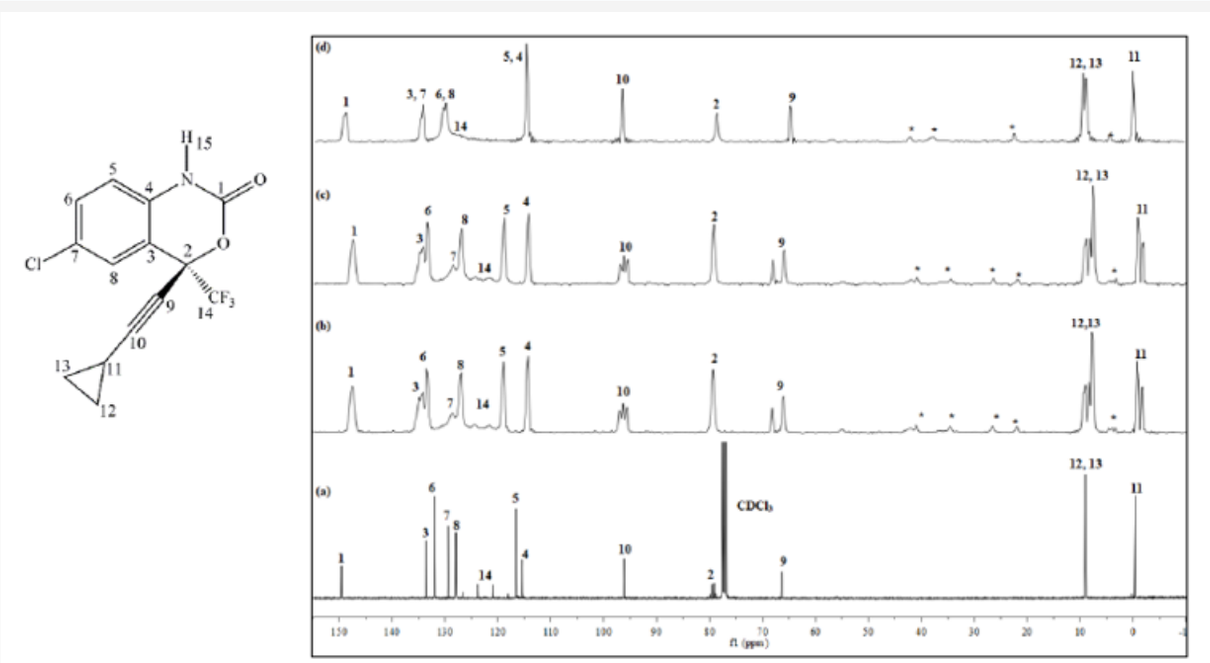


Figure 5: ^{13}C NMR spectra of EFZ samples: (a) EFZ/NPR, $CDCl_3$ solution; (b) EFZ/NPR, CPMAS; (c) EFZ/MIC, CPMAS; and (d) EFZ/HEPT, CPMAS. *denotes spinning side bands [14].

Acknowledgement

None.

Conflict of Interest

The authors declare no conflict of interest.

References

1. Zwanziger JW, Spiess HW (2010) Solid State NMR, Methods. In: Encyclopedia of Spectroscopy and Spectrometry (2nd edn.), Academic Press, San Diego, London, pp. 2587-2594.
2. Alcântara GB, Lião LM, San Gil RAS, Menezes SMC (2014) Fundamentos e Aplicações da Ressonância Magnética Nuclear: Ressonância Magnética Nuclear de Alta Resolução com Rotação em torno do ângulo Mágico: Uma abordagem teórico Prática (1ªed.), Auremn, Rio de Janeiro, Brasil 1-46.
3. Tishmack PA, Bugay DE, Byrn SR (2003) Solid-state nuclear magnetic resonance spectroscopy--Pharmaceutical applications. J Pharm Sci 92(3): 441-474.
4. Stejskal EO, Schaefer J (1977) Magic-angle spinning and polarization transfer in proton-enhanced NMR. J Magn Reason 28(1): 105-112.
5. Aguiar MRMP, Gemal AL, San Gil RAS (1998) Caracterização de polimorfismo em fármacos por ressonância magnética nuclear no estado sólido. Química Nova 22(4): 553-564.
6. Pines A, Gibby MG, Waugh JS (1973) Proton enhanced NMR of dilute spins in solids. J Chem Phys 59: 569-590.
7. Dixon WT, Schaefer J, Sefcik MD, Stejskal EO, Mckay RA (1982) Total suppression of sidebands in CPMAS C-13 NMR. J Magn Reson 49(2): 341-345.
8. Opella SJ, Frey MH (1979) Selection of Nonprotonated Carbon Resonances in Solid State NMR. J Am Chem Soc 101: 5854-5856.
9. Antzukin ON, Lee YK, Levitt MH (1998) and 15N-Chemical Shift Anisotropy of Ampicillin and Penicillin-V Studied by 2D-PASS and CP/MAS NMR. J Magn Res 135(1): 144-155.
10. Pindelska E, Szeleszczuk L, Pisklak DM, Mazurek A, Kolodziejski W (2015) Solid-state NMR as an effective method of polymorphic analysis: solid dosage forms of clopidogrel hydrogensulfate. J Pharm Sci 104(1): 106-113.
11. Aguiar DLM, San Gil RAS, Alencastro RB, Souza EF, Borré LB, et al. (2016) 6-aminopenicillanic acid revisited: A combined solid-state NMR and in silico refinement. Chemical Physics Letters 660: 214-220.
12. Skotnicki M, Apperley DC, Aguilar JA, Milanowski B, Pyda M, et al. (2016) Characterization of two distinct amorphous forms of valsartan by solid-state NMR. Mol Pharmaceutics 13 (1): 211-222.
13. Rezende CA, San Gil RAS, Borré LB, Pires JR, Vaiss VS, et al. (2016) Combining Nuclear Magnetic Resonance Spectroscopy and Density Functional Theory Calculations to Characterize Carvedilol Polymorphs. J Pharm Sci 105(9): 2648-2655.
14. Sousa EGR, Carvalho EM, San Gil RAS, Santos TC, Borré LB, et al. (2016) Solution and solid-state NMR spectroscopic characterization of efavirenz. J Pharm Sci 105(9): 2656-2664.
15. Silva RP, Ambrósio MFS, Piovesan LA, Freitas MCR, Aguiar DLM, et al. (2018) New Polymorph Form of Dexamethasone Acetate. Journal of Pharmaceutical Sciences 107(2): 672-681.
16. Romani LFA, Yoshida MI, Gomes ECL, Machado RR, Rodrigues FF, et al. (2018) Physicochemical characterization, the Hirshfeld surface, and biological evaluation of two meloxicam compounding pharmacy samples. Journal of Pharmaceutical Analysis 8(2): 103-108.
17. Szeleszczuk L, Pisklak DM, Gubica T, Matjakowska K, Kaźmierski S, et al. (2019) Application of combined solid-state NMR and DFT calculations for the study of piracetam polymorphism. Solid State Nucl Magn Reson 97: 17-24.

Pharmaceutical Research, Vol. 12, No. 7, 1995

Review

Pharmaceutical Solids: A Strategic Approach to Regulatory Considerations

Stephen Byrn,[1,4] Ralph Pfeiffer,[1] Michael Ganey,[2,3] Charles Hoiberg,[2] and Guirag Poochikian[2]

Purpose. This review describes a conceptual approach to the characterization of pharmaceutical solids. ***Methods.*** Four flow charts are presented: (1) polymorphs, (2) hydrates, (3) desolvated solvates, and (4) amorphous forms. ***Results.*** These flow charts (decision trees) are suggested as tools to develop information on pharmaceutical solids for both scientific and regulatory purposes. ***Conclusions.*** It is hoped that this review will lead to a more direct approach to the characterization of pharmaceutical solids and ultimately to faster approval of regulatory documents containing information on pharmaceutical solids.

KEY WORDS: polymorph; hydrate; amorphous form; desolvated solvate.

Interest in the subject of pharmaceutical solids stems in part from the Food and Drug Administration's (FDA's) drug substance guideline that states "appropriate" analytical procedures should be used to detect polymorphic, hydrated, or amorphous forms of the drug substance. These guidelines suggest the importance of controlling the crystal form of the drug substance. The guideline also states that it is the applicant's responsibility to control the crystal form of the drug substance and, if bioavailability is affected, to demonstrate the suitability of the control methods.

Thus, while it is clear that the New Drug Application (NDA) should contain information on solid state properties, particularly when bioavailability is an issue, the applicant may be unsure about how to scientifically approach the gathering of information and perhaps what kind of information is needed. This review is intended to provide a strategic approach to remove much of this uncertainty by presenting concepts and ideas in the form of flow charts rather than a set of guidelines or regulations. This is especially important because each individual compound has its own peculiarities which require flexibility in approach. The studies proposed herein are part of the Investigational New Drug (IND) process.

Solid drug substances display a wide and largely unpredictable variety of solid state properties. Nevertheless, application of basic physicochemical principles combined with appropriate analytical methodology can provide a strategy for scientific and regulatory decisions related to solid state behavior in the majority of cases. By addressing *fundamental* questions about solid state behavior at an early stage of drug development, both the applicant and the FDA are in a better position to assess the possible effects of any variations in the solid state properties of the drug substance. The resulting early interaction of the parties with regard to this area would not only tend to ensure uniformity of the materials used throughout the clinical trials but also fully resolve solid state issues before the critical stages of drug development. A further benefit of these scientific studies is the development of a meaningful set of solid state specifications which critically describe the solid form of the drug substance. These specifications would thus also facilitate the approval of a change in supplier or chemical process.

Our approach in this review is to suggest a sequence for collecting data on a drug substance that will efficiently answer specific questions about solid state behavior in a logical order. In "difficult" cases, perhaps where mixtures of forms must be dealt with, or other unusual properties are encountered, the suggested sequences would still have to be followed as a first stage in this investigation.

We have chosen to present this approach in the form of a series of decision trees, or flow charts (algorithms), one for each of the most common solid state forms. The charts are accompanied by examples from the literature representing the kind of data that would be useful in supporting the various decisions.

Decision trees provide conceptual frameworks for understanding how the justification for different crystal forms might be presented in the drug application. Industry may wish to use these decision trees as a strategic tool to organize the gathering of information early in the drug development process. Put another way, these decision trees provide a thought process that will lead to development of the most

[1] Department of Medicinal Chemistry and Pharmacognosy, Purdue University, West Lafayette, Indiana 47907.
[2] Division of Oncology and Pulmonary, Food and Drug Administration, 5600 Fishers Lane, Rockville, Maryland 20857.
[3] Current Address: Pfizer Central Research, Groton, Connecticut.
[4] To whom correspondence should be addressed.

0724-8741/95/0700-0945$07.50/0 © 1995 Plenum Publishing Corporation

appropriate analytical controls. One should also note that it is the responsibility of the industry to select the appropriate test or tests to identify the phase of the solid and determine its relevant pharmaceutical properties. This approach is superior to simply performing a broad range of tests without regard to their relevance.

We should point out that, from a regulatory standpoint, if a company can establish a specification/test to ensure production of a well defined solid form of the drug substance, then it is not necessary to do all of the physical/chemical testing outlined in the decision trees. From a scientific standpoint, however, such an approach is risky since new forms may appear unpredictably during various stages of the development process. The appearance of these new forms usually slows the drug approval process and makes planning difficult.

Four decision trees are described in the sections that follow: Polymorphs; Hydrates (Solvates); Desolvated Solvates; and Amorphous Forms. Polymorphs exist when the drug substance crystallizes in different crystal packing arrangements all of which have the same elemental composition (Note that hydrates can exist in polymorphs). Hydrates exist when the drug substance incorporates water in the crystal lattice in either stoichiometric or nonstoichiometric amounts. Desolvated solvates are produced when a solvate is desolvated (either knowingly or unknowingly) and the crystal retains the structure of the solvate. Amorphous forms exist when a solid with no long range order and thus no crystallinity is produced. It is apparent that the appropriate flow chart can only be determined after the solid has been characterized using some of the tests described in the first decision point of the decision trees/flow charts (i.e. X-ray powder diffraction, elemental analysis, etc.). If there is no interest in marketing or producing an amorphous form or desolvated solvate at any stage in the process, then the corresponding flow charts do not need to be addressed. As already mentioned, it is advisable to investigate the drug substance for the existence of polymorphs and hydrates since these may be encountered at any stage of the drug manufacturing process or upon storage of the drug substance or dosage form.

All of the flow charts end (see for example Figure 1) with an indication of the types of controls which will be required based on whether a single morphic form or a mixture will be produced as the drug substance. Although this ending provides a simplistic view of a very complicated process of selecting appropriate controls, it is included to illustrate the consequence of the decisions made with regard to the drug substance. The reader should realize that the actual selection of the appropriate control could be the subject of another review which might contain another set of flow charts or decision trees.

POLYMORPHS

The flow chart/decision tree for polymorphs is shown in Figure 1. It outlines investigations of the formation of polymorphs, the analytical tests available for identifying polymorphs, studies of the physical properties of polymorphs and the controls needed to ensure the integrity of drug substance containing either a single morphic form or a mixture.

A. Formation of Polymorphs—Have Polymorphs Been Discovered?

The first step in the polymorphs decision tree is to crystallize the substance from a number of different solvents in order to attempt to answer the question: Are polymorphs possible? Solvents should include those used in the final crystallization steps and those used during formulation and processing and may also include water, methanol, ethanol, propanol, isopropanol, acetone, acetonitrile, ethyl acetate, hexane and mixtures if appropriate. New crystal forms can often be obtained by cooling hot saturated solutions or partly evaporating clear saturated solutions. The solids produced are analyzed using X-ray diffraction and at least one of the other methods. In these analyses, care must be taken to show that the method of sample preparation (i.e. drying, grinding) has not affected the solid form. If the analyses show that the solids obtained are identical (e.g. have the same X-ray diffraction patterns and IR spectra) then the answer to the question "Are polymorphs possible?" is "No",

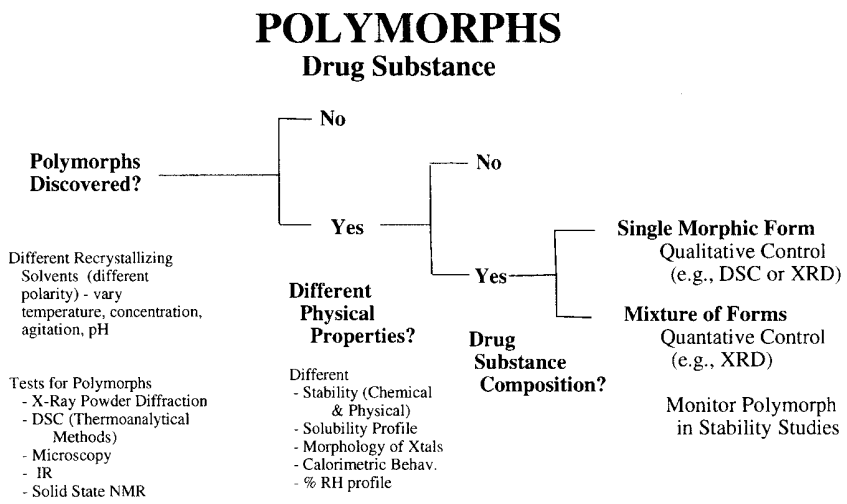


Figure 1. Flow chart/decision tree for polymorphs.

and further research is not needed. The work of Miyamae *et al.* serves as a good example of solid state studies of a drug substance which exists as polymorphs (1). Powder diffraction showed that there were two crystal forms (see Figure 2).

These workers also carried out single crystal analysis of the two crystal forms of the compound. The structures are shown in Figure 3. While such studies are not required, and indeed sometimes not possible, they provide an unequivocal confirmation of the existence of polymorphs. Moreover, once the single crystal structure of a phase has been determined, it is possible to calculate the corresponding X-ray powder pattern. This provides an irrefutable standard for identifying the phase by that method.

The DSC thermal curves of the two forms are slightly different, as shown in Figure 4 and thus may not be the preferred way of differentiating these polymorphs.

The IR spectra of the two polymorphs are quite similar(1), and IR does not appear to be a powerful method for differentiating the crystal forms in this case. Thus, for 8-(2-methoxycarbonylamino-6-methylbenzyloxy)-2-methyl-3-(2-propynyl)-imidazo{1,2-a}pyridine, powder diffraction appears to be the best method for differentiating the two forms.

Solid-state NMR is another powerful technique for analyzing different crystal forms (2,3). Figure 5 shows the solid-state C-13 NMR spectra of Forms I and II of prednisolone. Differences in the positions of the two resonances in the 120 ppm range clearly differentiate the two forms. In principle, solid state NMR is an absolute technique in which the signal intensity is proportional to the number of nuclei provided appropriate conditions are met. In addition, solid state NMR is a bulk technique which is not very sensitive to surface changes. This method appears to be very sensitive and will undoubtedly be used more often in the future as a tool to detect different crystal forms. However, with present technology, errors in solid-state quantitative studies may be rather large.

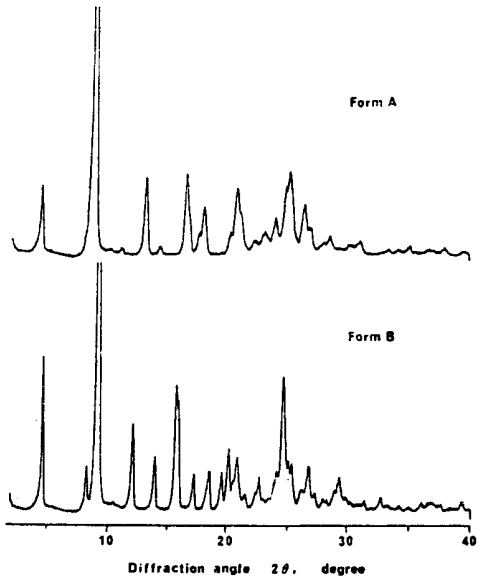


Figure 2. Powder X-ray diffraction patterns of the polymorphs of 8-(2-methoxycarbonylamino-6-methylbenzyloxy)-2-methyl-3-(2-propynyl)-imidazo{1,2-a}pyridine (1).

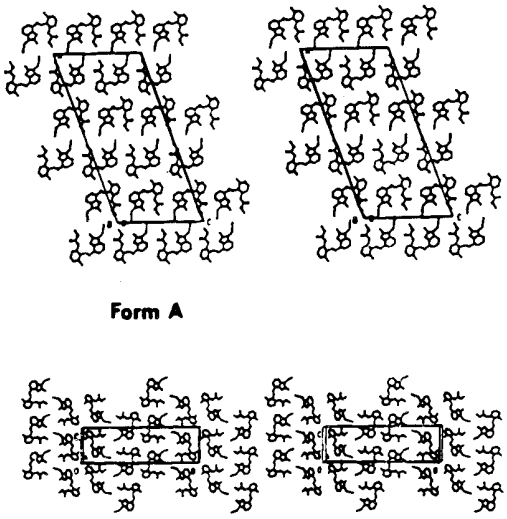


Figure 3. Stereoscopic drawings of the crystal packing of both polymorphs of 8-(2-methoxycarbonylamino-6-methylbenzyloxy)-2-methyl-3-(2-propynyl)-imidazo{1,2-a}pyridine viewed along the shortest axis (Form A, b-axis; Form B, a-axis) (1).

B. Do the Polymorphs Have Different Physical Properties?

If polymorphs exist then it is necessary to examine the physical properties of the different polymorphs that can affect dosage form performance (bioavailability and stability) or manufacturing reproducibility. The properties of interest are solubility profile (intrinsic dissolution rate, equilibrium solubility), stability (chemical and physical), and crystal morphology (including both shape and particle size), calorimetric behavior, and %RH profile. If there are no discernible differences between these physico-chemical properties, then the answer to the second question in the decision tree, "Different physical properties?" is "No."

The variable physical properties of several drugs with different polymorphs are reported in the literature. For example, the dissolution profiles of the polymorphs of chloramphenicol are significantly different (4). In addition, van't Hoff solubility analysis has been used to elucidate the dif-

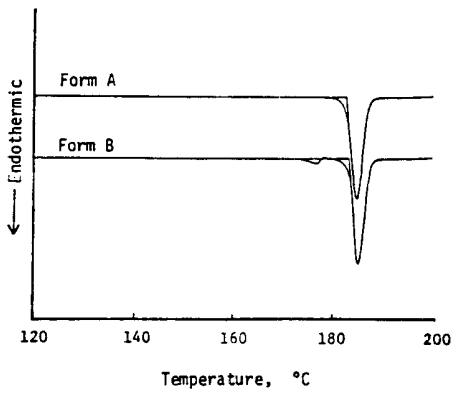


Figure 4. DSC thermal curves of the polymorphs of 8-(2-methoxycarbonylamino-6-methylbenzyloxy)-2-methyl-3-(2-propynyl)-imidazo{1,2-a}pyridine (1). These curves show that Form A melts whereas Form B undergoes a small endothermic transition and then melts at the same temperature as Form A.

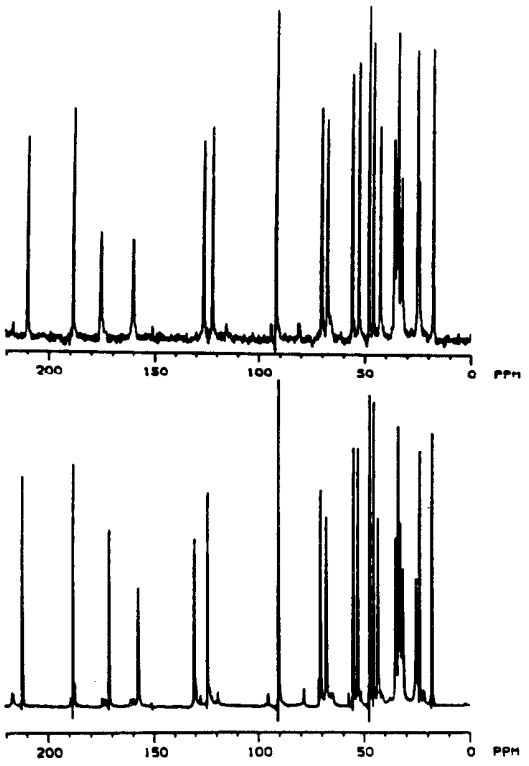


Figure 5. Solid state NMR of the two Crystal Forms of Prednisolone (2).

ferent solubilities of two polymorphs of methyl prednisolone(5). This method involves determining the equilibrium solubility of each polymorph at various temperatures. The log of the equilibrium solubility is then plotted vs 1/T. This should give straight lines for each polymorph and the temperature at which the curves intersect is the transition temperature. This technique does not work if the polymorphs interconvert.

For balance, it is important to point out that there are also cases where polymorphs exist but they have virtually identical dissolution properties(6).

C. Drug Substance Control

The important question lies in the properties that differ among polymorphs and whether those properties affect the dosage form performance (i.e., quality or bioavailability). If they do then from a regulatory standpoint it is appropriate to establish a specification/test (e.g. powder X-ray diffraction or IR) to ensure the proper form is produced. From a production standpoint, it is important to develop a process that reproducibly produces the desired polymorph.

If mixtures of forms cannot be avoided, then quantitative control is needed to ensure that a fixed proportion of forms is obtained. Furthermore, the method of analyzing for the proportion of forms would have to be validated. Also, the proportion of forms would have to remain within stated limits through the retest date of the drug substance and potentially throughout the shelf life of the product; a difficult requirement if the forms interconvert. Thus, the way to avoid a substantial amount of work in this area is to select a single solid form for production. Usually, this would be the most physically stable form when their bioavailabilities are not significantly different. Selection of the most stable from would, of course, insure that it there would be no conversion into other forms.

Powder diffraction is often a useful method to determine the percentages of polymorphs in a mixture; however, the detection limit is variable from case to case and can be as high as 15%. Matsuda (7) carried out a mixture analysis of phenylbutazone polymorphs. Diffraction lines disappear and appear as the ratio of the crystal forms change. Some of these calibration curves developed from this analysis are almost horizontal, meaning that any given mixture gives the same line intensity in this mixture range. However, other calibration curves are sloped and would appear to allow a reasonable analysis. It is fair (although Matsuda did not carry out an estimate) to estimate the errors in this analysis as $\pm 15\%$.

Tanninen and Ylirussi (8) used computer curve fitting to carry out a mixture analysis of prazosin. In this particular case, they reported a highly accurate analysis, and, in fact, showed a calibration curve that could detect 0.5% of one form in another. This is obviously a highly accurate mixture analysis by powder diffraction and shows the power of this method for some applications. However, this analysis required extreme care in sample preparation and may be more difficult to carry out in a production setting where particle size may not be controlled. Similar comments apply to the analysis of mixtures by IR, where the accuracy and precision may also vary considerably from case to case. Given the analytical problems in dealing with mixtures of forms, it may generally be simpler to develop a method to prepare only one crystal form.

In summary, it is important to determine whether polymorphs are present and to solve any problems before pivotal clinical studies are initiated.

D. Determination of the Polymorph Present in the Drug Product

In cases where stability or bioavailability issues exist, the solid form present in the drug product should be investigated, if possible.

For bulk drug substances, X-ray powder diffraction and other techniques can identify the polymorph; however, solid state NMR appears to be the best method for the study of the drug substance in the dosage form (2, 3). Solid-state NMR study of three commercial products containing prednisolone showed that the products A and B contain Form I, whereas product C contains Form II.. This analysis was possible even though these tablets contain approximately 95 mg of excipients and 5 mg of drug. There are numerous cases, often involving complex mixtures or low dose products, where solid state NMR (and, in fact, any technique) will not be sensitive enough to identify the polymorph present in the drug product. However, the safety and efficacy is, of course, controlled by the potency assays and by the physical tests (e.g., dissolution).

HYDRATES (SOLVATES)

The flow chart/decision tree for hydrates (solvates) is shown in Figure 6. It outlines investigations of the formation

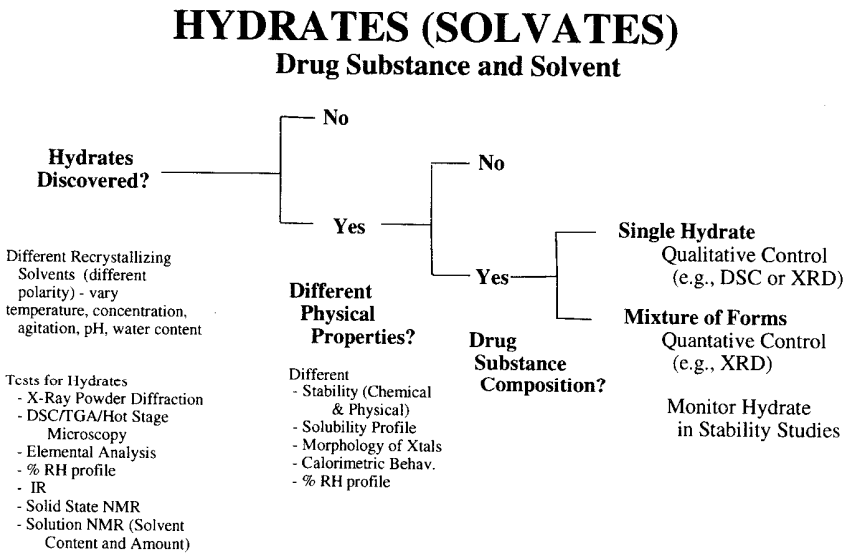


Figure 6. Flow chart for solvates or hydrates.

of hydrates (solvates), the analytical tests available for hydrates (solvates), studies of the physical properties of hydrates (solvates) and the controls needed to ensure the integrity of drug substance containing either a single morphic form or a mixture.

A. Have Hydrates (Solvates) Been Discovered?

The flow chart for hydrates (solvates) (Figure 7) is applied after the preliminary crystallizations have been completed. These are essentially the same as in the polymorph decision tree but, in addition, should include solvent-water mixtures in order to maximize the chance for hydrate formation. These experiments can be guided by the moisture uptake (% RH) studies. Any solids that indicate a significant change in water content as indicated by the % RH-moisture profile should also be examined. The resulting solid phases are preferably characterized by a combination of methods—two for phase identity and two to reveal composition and stoichiometry.

With a very few exceptions, the structural solvent contained in marketed crystalline drug products is water. It is nevertheless often desirable to characterize other solvated crystalline forms of a drug for several reasons: they may be the penultimate form used to crystallize the final product and thus require controlled characterization; they may form if the final crystallization from solvents, especially mixed solvents, is not well controlled; they may be the actual crystallized form of a final product that is desolvated during a final drying step; they may be the form used in recovery for subsequent rework. The relevance of these points will vary from case to case, but for the present discussion we shall treat the subject of solvates in its broadest form.

Examples taken from the literature serve to illustrate the kind of data that proves useful in characterizing solvated crystal forms. For example, a recent report from our laboratory showed that IR and solid state NMR was useful for the identification of the different crystal forms of dirithromycin(9). TGA is another powerful method for the analysis of solvates. For example, one early study showed that TGA could differentiate three different hydrated salts of fenoprofen(10). Combined with IR or other methods, TGA is an unequivocal method for the verification of the existence of solvates. In addition, TGA is a good method for looking at mixtures of solvated and unsolvated crystal forms, and probably can be developed into an analytical method for determining the ratios of solvated and unsolvated forms.

DSC is also a good method for detecting solvates since there is usually heat change involved in desolvation, especially for hydrates(11). Specifically, DSC by itself does not prove the existence of a solvate, but once other analytical

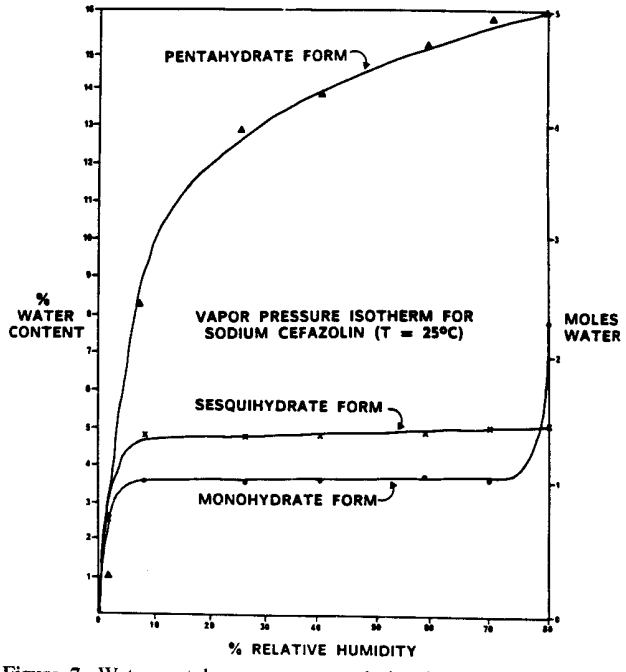


Figure 7. Water uptake vs percent relative humidity for sodium cefazolin.

data from TGA, NMR, etc. are available, DSC becomes a good method for analyzing solvates and determining a percentage of solvates present.

The three solvates of ethynylestradiol (0.5 acetonitrile, 1.0 methanol, 0.5 water) provides another interesting example (12). These solvates have different cell parameters and are crystallographically completely distinct materials. The hemihydrate was obtained from an organic solvent which is not completely miscible with water but was saturated with water. In fact, it is known that crystallization from water-immiscible solvents containing small but slightly different proportions of water can produce different hydrates of a substance.

The DSC/TGA of the three ethynylestradiol solvates(12) are unique and in this case it may be possible to develop DSC/TGA into an analytical procedure for determining the proportions of each solvate. The DSC in some of these traces appears to show a melt and recrystallization corresponding to the loss of solvent of crystallization. However, the exact interpretation of this is not possible without either a DSC microscope or interrupting the tracing to analyze the sample at various temperatures. The methanolate appears to lose solvent in two equal steps, indicating that there may also be a hemimethanolate of this compound. Again, confirmation of this would require interrupting the heating and analyzing the substance after the first solvent loss has occurred. In addition, the DSC/TGA traces suggest that all of the forms are converted to an anhydrous form which then melts at a higher temperature. Thus, interrupting any one of these thermal curves just prior to the final melt could reveal a new form that gives the powder pattern for the anhydrate. Unfortunately, no data of this type is provided in the case cited.

DSC analysis of solvates should be carried out using either an open pan or a pan with a pin-prick; otherwise, unusual and variable results will be obtained because the solvent is not provided a way of escape from the pan. One advantage of using an open pan for DSC is that it reproduces the conditions under which the TGA is performed.

Comparison of the ethinylestradiol powder diffraction patterns clearly establishes that these solvates are different crystal forms as would be expected from the single crystal data(12). In summary, DSC, TGA, and powder diffraction are all good methods for analysis of the different crystal forms of ethinylestradiol.

Figure 7 shows a percent relative humidity versus water uptake study of the type recommended by the USP committee on water(13) In this case, there are two hydrates which are relatively well behaved insofar as they are completely hydrated at about 10% relative humidity and remain uniformly hydrated throughout a wide humidity range. On the other hand, the so-called pentahydrate, which really is only a pentahydrate at very high humidity, changes water content considerably as the relative humidity is changed. The USP committee on moisture specifications recommended that moisture uptake vs relative humidity studies should be routinely performed on all drug substances and excipients (13).

B. Do the Hydrates (Solvates) Have Different Physical Properties?

The physical properties of hydrates are often quite different from the anhydrate form. Figure 8 shows the dissolution profile of theophylline hydrate and anhydrate. This figure shows that the anhydrate reaches a much higher solubility in water, and on extended exposure recrystallizes to the less soluble hydrate. Such differences must be further examined for possible effects on bioavailability.

In our laboratory we have described the different crystal forms of hydrocortisone-21-tertiary butylacetate(14). Our studies showed that the nonstoichiometric ethanolate is oxygen-sensitive and, of course, would show different physical properties from the stoichiometric ethanolate and the other solvates. Prednisolone tertiary-butylacetate also exists as a nonstoichiometric hydrate which is oxygen sensitive(15). Thus, these are cases where different crystal forms have different chemical stability, although there may be no significant differences in solubility.

C. Mixtures of Polymorphs and Hydrates

Other drug substances exist as both polymorphs and solvates. For example, furosemide exists in two polymorphs, two solvates, and an amorphous form (16, 17). The polymorphs are enantiotropically related, which means that at one temperature one polymorph is more stable, but at a different temperature the other polymorph is physically more stable. That is, plots of solubility versus temperature cross for the two polymorphs. In addition, the different crystal forms have different photostability (chemical stability in light) and moreover have different dissolution rates. Thus, there are significant differences in both chemical and physical properties.

The five different forms, or modifications of furosemide, give clearly different powder patterns. Thus, powder diffraction is a good method for analysis of these different forms. There are similarities between the IR spectra of the five different forms but there are also some significant differences, and expansion and careful analysis could lead to an FT/IR method for analysis of these different forms. IR would probably be a useful method for analysis at least for pairs of these compounds. However, it is not clear whether IR could be used to determine the percentages of several different forms in a more complex mixture. The DSC and TGA of the different forms are significantly different. As expected, the solvates show weight loss in the TGA.

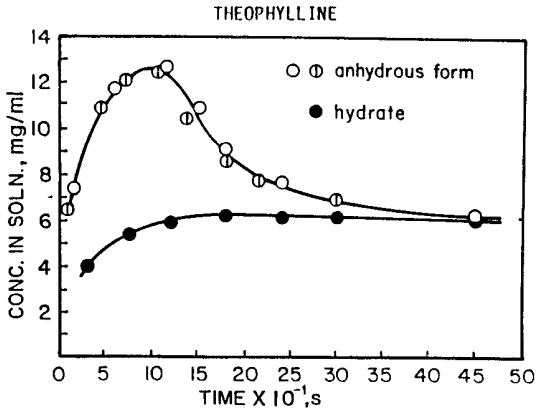


Figure 8. The dissolution-time curves for anhydrous and hydrated theophylline in water at 25°. The two types of open circles represent successive experiments (18).

The interconversion of the different forms of furosemide have been analyzed and a diagram constructed. Such a diagram can be experimentally difficult when so many pairs of crystal forms must be studied for possible interconversions and under different conditions. It is clear from this diagram that many of the forms of furosemide can be converted to form I. This study is one of the most complete reports of solvates and polymorphs available in the literature and serves as a model for studies of such systems for regulatory submissions.

D. Determination of the Hydrate Present in the Drug Product

Another important area is the analysis of the material which is produced after wet granulation of a substance which can form hydrates. We are aware of cases where the bulk drug substance is manufactured and stored as the anhydrate. However, upon wet granulation, there is a conversion (either partial or complete) to a hydrate. Subsequent drying is sometimes not adequate to convert the substance back to the anhydrate, and a hydrate or a mixture of hydrate and anhydrate remain. The formation of a hydrate and its subsequent drying can result in a change in particle size of the drug substance (19). It may also be possible to cause transformations during other processing steps. It is thus recommended that if wet granulation or processing that subjects the drug to even brief changes in temperature or pressure (e.g. milling or compression) is contemplated, then extensive studies of the ability to convert the drug substance to a new crystal form be carried out by mimicking the processing step in the laboratory.

DESOLVATED SOLVATES

The term "desolvated solvates" refers to compounds that are crystallized as solvates but undergo desolvation prior to analysis. Often these "desolvated solvates" retain the structure of the solvate with relatively small changes in the lattice parameters and atomic coordinates, but no longer contain the solvent. In addition, desolvated solvates are apt to be less ordered that their crystalline counterparts. These forms are particularly difficult to characterize properly since analytical studies indicate that they are unsolvated materials (anhydrous crystal forms) when, in fact, they have the structure of the solvated crystal form from which they were derived. Several observations may give clues that one is dealing with a desolvated form: (1) The form can be obtained from only one solvent; (2) On heating, the form converts to a structure known to be unsolvated; and (3) The form has a particularly low density compared to other forms of the same substance. Experiments that help to clarify whether an apparently solvent free modification is a desolvated form or a true anhydrate include: (1) Single crystal X-ray structure determination in the presence of mother liquor from the crystallization; (2) comparison of the X-ray powder diffraction patterns and solid state NMR spectra of the solvated and desolvated crystal forms; and (3) determination of the vapor pressure isotherm by varying the vapor pressure of the specific solvent involved. A desolvated form will often take up stoichiometric amounts of the relevant solvent. In addition, crystals of the form directly isolated from the crystallizing medium will show a plateau in their isotherm as the vapor pressure of the solvent is reduced.

Figure 9 shows the flow chart used to address regulatory issues involving desolvated solvates. It is similar to the polymorphs flow chart except that the first question involves determining whether a solvate was formed initially and then desolvated, perhaps by "air drying." The remaining questions are identical to the polymorphs flow chart.

Figure 10 shows the behavior of three different crystal forms of the same antibiotic. One crystal form takes up about two waters of hydration and further analysis indicated that it was the dimethanolate which had been desolvated by drying. The second crystal form takes up approximately one water and was originally the monomethanolate which had been desolvated by drying. The third crystal form also takes up

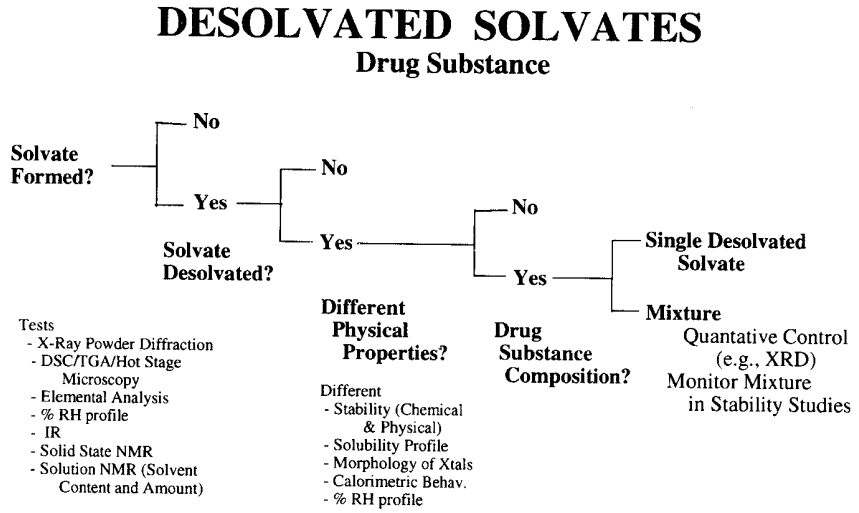


Figure 9. Flow chart for desolvated solvates.

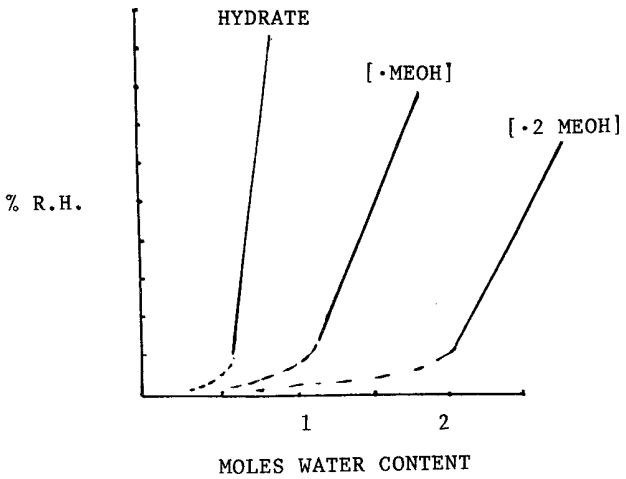


Figure 10. Water sorption by three crystal forms of cephaloridine. The brackets indicate the crystal form produced by desolvating the designated methanolate.

about one molecule of water and is the 0.75 hydrate typically obtained from water solution.

AMORPHOUS FORMS

Amorphous forms are of substantial interest because they usually are much more soluble than their crystalline counterparts. Indeed, there are cases where the amorphous forms is the only solid form that has adequate bioavailability. The initial question with this flow chart (Figure 11) is similar to the previous ones: "Are amorphous forms possible?" Amorphous forms can be prepared in different ways, for example, by spray drying or by freeze drying. One can test whether an amorphous form has been produced by using one of the methods listed. X-ray powder diffraction and microscopy are the two primary methods for determining whether an amorphous form has been produced. Powder diffraction is an excellent method for determining the existence of an amorphous form since they usually exhibit a broad hump between 2 and 20° 2θ. An amorphous form is expected to have no peaks in the powder diffraction pattern. The USP test for the presence of an amorphous form involves determining, by microscopy, whether the material lacks birefringence. IR and solid-state NMR may be useful for detecting amorphous forms since the amorphous nature of the solid sometimes results in broad lines, or in NMR, altered relaxation times. The next question on the flow chart is: "Do the amorphous forms have different physical properties?" The answer to this question will almost certainly be "Yes." Three differences from crystalline forms may generally be expected: 1) Amorphous forms would have greater solubility, 2) Amorphous forms take up water more extensively, and 3) Amorphous forms are sometimes less chemically stable. Another key question for an amorphous form is: "Does it crystallize, and how and when?" This question is very important since inadvertent crystallization can greatly affect the solubility and dissolution rate, and lead to other failures in formulation. Attempts to purposely cause amorphous forms to crystallize can provide information on the parameters involved in crystallization of amorphous forms. Specific questions include: (1) "Does the amorphous form crystallize upon exposure to heat and/or humidity?," and (2) "What other factors (e.g. mechanical pressure and seeding) can lead to the crystallization of the amorphous forms?"

The amorphous form of any substance can be partly characterized by the glass transition temperature, T_g (11). When heated to a temperature above T_g, the solid transforms from a glassy state to a more fluid-like rubbery state. The corresponding increased molecular mobility greatly raises the likelihood of two adverse events: (1) Crystallization and subsequent decreased solubility; and (2) Reduced chemical stability in the more reactive amorphous solid. Amorphous solids are also often prone to absorb moisture and this water sorption reduces the glass transition temperature further. The weight of water required to reduce the glass transition

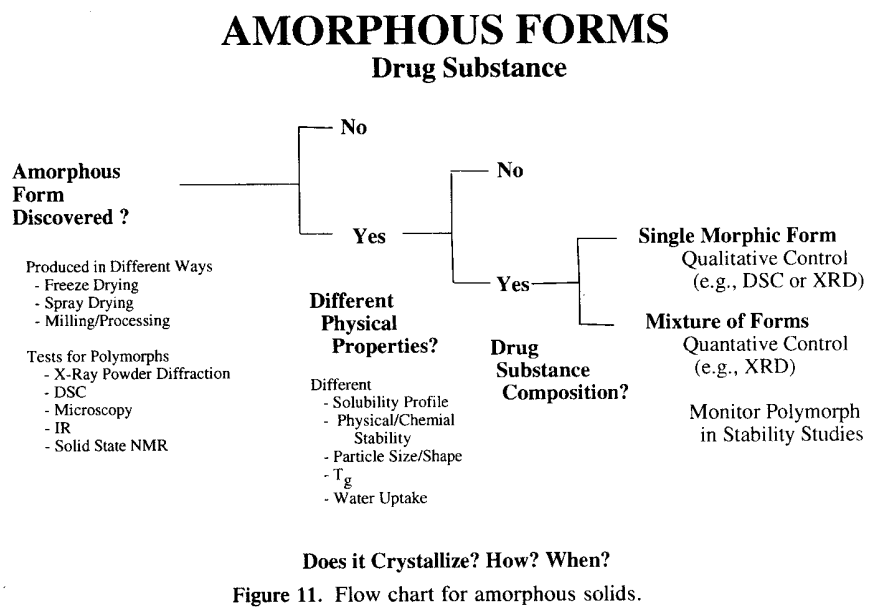


Figure 11. Flow chart for amorphous solids.

temperature to room temperature is of obvious interest and is termed W_g. Table I shows a series of interesting studies on amorphous forms of some common pharmaceuticals.

The table compares the glass transition temperatures (T_g) of a number of pharmaceutical solids with the melting temperatures (T_m). It is interesting that the average ratio of the glass transition temperature to the melting temperature is about 0.70. This table provides a simple rule of thumb which allows the prediction of the glass transition temperature of pharmaceuticals from the known melting point. Crystallization and other solid-state phenomena, such as degradation reactions, as we have said, would be more likely to occur at temperatures above the glass transition temperature. For stability, one might, therefore, wish to prepare amorphous forms only for drugs which have a T_g well above room temperature.

Amorphous indomethacin crystallizes upon standing at room temperature(Figure 12). Obviously, formulations containing amorphous indomethacin are at significant risk to crystallize and thus become less soluble. This has to some extent hampered preparing more bioavailable indomethacin dosage forms.

Quantitative analysis of mixtures of amorphous and crystalline forms provides some challenges. Cefixamine trihydrate is the subject of some early research in this area. This antibiotic, upon grinding, became a mixture of crystalline and amorphous forms. A calibration curve based upon analyzing the height of a selected powder X-ray peak was constructed and used to determine the crystallinity versus grinding time for this system. It is clear that powder diffraction provides a way to estimate the amount of amorphous cefiximine. These studies show that milling and other similar processing steps can create amorphous material and that this process may be detectable. As with wet granulation where transitions to hydrated forms can occur, processing of the drug substance can promote the formation of amorphous drug.

Pikal has compared the analysis of mixtures of crystalline and amorphous forms of several antibiotics by powder diffraction and calorimetry (20). His studies indicate that calorimetry can be a more accurate method for analysis of percent crystallinity but are complicated by water sorption. Zografi and co-workers (unpublished results) have developed a powerful method for the determination of low percentages of amorphous material based on the general propensity of amorphous materials to sorb moisture.

Table I. Pharmaceuticals Forming Glasses Above Room Temperature (21)

Pharmaceutical	T_g (K)	T_m (K)	T_g/T_m
Cholecalciferol	296	352	0.84
Sulfisoxazole	306	460	0.67
Stilbestrol	308	439	0.70
Phenobarbital	321	443	0.72
Quinidine	326	445	0.73
Salicin	333	466	0.71
Sulfathiazole	334	471	0.71
Sulfadimethoxine	339	465	0.73
Dehydrocholic acid	348	502	0.69
17β-Estradiol	351	445	0.80

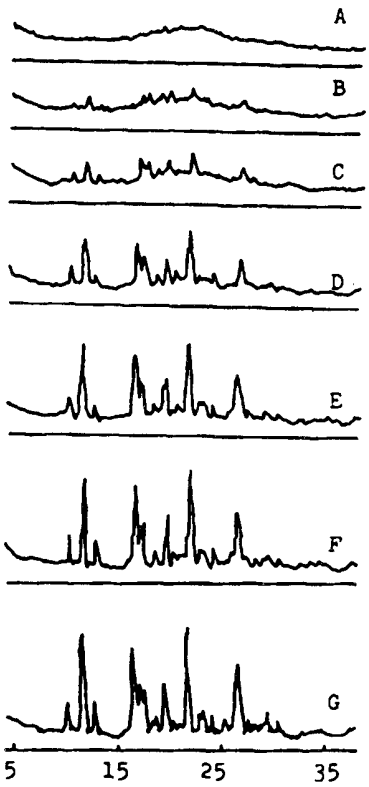


Figure 12. Behavior of amorphous indomethacin upon standing: A, at start; B 24 h; C, 48 h; D, 7d; E, 14d; F, 30d; G, 67d (22).

SUMMARY

Four flow charts which describe approaches to regulatory issues involving pharmaceutical solids have been developed. These flow charts are for the different types of solids generally encountered (polymorphs, solvates, desolvated solvates, and amorphous forms). It is hoped that these flow charts will guide the solid-state research needed to prepare a comprehensive regulatory submission on the physicochemical properties of a pharmaceutical. It is also hoped that this review has provided enough information to allow the generation of results and information necessary to prepare a drug substance submission that will be quickly approved.

ACKNOWLEDGMENTS

This review was supported in part by funds from the Purdue-Wisconsin Joint Project for the Study of the Effect of Water on the Molecular Mobility of Solid Pharmaceuticals (Members: Merck, Sandoz, Upjohn, Glaxo, Pfizer, 3M, Hoffmann-LaRoche, Syntex, Bristol-Myers Squibb). Helpful comments were provided by scientists from Merck (West Point and Montreal), Glaxo, Bristol-Myers Squibb, Syntex, Upjohn, Pfizer, Lilly, Sandoz, Pfizer, and Roche.

REFERENCES

1. A. Miyamae, S. Koda, S. Kitamura, Y. Okamoto, and Y. Morimoto. X-ray crystallographic characterization of two poly-

morphs of 8-(2-methoxycarbonylamino-6-methylbenzyloxy)-2-methyl-3-(2-propynyl)imidazo[1,2-a]pyridine, *J. Pharm. Sci.* **79**:189–195 (1990).
2. P. A. Saindon, N. S. Cauchon, P. A. Sutton, C. J. Chang, G. Peck, and S. R. Byrn. Solid-state nuclear magnetic resonsance (NMR) spectra of pharmaceutical dosage forms, *Pharm. Res.* **10**:197–203 (1993).
3. D. E. Bugay. Solid-state nuclear magnetic resonance spectroscopy: Theory and pharmaceutical applications, *Pharm. Res.* **10**:317–327.
4. J. K. Haleblian and W. C. McCrone. Pharmaceutical Applications of Polymorphism, *J. Pharm. Sci.* **58**:911 (1969).
5. W. I. Higuchi, P. K. Lau, T. Higuchi, and J. W. Shell. Polymorphism and Drug Availability, *J. Pharm. Sci.* **52**:150–153 (1963).
6. D. P. Ip, G. S. Brenner, J. M. Stevenson, S. Lindenbaum, A. W. Douglas, S. D. Klein, and J. A. McCauley. High resolution spectroscopic evidence and solution calorimetry studies on the polymorphs of enalapril maleate, *Int. J. Pharm.* **28**:183–191 (1986).
7. Y. Matsuda, E. Tatsumi, E. Chiba, and Y. Miwa. Kinetic study of the polymorphic transformations of phenylbutazone, *J. Pharm. Sci.* **73**:1453–1460 (1984).
8. V. P. Tanninen and J. Yliruusi. X-ray powder diffraction profile fitting in quantitative determination of two polymorphs from their powder mixture, *Int. J. Pharm.* **81**:169–177 (1992).
9. G. A. Stephenson, J. G. Stowell, P. H. Toma, D. E. Dorman, J. R. Greene, and S. R. Byrn. Solid-State Analysis of Polymorphic, Isomorphic, and Solvated Forms of Dirithromycin, *J. Am. Chem. Soc.* **116**:5766–5773 (1994).
10. C. A. Hirsch, R. J. Messenger, and J. L. Brannon. Fenoprofen: drug form selection and preformulation stability studies, *J. Pharm. Sci.* **67**:231–236 (1978).
11. S. Niazi. Thermodynamics of mercaptopurine dehydration, *J. Pharm. Sci.* **67**:488–491 (1978).
12. T. Ishida, M. Doi, M. Shimamoto, N. Minamino, K. Nonaka, and M. Inoue. Physicochemical properties of crystalline forms of ethynylestradiol solvates: comparison of thermal behavior with x-ray crystal structure, *J. Pharm. Sci.* **78**:274 (1989).
13. G. Zografi, D. Hollenbeck, S. Laughlin, M. Pikal, J. Schwartz, and L. VanCampen. Report of the advisory panel on moisture specifications, *Pharmacopeial Forum:* 1459–1474 (1991).
14. C. T.Lin, P. Perrier, G. G. Clay, P. A. Sutton, and S. R. Byrn. Solid-State Photooxidation of Cortisol-21-tert-butylacetate to Cortisone-21-tert-butylacetate, *J. Org. Chem.* **47**:2978–82 (1982).
15. S. R. Byrn, P. A. Sutton, B. Tobias, J. Frye, and P. Main. Crystal structure, solid-state NMR spectra, and oxygen reactivity of five crystal forms of prednisolone tert-butylacetate, *J. Am. Chem. Soc.* **110**:1609–1614 (1988).
16. Y. Matsuda and E. Tatsumi. Physicochemical characterization of furosemide modifications, *Intl. J. Pharm.* **60**:11–26 (1990).
17. C. Doherty and P. York. Furosemide crystal forms; solid state and physicochemical analyses, *Int. J. Pharm.* **47**:141–155 (1988).
18. E. Shefter and T. Higuchi. Dissolution behavior of crystalline solvated and nonsolvated forms of some pharmaceuticals, *J. Pharm. Sci.* **52**:781–791 (1963).
19. I. Himuro, Y. Tsuda, K. Sekiguchi, I. Horikoshi, and M. Kanke. Studies on the method of size reduction of medicinal compounds. IV. Solvate formation of chloramphenicol and its application to size reduction, *Chem. Pharm. Bull.* **19**:1034–1040 (1971).
20. M. J. Pikal, A. L. Lukes, J. E. Lang, and K. Gaines. Quantitative crystallinity determinations for beta-lactam antibiotics by solution calorimetry: correlations with stability, *J. Pharm. Sci.* **67**:767–769 (1978).
21. E. Fukuoka, M. Makita, and S. Yamamura. Some physicochemical properties of glassy indomethacin, *Chem. Pharm. Bull.* **34**:4314–4321 (1986).
22. E. Fukuoka, M. Makita, and S. Yamamura. Glassy state of pharmaceuticals III. Thermal properties and stability of glassy pharmaceuticals and their binary glass systems, *Chem. Pharm. Bull.* **37**:1047–1050 (1989).

Crystals from first principles

A new calculation of the polymorphs of silica appears to have broken new ground in deriving crystal structure from chemical composition. But X-ray crystallographers need not worry — yet.

ONE of the continuing scandals in the physical sciences is that it remains in general impossible to predict the structure of even the simplest crystalline solids from a knowledge of their chemical composition. Who, for example, would guess that graphite, not diamond, is the thermodynamically stable allotrope of carbon at ordinary temperature and pressure? Solids such as crystalline water (ice) are still thought to lie beyond mortals' ken.

Yet one would have thought that, by now, it should be possible to equip a sufficiently large computer with a sufficiently large program, type in the formula of the chemical and obtain, as output, the atomic coordinates of the atoms in a unit cell.

That time may not yet have arrived, but S. Tsuneyuki, M. Tsukada and H. Aoki from the University of Tokyo, with Y. Matsui from Okayama University, have brought it a good step nearer. Starting with the information that the polymorphic forms of pure silica consist exclusively of SiO_2, they first calculate, from first principles, the force constants in clusters of the atoms and then, by molecular dynamics, the lattice constants of the four common polymorphs of silica (α-quartz, α-cristobalite, coesite and stishovite — the two last first recognized in the debris from meteoritic impacts).

The authors thank two computer centres in Japan for access to computing machinery, although they do not say how many Cray-equivalent hours their calculations occupied (*Phys. Rev. Lett.* **61** 871; 1988).

The calculation is not merely a taste of things to come but a pointer to the obstacles that remain, as well as being, in its own right, a considerable achievement. What the group has done is to invert the usual procedure in which force constants are calculated empirically from the properties of crystals. Their strategy is instead to calculate the force constants from first principles, for which purpose they must calculate the electronic structure of a complex of silicon and oxygen atoms.

The snag is that, even with the the price of Cray machines and their equivalents falling year by year, it remains beyond the capacity of computation to calculate the properties of a real crystal. So Tsuneyuki *et al.* start with the simplest of all relevant structures — the tetrahedral cluster SiO_4^{4-}.

But why SiO_4^{4-}, not SiO_4? Because Si readily surrenders electronic charge to oxygen atoms — the authors estimate 0.7 of an electron charge for every SiO bond, or close on two electron charges for those O atoms bound to two Si atoms. So, to ensure that their calculated structures are electrically neutral, the authors place electronic charges at points 1.65 Å along the four tetrahedral axes of the cluster, neatly simulating in the process the electrostatic effects of the neighbouring oxygen ions found in structures such as quartz.

It would be wrong to say that, from this point, everything depends on what the programmers have done, but that is how the article reads. Tsuneyuki *et al.* essentially calculate the electronic structure of the cluster for various departures of the atoms from their mean positions. They use pre-calculated atomic orbitals in a Hartree–Fock self-consistent field procedure (one of the means of allowing for electron–electron interactions in many-electron atoms).

In principle, there is every reason why the energy of the system should be quite a complicated function of the atomic positions. The surprise is that the parts of the energy surface so far calculated can be accurately represented by potential functions depending only on the distances between pairs of atoms in the cluster. Not surprisingly, one of these is a Coulomb term, another corresponds to the van der Waals attractive potential proportional to r^{-6} where r is the separation.

The molecular dynamics is made to seem just routine, no doubt because of the careful development of the appropriate programs by Japanese colleagues. Pressure and temperature are determined by the size of a repeating three-dimensional unit in a periodic lattice and by total kinetic energy respectively. The known structures of the four polymorphs of silica are each dealt with separately. In each case, the object of the exercise is to tell whether the polymorphs are dynamically stable, or that they are not spontaneously converted into each other, which all four prove to be. This is taken as an explanation of why they are all apparently stable under ordinary conditions even though, thermodynamically, they are metastable.

Given previous difficulties in calculating from first principles the properties of real solids, the results are extremely good. Unit cell dimensions turn out to be within 5 per cent of their measured values, bulk properties such as density and bulk modulus within 10 per cent. The agreement between calculated energy (enthalpy) of the polymorphs and the few measurements available is even better (1 per cent), but the authors say they could probably do even better if they allowed for the band structure of these polymorphs and the extent to which the bands are filled at different temperatures.

Several refinements remain to be explored. The chances are that three-body potentials and even more complicated variations of energy with configuration can be demonstrated by calculation and by comparison, for example, with measured specific heats. Evidently the treatment of charge transfer between Si and O, while effective, is somewhat artificial and does not allow for cooperative configurations extending over more than one SiO_4^{4-} tetrahedron.

In themselves, of course, these results are not a fulfilment of the goal of calculating from first principles the crystal structure of a compound of which nothing is known except chemical composition. But that cannot be far away.

On the face of things, the most obvious artificially introduced variables are the known crystal structures of the polymorphs of silica, used as a starting point for the molecular dynamics. It should not be beyond the wit of Tsuneyuki and his colleagues, with the help of a few computer centres, to select from a listing of all possible structures of an arbitrary material those that can be considered plausible on crystallographic and other grounds.

Perhaps the most striking feature of this laconic paper is the contrast it presents with the state of the art of calculating the properties of solids as recently as a decade ago, when it seemed that even the use of force constants derived empirically from the measured properties of crystals did not regenerate, on calculation, the authentic properties of those same crystals. But the practical importance of the new calculation could be considerable, especially with the need to learn something of the crystal structure of materials that are either very small ('microdot' zero-dimensional quantum wells, for example) or which vary in composition over distances smaller than the limits of X-ray crystallography (such as doped semiconductors). In applying calculations to these needs, a demonstration of success can rank, psychologically, with the example set by those who first climbed Everest.

John Maddox

IUCr Monographs on Crystallography

1 *Accurate molecular structures: their determination and importance*
A. Domenicano and I. Hargittai, *editors*
2 *P. P. Ewald and his dynamical theory of X-ray diffraction*
D. W. J. Cruickshank, H. J. Juretschke, and N. Kato, *editors*
3 *Electron diffraction techniques, Volume 1*
J. M. Cowley, *editor*
4 *Electron diffraction techniques, Volume 2*
J. M. Cowley, *editor*
5 *The Rietveld method*
R. A. Young, *editor*
6 *Introduction to crystallographic statistics*
U. Shmueli and G. H. Weiss
7 *Crystallographic instrumentation*
L. A. Aslanov, G. V. Fetisov, and J. A. K. Howard
8 *Direct phasing in crystallography: fundamentals and applications*
C. Giacovazzo
9 *The weak hydrogen bond in structural chemistry and biology*
G. R. Desiraju and T. Steiner
10 *Defect and microstructure analysis by diffraction*
R. L. Snyder, J. Fiala, and H. J. Bunge
11 *Dynamical theory of X-ray diffraction*
A. Authier
12 *The chemical bond in inorganic chemistry*
I. D. Brown
13 *Structure determination from power diffraction data*
W. I. F. David, K. Shankland, L. B. McCusker, and Ch. Baerlocher, *editors*
14 *Polymorphism in molecular crystals*
J. Bernstein

IUCr Texts on Crystallography

1 *The solid state: from superconductors to superalloys*
A. Guinier and R. Julien, *translated by* W. J. Duffin
4 *X-Ray charges densities and chemical bonding*
P. Coppens
5 *The basics of crystallography and diffraction, second edition*
C. Hammond
6 *Crystal structure analysis: principles and practice*
W. Clegg, *editor*
7 *Fundamentals of crystallography, second edition*
C. Giacovazzo, *editor*

Polymorphism in Molecular Crystals

JOEL BERNSTEIN
Department of Chemistry
Ben-Gurion University of the Negev

CLARENDON PRESS • OXFORD
2002

8.3.1 Quinacridones 259
8.3.2 Perylenes 263
8.3.3 Phthalocyanines 264
8.3.4 Some other pigments—old and new 270
8.4 Isomorphism of pigments 271

9 Polymorphism of high energy materials 275
9.1 Introduction 275
9.2 The 'alphabet' of high energy molecular materials 276
9.3 Individual systems 278
9.3.1 Aliphatic materials 278
9.3.2 Aromatic materials 287

10 Polymorphism and patents 297
10.1 Introduction 297
10.2 Ranitidine hydrochloride 298
10.3 Cefadroxil 301
10.4 Terazosin hydrochloride 304
10.5 Aspartame 305
10.6 Concluding remarks 307

References 308

Index 401

1

Introduction and historical background

With the accumulation of data, there is developing a gradual realization of the generality of polymorphic behavior, but to many chemists polymorphism is still a strange and unusual phenomenon. (Buerger and Bloom 1937)

In spite of the fact that different polymorphs of a given compound are, in general, as different in structure and properties as the crystals of two different compounds, most chemists are almost completely unaware of the nature of polymorphism and the potential usefulness of knowledge of this phenomenon in research. (W. C. McCrone 1965)

1.1 Introduction

In spite of chemists' occupation and fascination with structure and the connection between structure and properties, in McCrone's view in the nearly three decades following the observation of Buerger and Bloom there had not been any serious change in their awareness of polymorphism, its importance to chemistry and its potential usefulness. More than thirty-five additional years have passed, and that awareness is now increasing. As analytical methods have become more sophisticated, more precise and more rapidly carried out, the proliferation of data has revealed differences in structure and behaviour which can be attributed to polymorphism. The increasingly rapid accumulation and archiving of structural data allow for the systematic search and retrieval of those data for the purpose of correlating structure with properties. In short, polymorphism in chemistry is moving from a 'strange and unusual phenomenon' to one which is a legitimate and important area of research in and of itself that can also be utilized by chemists in unique and efficient ways for the study, understanding and development of structure–property relations in solids.

Structural diversity surfaces in almost every facet of nature. Chemistry in general is no exception, nor, in particular is structural chemistry, and crystal polymorphism is one manifestation of that diversity. The emphasis here will be on molecular crystals for a number of reasons. Inorganic compounds and minerals traditionally have been the purview of geologists and inorganic chemists and their innate interest in structure–property relationships led naturally to more organization and more awareness of polymorphism than in other pursuits. Monographs such as Wells' (1989) 'Structural Inorganic Chemistry' and Verma and Krishna's (1966) 'Polytypism and Polymorphism' are typical examples. On the other hand, organic solid state chemistry is a relatively new discipline (or multidiscipline), founded (or refounded) in the 1960s by the schools of Schmidt (1971) in Israel and Paul and Curtin (1973, 1975)

7

Polymorphism of pharmaceuticals

After discovery of the first cases of polymorphism with dramatic differences in biological activity between two forms of the same drug . . . no pharmaceutical manufacturer could neglect the problem. (Borka 1991)

There are many mysteries of nature that we have not yet solved. Hurricanes, for example continue to occur and often cause massive devastation. Meteorologists cannot predict months in advance when and with what velocity a hurricane will strike a specific community. Polymorphism is a parallel phenomenon. We know that it will probably happen. But not why or when. Unfortunately, there is nothing we can do today to prevent a hurricane from striking any community or polymorphism from striking any drug. (Sun 1998)

7.1 Introduction

The increasing awareness and importance of polymorphism in the past 30 years or so is perhaps nowhere more evident than in the field of pharmaceuticals (Bavin 1989). The landmark chapters of Buerger and Bloom (1937) and McCrone (1965) did not place any special emphasis on pharmaceutical materials. One outstanding exception was the book of Kofler and Kofler (1954), whose authors were members of an academic department of pharmacognosy (Webster: the branch of pharmacology that treats or considers the natural and chemical history of unprepared medicines). The seminal paper on the subject of polymorphism of pharmaceuticals was the review of Haleblian and McCrone (1969), which set the scope and the standards for many subsequent works. The literature on the polymorphism of pharmaceuticals is now best described as vast. A multiauthored monograph has appeared covering various aspects of the subject (Brittain 1999*b*), along with major sections of other books (Byrn 1982; Byrn *et al.* 1999), and an ever increasing number of reviews (Haleblian 1975; Kuhnert-Brandstätter 1975; Bouche and Draguet-Brughmans 1977; Giron 1981; Burger 1983; Threlfall 1995; Streng 1997; Caira 1998; Yu *et al.* 1998; Winter 1999; Vippagunta *et al*. 2001) covering various aspects of polymorphism as related directly to problems in the pharmaceutical field and/or pharmaceutical compounds, including some of the economic and intellectural property implications (Henck *et al.* 1997). Therefore, it would be foolhardy to attempt to present a comprehensive review of the subject here. Rather, in keeping with the general philosophy of this book, the aim is to provide a general introduction to the subject, with sufficient examples to demonstrate the points raised, and commensurate relevant references for the reader to seek further details and information.

7.2 Occurrence of polymorphism in pharmaceuticals

7.2.1 *Drug substances*

The development of a new drug from a promising lead compound to a marketed product is a long and expensive process, with odds of success estimated at 1 in 10 000 (Yevich 1991). The strict quality control requirements and the intellectual property implications of the drug industry lead to thorough and intensive investigations of the formation and properties of solid substances intended for the use in pharmaceutical formulations, both active ingredients and excipients. These efforts, often extending over long periods of time and with many potential experimental and environmental variables, can create conditions that can lead to the appearance of polymorphic forms, intentionally or serendipitously. While it may not be surprising that many pharmaceutically important materials have been found to be polymorphic, or that any particular compound may turn out to be polymorphic, every compound is essentially a new situation, and the state of our knowledge and understanding of the phenomenon of polymorphism is still such that we cannot predict with any degree of confidence if a compound will be polymorphic, prescribe how to make possible (unknown) polymorphs, or predict what their properties might be (Beyer *et al.* 2001).

There have been a few attempts to compile instances of polymorphism in pharmaceutically important materials. Since even the definition of what comprises 'pharmaceutically important materials' is itself subject to debate it is difficult to judge how comprehensive such compilations might be. However, generally they serve as useful references and are given here. One of the first organized attempts at such a compilation for steroids, sulphonamides and barbiturates was by Kuhnert-Brandstätter (1965) (see also Kuhnert-Brandstätter and Martinek 1965). Much of those data may be found in her subsequent book (Kuhnert-Brandstätter 1971), which also contains a compilation of many of the thermal studies of pharmaceutical compounds that revealed polymorphic behaviour. Numerous additional reports of studies by the Innsbruck school of polymorphic pharmaceutical compounds (using thermomicroscopy and IR spectroscopy) have appeared in the literature since the middle 1960s; many of those have been listed by Byrn *et al.* (1999). Borka and Haleblian (1990) compiled a list of over 500 references to reports of polymorphism in over 470 pharmaceutically important compounds.[1] This was shortly followed (Borka 1991) by a review of polymorphic substances included in Fasciculae 1–12 of the European Pharmacopoeia (EP), including a comparison of melting points in the EP and the original literature. The latter review was subsequently updated in 1995 by including EP entries for Fasciculae 13–19 (Borka 1995).

Griesser and Burger (1999) compiled the information regarding 559 polymorphic forms, solvates (including hydrates) of drug solids at 25 °C in the 1997 edition of

[1] Dr Borka has communicated with this author that he and Dr Haleblian did not receive galley proofs of this paper, which unfortunately contains 'numerous printing errors'. The list of errata actually contains 48 of them. Even with that cautionary note, it is a useful compilation.

Solid-State Pharmaceutical Chemistry

S. R. Byrn,*,† R. R. Pfeiffer,† G. Stephenson,† D. J. W. Grant,‡ and W. B. Gleason§

Department of Medicinal Chemistry and Pharmacognosy, Purdue University, West Lafayette, Indiana, 47907 and Department of Pharmaceutics and Department of Laboratory Medicine and Pathology, Biomedical Engineering Center, University of Minnesota, Minneapolis, Minnesota 55455

Received February 8, 1994. Revised Manuscript Received June 24, 1994®

Solid-state pharmaceutical chemistry encompasses a wide range of studies on pharmaceutical solids including (1) determination of the physical properties of polymorphs and solvates, (2) physical transformations between polymorphs and solvates, (3) chemical reactions in the solid state, and (4) solid–solid reactions which occur in pharmaceutical preparations. Recent advances in this field include improved understanding of crystallization processes, improved understanding of the need for characterization of polymorphs and solvates for both control and regulatory purposes, and a better understanding of the mechanisms of solid-state degradations and solid–solid reactions. This review will briefly describe recent advances in the following areas: (1) crystallization and the properties of crystals of pharmaceutical solids; (2) characterizations of crystal forms of drugs using solid-state NMR spectroscopy.

The study of the solid-state chemistry of drugs not only encompasses many scientific disciplines but also impinges on virtually all phases of the pharmaceutical industry, from discovery to successful marketing. It is clear that an understanding of the molecular structure of the solid state can lead to better design and control of drug performance.

The mission of those working in the field of solid-state pharmaceutical chemistry is to provide each drug in a solid form that has optimum performance in a given application. Pursuit of this mission requires recognition of several general, interrelated points: (1) Drugs can exist in a number of solid forms, each having different properties of pharmaceutical importance, including stability and bioavailability; the number and properties of these forms are largely unpredictable and vary considerably from case to case. (2) The forms of a drug may interconvert under various conditions. (3) Once a solid form is chosen for a product, methods for analysis and control of the form must be devised.

Let us briefly review each of these points with regard to their status in current practice and to some associated scientific challenges that remain.

(1) The most common solid forms that may be found for a given drug substance are as follows: **crystalline polymorphs**, forms having the same chemical composition but different crystal structures and therefore different densities, melting points, solubilities, and many other important properties; **solvates**, forms containing solvent molecules within the crystal structure, giving rise to unique differences in solubility, response to atmospheric moisture, loss of solvent, etc. Sometimes a drug product may be a **desolvated solvate**, formed when solvent is removed from a specific solvate while the crystal structure is essentially retained—again, many important properties are unique to such a form; finally, **amorphous** solid forms that have no long-range molecular order (i.e., no crystallinity) and which tend to be more soluble, more prone to moisture uptake, and less chemically stable than their crystalline counterparts (pharmaceutical processing operations may produce solids of low crystallinity intermediate between that of a crystalline solid and an amorphous solid).

To be sure, differentiating among the various solid forms of a substance is generally a routine matter. A number of analytical methods, used together, make this possible. Various familiar methods reveal the chemical composition of the solid and reveal the presence of solvent. The physical form is further characterized by X-ray powder diffraction, infrared and solid-state NMR spectroscopy, differential scanning calorimetry, and microscopy. The single most valuable piece of information about a crystalline solid, although not always available, is the molecular structure, determined by single-crystal X-ray diffraction.

Perhaps the chief challenge in managing the phenomenon of multiple solid forms of drugs is our inability to predict how many forms can be expected in a given case: too often costly delays are encountered when a less soluble solid form suddenly appears late in a development program. Progress along these lines awaits analysis and quantification of the myriad intermolecular forces within any proposed crystal structure as well as the ability to postulate the likely packing modes for a given molecule in all its configurations. Further research similar to that of Margaret Etter and co-workers, reviewed in section A, will doubtless lead to better success in predicting alternative solid forms of new drugs.

A second challenge relates to the strikingly different reactivity of different solid forms of many substances, whether it be oxidation, dehydration, decarboxylation, or other chemical reactions. Kinetics involving the solid state, in which specific contacts (or noncontacts) between reactive groups are dictated by the structure of a given solid form, are apt to be more complex than kinetics in solution, where the corresponding molecular encounters are much more random. Much the same can be said about the relative difficulty of elucidating mechanisms in these two states. Moreover, reactions in the solid state may be further complicated by other, often unknown factors such

† Purdue University.
‡ Department of Pharmaceutics, University of Minnesota.
§ Department of Laboratory Medicine and Pathology, University of Minnesota.
® Abstract published in *Advance ACS Abstracts*, August 15, 1994.

0897-4756/94/2806-1148$04.50/0 © 1994 American Chemical Society

as nucleation of a reaction product phase, presence of various amounts of amorphous component, strain or disorder in the crystal structure, and multiplicity of reaction products. As a result, there is very little information available to guide in any general way the prediction of the stability of compounds in the solid state, let alone in their different solid forms or different formulations. Thus, the stability of all but the most rugged products is generally characterized empirically at actual storage temperatures, and the value of studies at elevated temperatures must be assessed case by case. Elucidation of the kinetics and mechanisms of solid-state reactions is pursued in only the most pressing cases.

(2) A dictate of formulation technology is that the physical form of the drug substance, after being defined and verified, should not change once the product has been manufactured. Therefore, in addition to identifying various solid forms of a drug, an understanding of the specific factors that may bring about *transformations* between the forms is also essential.

Rates of solid-to-solid transformations in drugs are affected by one or more of the following variables: temperature, solubility in a given liquid phase, and vapor pressure of solvent. At a minimum, the investigator must therefore first identify and obtain certain physicochemical data on each relevant solid form:

- transition temperature(s) between polymorphs
- solubility of the drug in all solvents and solvent mixtures used in preparation of the final drug substance and throughout the formulation process
- equilibrium water vapor pressure *vs* composition isotherm

This information reveals which solid form is the most physically stable (least soluble) under specific conditions of temperature and composition; thus, if that form is already the one present, no transformation will occur. If, however, a less physically stable (more soluble) form is present, the *direction* of any transformation can now be predicted for given conditions. One might well ask why the most stable form is not always selected and, indeed, that is usually the case. There are however, situations where the peculiar properties of a less stable solid form are required for a product's performance—achieving higher solubility, for example. In such cases, the manufacturer has the added burden of demonstrating the *lack* of transformation to a more stable solid form throughout the life of the product. As discussed in the previous section, this task requires dealing with the problems of solid-state kinetics and must usually be approached empirically.

(3) Two main challenges to the analysis of pharmaceutical solids are dealing quantitatively with mixtures of forms in the drug substance and identifying the solid form of the active ingredient in the formulated product, particularly when the drug is a minor component in the presence of numerous other materials (excipients).

With this background on the current status of solid-state pharmaceutical chemistry, we can now turn to a number of recent advances in this field.

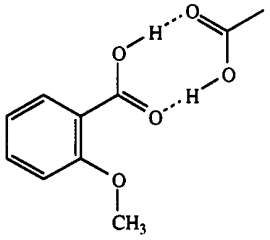
The work of Margaret Etter and co-workers, treated in section A, is an example of how present research addresses some of the issues of structure prediction raised above.

The topics discussed in sections B–D have significant bearing on many of the issues discussed in all three of the introductory subsections.

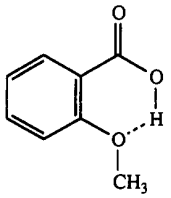
A. Forces Holding Crystals Together

Two main types of forces are responsible for holding drug crystals together: nonbonded interactions and hydrogen bonding. Nonbonded interactions occur in all crystals while hydrogen bonding is important in many compounds, especially pharmaceuticals. Etter has reviewed the extent and types of hydrogen bonding which can exist in organic solids.[1,2]

Carboxylic acids have been a particularly useful class of compounds for investigating alternative hydrogen bonding possibilities. For example, in *o*-alkoxybenzoic acids both dimerization and formation of intramolecular hydrogen bonding are observed.[3] In *o*-anisic acid, dimers are observed in the solid state while intramolecular hydrogen bonds are observed in dilute solution. However,

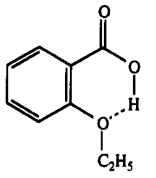


Solid State



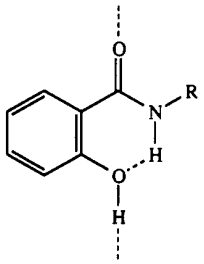
Solution

in *o*-ethoxybenzoic acid, only intramolecular hydrogen bonds are observed in the solid state and in solution.



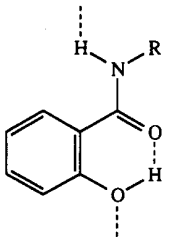
Solution and Solid State

The Etter group studied the hydrogen bonding in salicylamide derivatives and pointed out that two types of hydrogen bonding are possible in these compounds.[4] One type involves an intramolecular NH···O hydrogen bond and an intermolecular C=O···HO— hydrogen bond and the other an intramolecular C=O···HO— hydrogen bond and an intermolecular NH···O hydrogen bond.



Intra: HN··· O

Inter: C=O··· HO



Intra: C=O··· HO

Inter: HN··· O

(1) Goerbitz, C. H.; Etter, M. C. *Int. J. Pept. Protein Res.* **1992**, *39*, 93–110.
(2) Etter, M. C. *Acc. Chem. Res.* **1990**, *23*, 120–6.
(3) Etter, M. C.; Urbanczyk-Lipkowska, Z.; Fish, P. A.; Panunto, T. W.; Baures, P. W.; Frye, J. S. *J. Crystallogr. Spectrosc. Res.* **1988**, *18*, 311–25.

Table 1. Reliable and Occasional Hydrogen-Bond Donors and Acceptors

type	functional group involved
reliable donor	–OH,[a] $-NH_2$, –NHR, $-CONH_2$, –CONHR, –COOH
occasional donor	–COH, –XH, –SH, –CH
reliable acceptors	–COOH, –CONHCO–, –NHCONH–, –CON< (1–3°), >P=O, >S=O, –OH
occasional acceptors	>O, $-NO_2$, –CN, –CO, –COOR, –N<, –Cl

[a] Not COH.

Etter, MacDonald, and Bernstein developed a graph-theory-based approach to classifying and symbolically representing the different types of hydrogen bonds that can be formed.[5]

Etter also developed rules governing hydrogen bonding in solids. These rules require a classification of hydrogen bond donors and acceptors into "reliable" hydrogen-bond donors and acceptors and "occasional" donors and acceptors (Table 1). Using these classifications, three rules were devised: (1) All (or as many as possible) good proton donors and acceptors are used in hydrogen bonding. (2) Six-membered ring intramolecular hydrogen bonds form in preference to intermolecular hydrogen bonds. (3) The best proton donors and acceptors remaining after intramolecular hydrogen bond formation will form intermolecular hydrogen bonds. These rules apply quite well to hydrogen bonding of small molecules. However, in some larger molecules, e.g., erythromycins, steric factors make it impossible to satisfy all of the possible hydrogen bonded interactions, and some donors and acceptors are not involved in any hydrogen bonds.

Cocrystals. An important aspect of research into hydrogen bonding involves the realization that cocrystals can be obtained from certain solutions containing more than one molecular species. Cocrystals can also be formed by mixing or grinding two solids together. Cocrystals are usually formed between a hydrogen-bond donor molecule and a hydrogen-bond acceptor molecule. The nature of hydrogen bonding in cocrystals can also be described using the above rules. The cocrystals observed by Etter's group include numerous ureas with ketones, carboxylic acids with 2-aminopyridine, and also adenine or cytosine combined with many acidic organic compounds[6] such as carboxylic acids and *N*-acylamino acids. Other classes of cocrystals investigated by Etter's group are

pyrimidine, pyridines: carboxylic acids

pyridine-N-oxides: acids, alcohols, amines

phosphine oxides: acids, amides, alcohols, ureas sulfonamides, amines, water

carboxylic acids: other carboxylic acide, amides

m-dinitroureas: acids, ethers, phosphine oxides, sulfoxides, nitroanilines

imides: other imides, amides

The formation of cocrystals may be quite important in explaining solid–solid interactions in many fields including those of pharmaceuticals.

This elegant work of Etter and co-workers has greatly increased our understanding of the hydrogen-bonding interactions of molecules in both the solid state and in solution.

B. How Crystals Form

Crystallization and the factors controlling the formation of crystals is an extremely important area in solid-state pharmaceutical chemistry. Dr. Margaret Etter made an extremely important observation when she pointed out that molecules in solution often tend to form different types of hydrogen-bonded aggregates and hypothesized that these aggregate precursors are related to the crystal structures that form from the supersaturated solution.[2] This concept helps to explain the many different hydrogen-bonding motifs seen in different solids.

A number of factors can affect the crystal formed either by influencing the hydrogen-bonded aggregate precursors in solution or influencing one of the many other factors involved in crystallization. These include (1) solvent composition or polarity, (2) concentration or degree of supersaturation, (3) temperature including cooling rate and the cooling profile, (4) additives, (5) seeds and the presence of seeds, (6) pH (pH is important for crystallization of salts), and (7) agitation.

The composition of the solvent used is known to influence crystallizations either directly or by influencing the temperature at which the crystallization is initiated. For example, in the mannitol system, the α-polymorph is formed by evaporation of 100% ethanol while the β-polymorph is formed by crystallization from aqueous ethanol.[7] In a study of inosine, Suzuki showed that crystallization from water gave the α-form whereas crystallization from 70% DMSO gave the β-form.[8]

A second important factor influencing crystallization is the degree of supersaturation—the ratio of the concentration of the solution to that of a saturated solution. In his study of the polymorphism of cimetidine, Sudo showed[9,10] that in isopropyl alcohol at high supersaturation ratios (greater than 3.6) form A crystallized spontaneously or in the presence of seeds of either form A or form B, whereas in lower supersaturation ratios (less than 2) form A crystallized if there were A seeds and B crystallized if there were B seeds.

Temperature can have a very significant effect on the polymorph produced. Studies by Kitamura[11] on the crystallization of L-glutamic acid showed that at 45° the α-form nucleates slowly resulting in β-form growth, whereas at 25 °C the α-form nucleates rapidly causing α-form growth.

The effect of additives on crystallization has been of interest for many years. Early work by Simonelli indicated that polymeric additives could prevent the crystallization of certain phases.[12] Significantly, studies in recent years by Lahav and co-workers[13] have shown that additives (as

(4) Etter, M. C.; Reutzel, S. M. *J. Am. Chem. Soc.* **1991**, *113*, 2586–98.
(5) Etter, M. C.; MacDonald, J. C.; Bernstein, J. *Acta Crystallogr., Sect. B* **1990**, *B46*, 256–62.
(6) Etter, M. C.; Reutzel, S. M. *J. Am. Chem. Soc.* **1991**, *113*, 2586–98.
(7) Berman, H. M.; Jeffrey, G. A.; Rosenstein, R. D. *Acta Crystallogr.* **1968**, *B24*, 442–449.
(8) Suzuki, Y. *Bull. Chem. Soc. Jpn.* **1974**, *47*, 2551–2552.
(9) Sudo, S.; Sato, K.; Harano, Y. *J. Chem. Eng. Jpn.* **1991**, *24*, 237–242.
(10) Sudo, S.; Sato, K.; Harano, Y. *J. Chem. Eng. Jpn.* **1991**, *24*, 628–632.
(11) Kitamura, M. *J. Cryst. Growth* **1989**, *96*, 541–546.
(12) Simonelli, A. P.; Mehta, S. C.; Higuchi, W. I. *J. Pharm. Sci.* **1970**, *59*, 633.
(13) Weissbuch, I.; Addadi, L.; Lahav, M.; Leiserowitz, L. *Science* **1991**, *253*, 637–646.

little as 0.03%) can inhibit nucleation and crystal growth of a stable polymorph, thus favoring the growth of a metastable polymorph. They also showed that it is possible to design crystal nucleation inhibitors to control polymorphism.

In addition, Grant et al. have shown the effects of additives on the properties of adipic acid, acetaminophen (paracetamol), and (*R,S*)-(−)-ephedrinium-2-naphthalenesulfonate, a chiral drug. The effects on each of these crystalline solids will now be considered in turn.

When adipic acid is crystallized from water containing traces of *n*-alkanoic acids[14] or oleic acid,[15] the additive is taken up by the crystals, while the very small water content is not significantly affected. Changes in crystal habit and in the crystal growth kinetics are consistent with a structural model in which the added *n*-alkanoic acid molecules occupy lattice sites at the crystal surfaces.[16] The incorporated additive also changes the thermodynamic properties of the crystal. Notably, the crystal energy and entropy are increased, as measured by reductions in the enthalpies of fusion and solution, while the melting point is little affected.[14,15] In addition, the Gibbs free energy of the crystal increases, as measured by the dissolution rate and the specific surface area, and the density of the crystals is changed. Furthermore, the compaction properties, as measured by Hiestand's indices of tableting performance of the crystals are also modified.[17] Low levels of incorporated *n*-octanoic acid produce an increase in lattice strain, reducing the energy required for plastic deformation leading to improved tableting performance. At higher levels of incorporated *n*-octanoic acid, the tableting performance again approaches that of the pure crystal, indicating a reduction in plasticity. The above results with adipic acid may be explained by the impurity defects and attendant dislocations introduced by incorporated additive, resulting in increased lattice strain at low concentrations of additive and in reversal of the effects at higher concentrations. These proposed changes in lattice strain have recently been confirmed by corresponding increases and decreases in the mosaic spread of the Laue diffraction pattern when single crystals are irradiated by white X-radiation from a synchrotron source.[18]

When acetaminophen is crystallized from water containing the structurally related synthetic impurity, *p*-acetoxyacetanilide (PAA), the additive is incorporated and the crystals become acicular (needle-shaped). Increasing concentrations of PAA lead to increasing uptake of PAA to a maximum constant value (suggesting a saturated solid solution), to a decrease in water content, and to an increase in the length/width ratio.[15] Higher concentrations of PAA cause the length/width ratio and the water content to return to nearly the initial values. The maximum length/width ratio and the minimum in water content correspond approximately to maxima in the enthalpy and entropy of fusion and in the intrinsic dissolution rate of the crystals, the melting point being little affected. The physical properties of the acetaminophen crystals mentioned above were measured under 29 different crystallization conditions, defined by the initial concentration of PAA, the initial supersaturation of acetaminophen, and the rate of stirring of the crystallization solution.[19] Statistical analysis of the properties of these crystals, crystallized and analyzed in triplicate, showed strong correlations between the length/width ratio and the concentration of PAA taken up by the crystal and between the intrinsic dissolution rate and the length/width ratio, the thermodynamic quantities playing a minor role.[20] These results demonstrate the significance of additive-induced changes in crystal habit in influencing the intrinsic dissolution rate of acetaminophen crystals. Thus, whereas the behavior of doped crystals of adipic acid may be attributed to differences in lattice strain, the behavior of doped acetaminophen crystals may be attributed to differences in crystal habit.

In the above examples, adipic acid and acetaminophen exist as achiral molecules and crystallize in achiral space groups. The question arises as to the effect of traces of the opposite enantiomer on the crystal properties of a chiral drug. To help answer this question, the chiral drug (*R,S*)-(−)-ephedrinium 2-naphthalenesulfonate [(−)-EN] was crystallized from aqueous solutions containing traces of the opposite enantiomer (*S,R*)-(+)-ephedrinium 2-naphthalenesulfonate [(+)-EN].[21] Crystals of (−)-EN took up the opposite enantiomer with an appreciable segregation coefficient (0.153), while the water content and melting point of the crystals remained constant. Uptake of the opposite enantiomer led to changes in the thermodynamic properties and intrinsic dissolution rate. These changes are similar to those observed when adipic acid incorporated *n*-alkanoic acid from the crystallization solution. The similar behavior suggests an analogous molecular mechanism in the solid state, implying that doping with the opposite enantiomer produces changes in crystal properties that are analogous to doping of a foreign molecule of different, but related structure. Interestingly, (−)-EN and (+)-EN when heated together give a phase equilibrium diagram with a eutectic (together with limited solid solution formation) between each enantiomer and the racemic compound. This observation suggests that the observed changes in the thermodynamic properties and intrinsic dissolution rate of (−)-EN may be attributed to doping of the crystals with [(+)-EN/(−)-EN] molecular pairs or clusters rather than simply with the added (+)-EN molecules.

Seeding is used extensively to control crystal form and also to control the extent of nucleation (i.e., final particle size). In almost all cases, seeding can be used to control the desired crystal form. For example, Suzuki et al.[8] showed that the α-form of inosine could be obtained by crystallization from water whereas to obtain the β-form, seeds of the β-form must be used. An interesting study of the effect of seeding was reported by Konapudi, and the mechanism of crystallization was elucidated by McBride and Carter.[22] Sodium chlorate crystallizes in both a chiral and a racemic form. Since sodium chlorate is not chiral in solution, crystallization from aqueous solution produces equal numbers of L and D crystals.

(14) Chow, K. Y.; Go, J.; Mehdiadeh, M.; Grant, D. J. W. *Int. J. Pharm.* **1984**, *20*, 3–24.
(15) Chow, A. H. L.; Chow, P. K. K.; Wang, Z.; Grant, D. J. W. *Int. J. Pharm.* **1985**, *25*, 41–55.
(16) Davey, R. J.; Black, S. N.; Logan, D.; Maginn, S. J.; Fairbrother, J. E.; Grant, D. J. W. *J. Chem. Soc., Faraday Trans.* **1992**, *88*, 3461–3466.
(17) Law, D.; Grant, D. J. W. *Pharm. Res.* **1993**, *10*, S-152, PT-6102.
(18) Grant, D. J. W.; Law, D.; Ristic, R.; Shekunov, B.; Sherwood, J. N. *24th Annual Meeting of the Fine Particle Society, August 24–28, Chicago, IL*, 1993.
(19) Chow, A. H. L.; Grant, D. J. W. *Int. J. Pharm.* **1988**, *42*, 123–133.
(20) Chow, A. H. L.; Grant, D. J. W. *Int. J. Pharm.* **1989**, *51*, 129–135.
(21) Duddu, S. P.; Fung, F. K. Y.; Grant, D. J. W. *Int. J. Pharm.* **1993**, *94*, 171–179.
(22) McBride, J. M.; Carter, R. L. *Angew. Chem., Int. Ed. Engl.* **1991**, *30*, 293–295.

Surprisingly, crystallization of an aqueous solution with stirring gives mostly crystals of one chirality, either L or D. Investigation showed that this effect was due to the fact that once a particular crystal (either L or D) has formed, when that initial crystal collides with the stirrer and is broken into many small seeds which then nucleate further crystallization of that hand crystal (either L or D). This observation supports the idea that one nucleating seed can produce a single crystalline form. It also suggests that in this particular crystallization, if one added a seed of either L or D crystals then one would obtain entirely that crystal form. This is one of the best examples of the concept: one seed, one crystal.

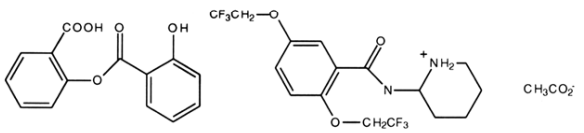
McCrone, in a letter to the editor of the *Journal of Applied Crystallography*, suggested that nucleation by seeding was the best explanation for the situation in which one unexpectedly obtains a new, more stable crystal form and then finds it is difficult or impossible to obtain the older less stable crystal form.[23] In response to this letter Jacewicz et al.[24] suggested that it is not impossible to produce the earlier form. They stated that the original crystal form should be capable of being produced but that the selection of the right conditions may require some time and trouble.

C. Disorder in Crystals of Pharmaceutical Solids

Another solid-state phenomenon which has important implications for pharmaceutical solids is disorder. Just as crystals of chiral and racemic drugs may have different physical properties, the presence of disorder in a crystal may also affect the physical properties of a crystal. One method of classifying disorder is to distinguish between cases involving static and dynamic disorder. Because single-crystal X-ray techniques give results which are averages over a long time period relative to molecular motion, X-ray crystallography at one temperature is usually unable to distinguish between static and dynamic disorder. Static and dynamic disorder can often be distinguished by comparing X-ray thermal parameters (ADPs) for two different temperatures. If the disorder results in observable resonance peaks in solid-state NMR spectra, then clearly this technique can be used to study this disorder.

In the crystallographic literature there are numerous examples of disorder which are caused by a molecule crystallizing in a single conformation but in a different orientation relative to other molecules in the crystal. There are also examples where the disorder is due to molecules crystallizing in different conformations.

Two such examples of conformational disorder are the crystal structures of nonsteroidal antiinflammatory (NSAID) drug salicylsalicylic acid (SALSALATE)[25,26] and the antiarrhythmic compound flecainide (TAMBOCOR).[27]



(23) McCrone, W. C. *J. Appl. Crystallogr.* **1975**, *8*, 342.
(24) Jacewicz, V. W.; Nayler, J. H. C. *J. Appl. Crystallogr.* **1979**, *12*, 396–397.

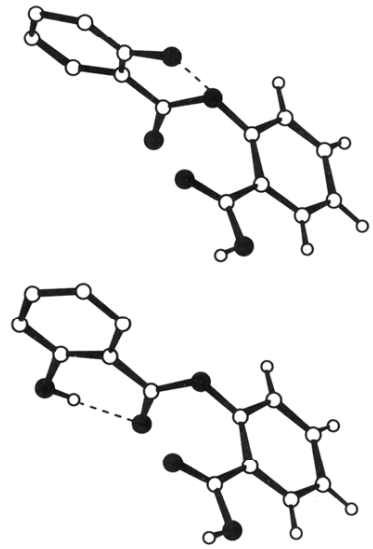


Figure 1. The two geometries of the SALSALATE molecule which are incorporated into the disordered crystal.

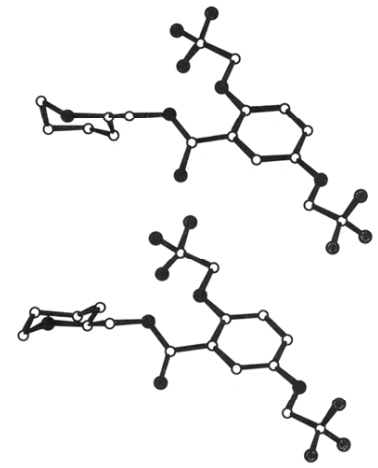


Figure 2. The two geometries of the TAMBOCOR which are incorporated into the disordered crystal.

The salsalate molecule can crystallize in two different conformations, each of which is intramolecularly hydrogen-bonded. Presumably, these two different intramolecular modes of hydrogen bonding are roughly equivalent energetically and the gross shape of the molecule in both conformations is similar so that both conformations can be incorporated into a single crystal as shown in Figure 1.

The other interesting example is the antiarrhythmic compound flecainide which is disordered in the solid state. The form of the compound which exhibits this disorder is actually the acetate salt, which was originally used for therapeutic purposes. Here the piperidinium ring takes on two alternate chair conformations as shown in Figure 2.

What are the consequences of such disorder? At the level of processing, the difficulty in reproducing material with the same properties may be responsible for different

(25) Frink, N.; Gleason, W. B.; Sweeting, L. M. In *IVth Midwest Organic Solid-State Chemistry Symposium*; Lincoln, NE, 1992.
(26) Frink, N.; Beaurline, J.; Gleason, W. B. In *Am. Cryst. Assoc. Annual Meeting*; Pittsburgh, PA, 1992.
(27) Gleason, W. B.; Bannit, E. H. In *Am. Cryst. Assoc., Annual Meeting*, 1987; p PE18.

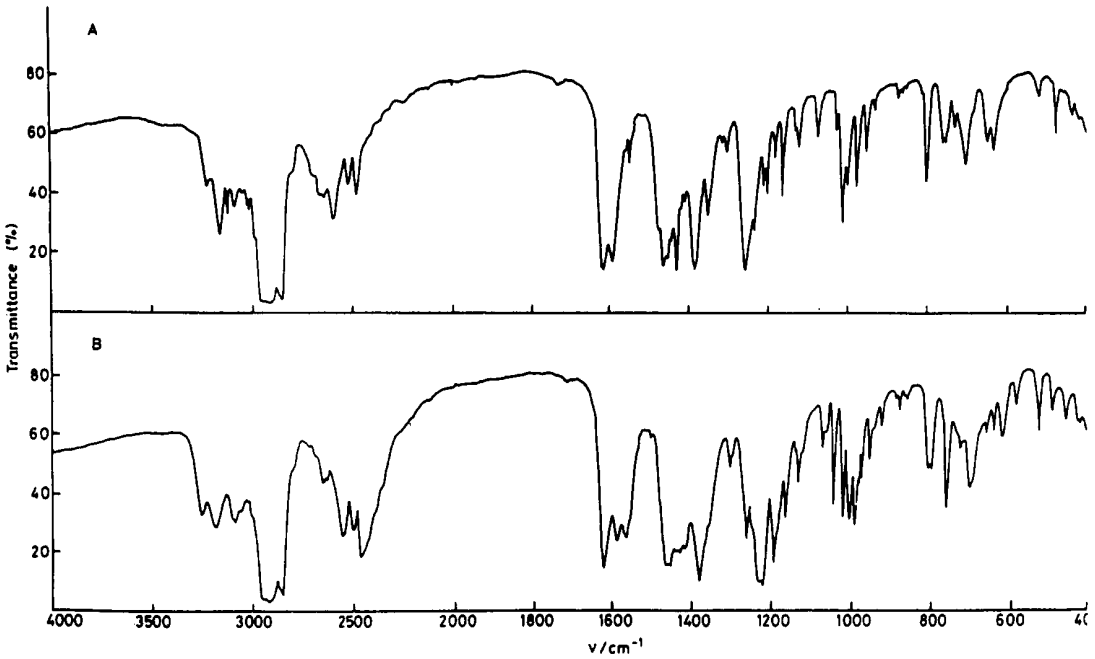


Figure 3. IR spectra of Nujol mulls of the two polymorphs of ranitidine hydrochloride: A, form 1; B, form 2.[29]

batches having dissimilar behavior. Batch-to-batch variability may be caused by differences in the ratio of the different conformations of molecule in the bulk sample.

Although disorder is a well-known phenomenon in the crystallography of small organics, the consequences of disorder in drug molecules appears not to have been widely considered. Just as crystals of chiral and racemic drugs may have different physical properties, the presence of disorder in a crystal may also affect the physical properties of the crystal. The amount of disorder (overall ratio of high occupancy to low occupancy conformations in the batch sample) found in a material may be highly dependent on the exact crystallization conditions. In turn the physical properties of individual batches may range from free-flowing powders to flocculent precipitates suffering badly from the effects of static electricity.

In addition, dynamic disorder reflects enhanced molecular mobility in the solid state. This enhanced molecular mobility may lead to enhanced chemical reactivity as suggested by the four-step mechanism of solid-state reactions first advanced by Paul and Curtin.[28] In this mechanism the first step is molecular loosening. Obviously, crystals possessing dynamic disorder are relatively loosely packed (at least near the site of disorder) and thus may be expected to be more reactive. At Purdue University, we are presently investigating cases in which the disorder of the system may relate to enhanced reactivity.

Are disordered samples with different amounts of disorder distinguishable? One method to distinguish this is discussed later in this review, solid-state NMR spectroscopy. Another approach is powder diffraction. Whether a particular sample will give a powder diffraction line which will change as a function of the disorder is a function of the scattering power of atoms in the alternate conformations and their contribution to scattering for a particular scattering plane. Computer programs are available for the calculation of powder diffraction patterns from single-crystal X-ray diffraction data. In one case we have examined, that of salicylsalicylic acid, our calculations indicate that certain diffraction lines are sensitive to the ratio of high occupancy to low occupancy conformations present in the salicylsalicylate sample. Thus the ratio of the intensities calculated for the two strongest lines in the powder pattern (311/202) varies from 0.80 to 1.75 as the amount of the "major conformer" is varied from 30% to 95%. Even though one must always be concerned with the effect of preferred orientation upon intensities for a powder sample, this calculation is encouraging for the possibility of using powder diffraction as a monitor for disorder in a material intended for pharmaceutical, or other use.

Salicylsalicylic acid crystallizes in Fdd2, an acentric space group, even though the molecule itself is not chiral.[25,26] This compound, as other salicyl esters, also exhibits strong triboluminescence. It is also disordered in the solid. The exact crystallization conditions for this compound can lead to solid material with a broad range of physical behavior. The variability in physical properties of this material may be tied to disorder in the crystalline material and may be a function of the amount of disorder found in the bulk sample.

D. Characterization of Pharmaceutical Solids

In this section the characterization of pharmaceutical solids will be briefly reviewed. This section is intended to provide the reader with a picture of the structure and properties of the various solid forms of pharmaceuticals.

The clearest indication of the existence of polymorphs and solvates comes from X-ray crystallographic examination of single crystals of various samples that are known to have the same composition but which may be suspected of being polymorphic. If single crystals of these materials have different unit-cell parameters then they may be polymorphs. Often, however, X-ray powder diffraction is sufficient to establish the existence of polymorphs. Thus polymorphs can be uniquely identified by their X-ray powder diffraction pattern and their structure completely elucidated by single-crystal X-ray diffraction.

(28) Paul, I. C.; Curtin, D. Y. *Acc. Chem. Res.* **1973**, *7*, 223.

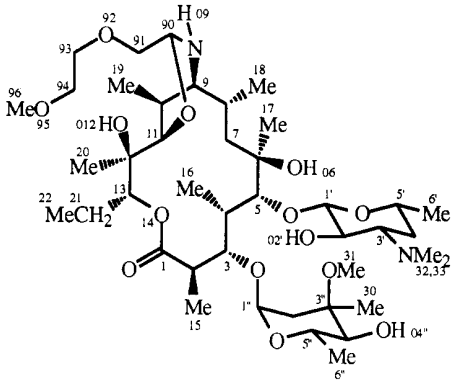
Knowledge of the polymorphs, solvates, and habits in which a drug crystallizes can lead to a dramatic improvement in understanding the stability, bioavailability, and ease of processing of pharmaceutical solids.

1. Infrared Spectroscopy of Solids. Infrared spectroscopy is quite useful for the analysis of solids, because it can be performed on small amounts of the solid substance. The method involves grinding the sample and measuring its infrared spectrum in one of several types of cells available. Infrared spectra of solids can also be obtained after suspending the sample in Nujol or grinding the sample with KBr and compressing this mixture into a disc. FT-IR microscopy can be used to measure the infrared spectrum of a single crystal or group of crystals. If care is taken to study only crystals of the same morphology, this method minimizes the possibility of obtaining infrared spectra of mixtures of crystal forms which is a distinct advantage over approaches that use powdered samples.

The infrared spectrum is extremely sensitive to the structure and conformation of a compound and, thus, can be used to compare the structure and conformation of the compound in different solids or in solid and solution. Infrared spectroscopy is thus a powerful method for the determination of polymorphs.

Cholerton et al.[29] reported the use of infrared spectroscopy to differentiate form 1 and form 2 of ranitidine hydrochloride (Figure 3). This is a classic example of the power of infrared analysis in polymorph studies.

Infrared spectroscopy is also useful for the investigation of solvates, as demonstrated by a study of erythromycin derivative (I).[30] Figure 4 shows the spectra of forms I and



II and the amorphous form of this compound. Clearly these three forms have different spectra especially in the carbonyl region. Note that form I shows two carbonyl absorptions, whereas the amorphous form and form II show only a single carbonyl absorption. Figure 5 shows the infrared spectra of three of the many solvates of this erythromycin derivative. These spectra are fairly similar except for the obvious C≡N stretching absorption in the acetonitrile·$3H_2O$ solvate. There are also slight differences among these three solvates in the fingerprint region. Figure 6 shows the infrared spectra of six solvates which are isomorphous (have the same crystallographic unit cell). These spectra are fairly similar as might be expected since they crystallize in the same unit cell. In cases where the solvents contain keto groups (e and f) the ketone absorption is obvious as a second carbonyl absorption in the spectrum.

(29) Cholerton, T. *J. Chem. Soc., Perkin Trans 2* **1984**, 1761.
(30) Stephenson, G. Unpublished observations, 1993.

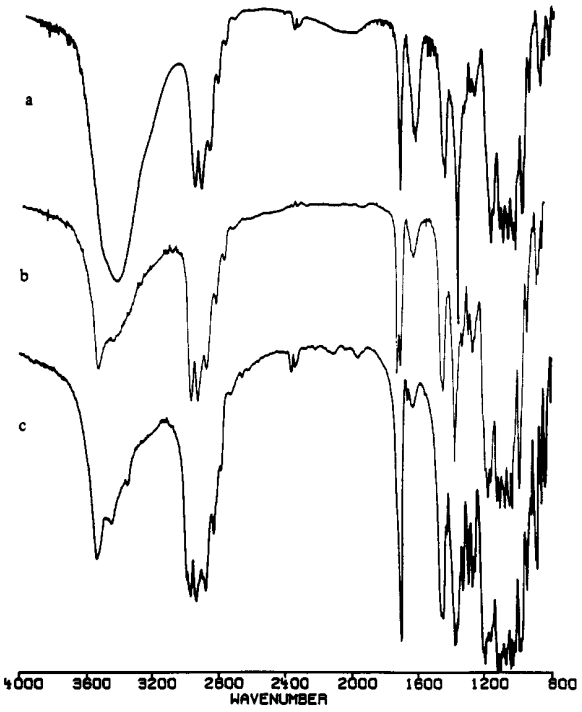


Figure 4. Infrared spectra of the amorphous form (a) and two anhydrous forms, I and II, (b and c) of an erythromycin derivative.[30]

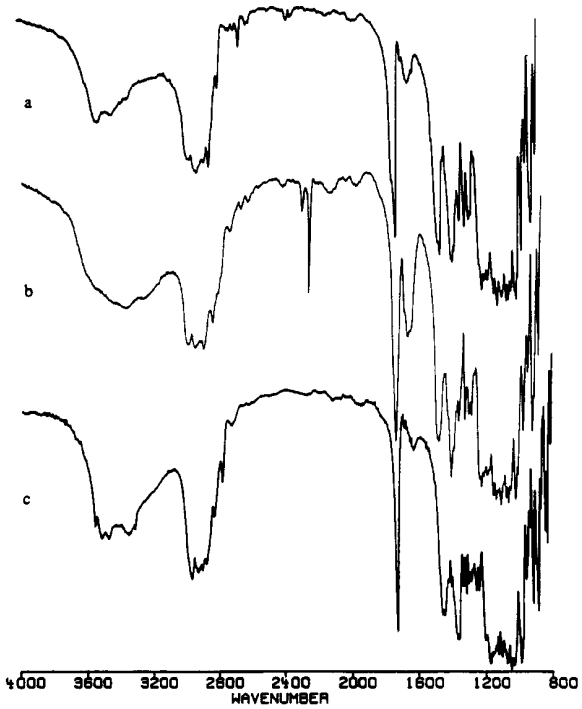


Figure 5. Infrared spectra of three nonisomorphic solvates of an erythromycin derivative: (a) tricyclohexane, (b) acetonitrile·$3H_2O$, and (c) *tert*-butyl alcohol solvate.[30]

Figure 7 shows an enlarged view of the ester carbonyl region of the spectrum in three of the crystal forms of the erythromycin derivative. These spectra suggest that the *n*-propanol solvate contains non-hydrogen-bonded carbonyl groups, that form II contains hydrogen-bonded carbonyl groups, and that form I contains both hydrogen-bonded and non-hydrogen-bonded carbonyl groups. These suggestions have been confirmed by the crystal structures

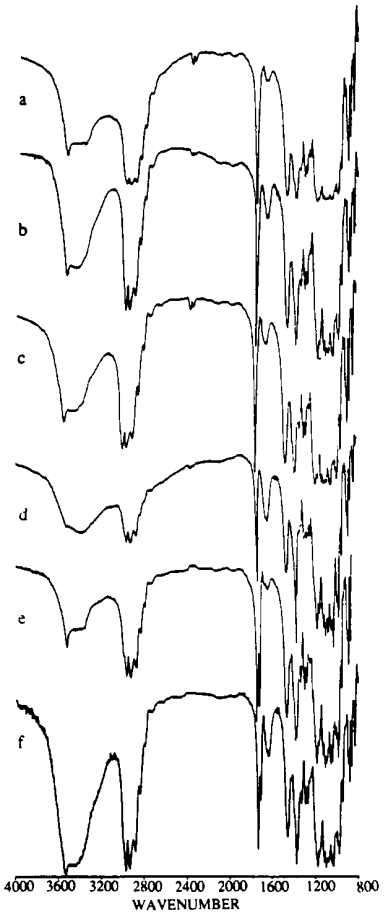


Figure 6. Infrared spectra of the isomorphic solvates of an erythromycin derivative: (a) ethanol, (b) *n*-propanol, (c) isopropyl alcohol, (d) *n*-butanol, (e) acetone, (f) methyl ethyl ketone.[30]

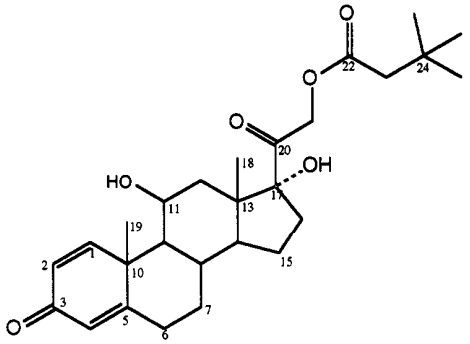
of the *n*-propanol solvate and hydrogen-bonded form II. Unfortunately, the crystal structure of form I could not be determined. Solid-state NMR confirms these suggestions as shown in Figure 8. Again, form I, which shows two carbonyl stretching vibrations in the IR also shows two carbonyl resonances in the solid-state NMR spectrum and the hydrogen bonded form shows a shift to lower field as expected based on model studies (see below).

2. Solid-State NMR Spectroscopy of Pharmaceutical Solids. Solid-state ^{13}C CP/MAS NMR offers significant advantages for the study of solid drugs.[31,32] Figure 9 shows the solid-state ^{13}C NMR spectra of two crystal forms of prednisolone and shows that they can be differentiated on the basis of differences in these spectra. Apparently changing the crystal packing results in significantly different magnetic environments for some of the carbon nuclei. This observation has considerable practical value: Figure 10 shows the ^{13}C CP/MAS NMR spectra of three prednisolone tablets from different vendors. It is clear that one can still observe resonances due to prednisolone, although these tablets contain only 5 mg of prednisolone in 95 mg of excipients. Comparison of Figures 9 and 10 shows that in tablets A and B form I exists, whereas in tablet C form II exists.

(31) Saindon, P. A.; Cauchon, N. S.; Sutton, P. A.; Chang, C. J.; Peck, G.; Byrn, S. R. *Pharm. Res.* **1993**, *10*, 197.
(32) Byrn, S. R.; Sutton, P. A.; Tobias, B. *J. Am. Chem. Soc.* **1988**, *110*, 1609–14.

Other reports show that different polymorphs of cellulose show different ^{13}C CP/MAS NMR spectra.[33] Moreover, solid-state ^{13}C CP/MAS NMR spectroscopy also offers the possibility of the analysis and characterization of amorphous forms. A particularly important question in this area is, What is the mobility of the molecule in amorphous forms? This question can be addressed by comparing the T_1 relaxation times of carbon atoms in the crystalline and amorphous state. In addition, the technique can be used to examine conformational and dynamic changes which occur in solid drugs by determining the coalescence temperature and associated rate constants for the process. In addition, because the time-scale of solid-state NMR spectroscopy is much shorter than X-ray crystallography, it offers the potential for analysis of a range of dynamic processes which cannot be studied by X-ray crystallography. These facts could lead to the widespread use of solid-state NMR spectroscopy in the pharmaceutical industry.

In our laboratory, we have used solid-state NMR to study the different crystal forms of prednisolone *tert*-butylacetate.[32] These studies show that the different crystal forms of prednisolone *tert*-butylacetate have different



Prednisolone 21-*tert*-butylacetate

solid-state NMR spectra. This is no doubt due to different crystal packing. Even forms I and II which have very similar unit cells have slightly different chemical shifts. However, the biggest difference between forms I and II is the position of the solvent peaks. In form I the ethanol solvent shows resonances at 18.1 and 58.2 ppm; in form II the propanol solvent shows resonances at 26.3 and 64.3 ppm. The solid-state NMR spectra of forms III, IV, and V are much different from those of form I and II and from each other. The biggest difference involves carbon 1 which shows chemical shifts which differ by up to 8 ppm from each other in the different crystal forms. Several of the other carbon atoms also show fairly large chemical shift differences. Figure 11 shows a plot of the difference between the solid state and solution chemical shift of carbon 1 vs the hydrogen-bond distance to the O3 carbonyl oxygen which is part of the α,β-unsaturated ketone system which contains carbon 1. It is important to note that this hydrogen bond to O3 is intermolecular and one of the forces responsible for holding the crystals of this steroid together. As can be seen from this plot (Figure 11), there is a more or less gradual shift to larger changes in ppm as the hydrogen-bond distance gets shorter and shorter. This observation is consistent with other studies of hydrogen bonding and also with solution studies

(33) Atalla, R. H.; Gast, J. C.; Sindorf, D. W.; Bartuska, V. J.; Maciel, G. E. *J. Am. Chem. Soc.* **1980**, *102*, 3249.

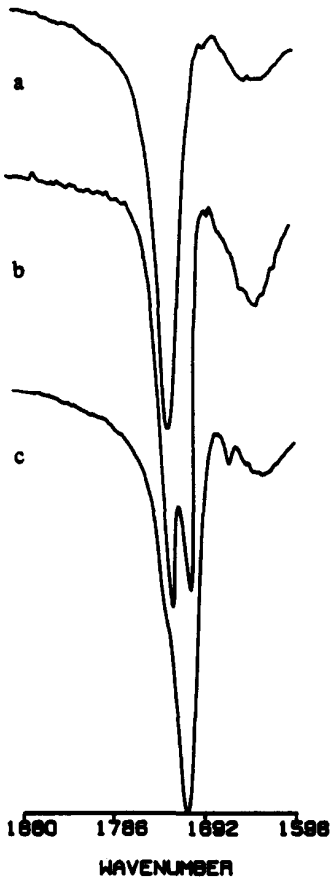
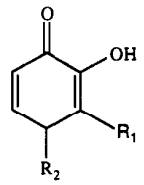


Figure 7. Ester carbonyl region of the *n*-propanol solvate (a), form I (b), and form II (c).[30]

where the stronger the hydrogen bonding the greater the chemical shift changes in ppm.

This type of correlation for different polymorphs and solvates shown in Figure 11 may also apply to members of a series of closely related compounds. Figure 12 shows that the $^{13}C(4)$ chemical shift difference between solid state and solution is a negative linear function of the crystallographic O(4)···O hydrogen bond distance in the crystal structures of a series of 1,2-dialkyl-3-hydroxy-4-pyridones (DAHPs) whose molecular structures are shown below:[34]



EMHP	$R_1 = CH_3$	$R_2 = C_2H_5$
PMHP	$R_1 = CH_3$	$R_2 = C_3H_7$
BMHP	$R_1 = CH_3$	$R_2 = C_4H_9$
MEHP	$R_1 = C_2H_5$	$R_2 = CH_3$
DEHP	$R_1 = C_2H_5$	$R_2 = C_2H_5$
EMHP	$R_1 = C_2H_5$	$R_2 = C_3H_7$

The DHAPs are iron chelators some of which may be promising drugs for oral administration in the treatment of diseases associated with iron overload. Although the crystal structure of the compound BMHP could not be determined, this compound provided an excellent ^{13}C NMR spectrum. The measured $^{13}C(4)$ chemical shift of BMHP might enable the O(4)···O hydrogen bond distance to be predicted using Figure 12, if this correlation is generally applicable.

(34) Ghosh, S. Ph.D. Thesis, University of Minnesota, 1993.

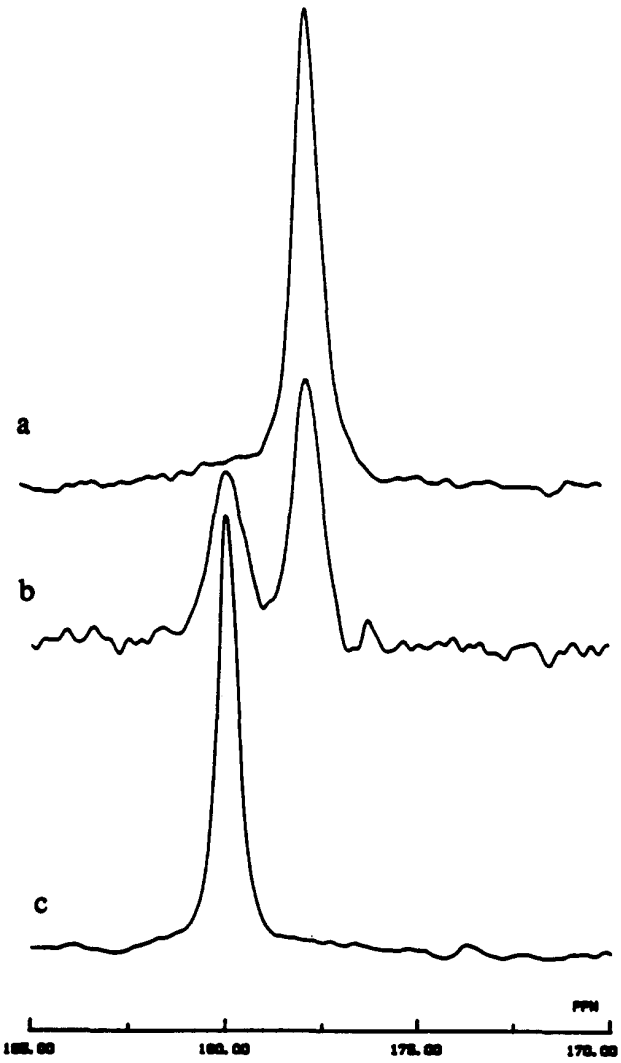


Figure 8. Solid-state NMR spectra of the ester carbonyl carbon: (a) *n*-propanol solvate, (b) form I, and (c) hydrogen-bonded form II.[30]

Solid-state NMR is also useful for the study of mobility in solids. The rate of relaxation of the carbon spins toward equilibrium is characterized by the spin lattice relaxation time, T_1.[35] In this process the excess energy from the spin system is transferred to "the lattice". Interactions of randomly fluctuating magnetic fields at the Larmor frequency of the nucleus stimulate these transitions. Such fields arise from motions of other nuclear magnetic moments such as protons. Spin–lattice relaxation is thus most efficient when these motions are near the Larmor frequency of the nucleus being observed. Studies of relaxation times can give valuable information about fast motions in the megahertz range such as methyl group rotations. Numerous studies of molecular motion using

(35) Fukushima, E.; Roeder, S. B. W. *Experimental Pulse NMR*; AddisonWesley: Reading, MA, 1988.

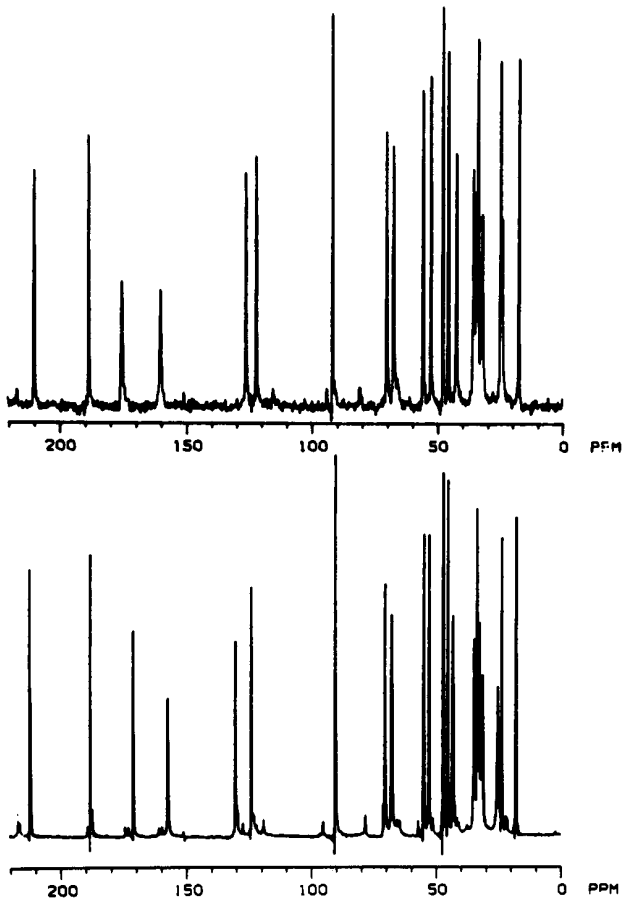


Figure 9. Solid-state ^{13}C CP/MAS NMR spectra of two polymorphs of prednisolone.[31] The top spectrum is form 1 and the bottom spectrum is form 2.

relaxation times have been published.[36] In particular, applications in the field of polymer science have been widespread. For example, solid-state NMR has been used to study both main chain and side group motion in polymers.[37-40] In addition, studies have been made of the relationship between polymer crystallinity and relaxation parameters including T_1, $T_{1\rho}$, and T_2.[41-43]

The mobility of functional groups in solids has been of interest for many years. An understanding of this mobility can lead to insight into the mobility of molecules, the forces responsible for conformational interconversions, and the factors responsible for solid-state reactions. In 1973, Paul and Curtin[28] suggested that molecular loosening or molecular mobility is the first step in a solid-state reaction, and, in our laboratory, we have suggested that solid-state

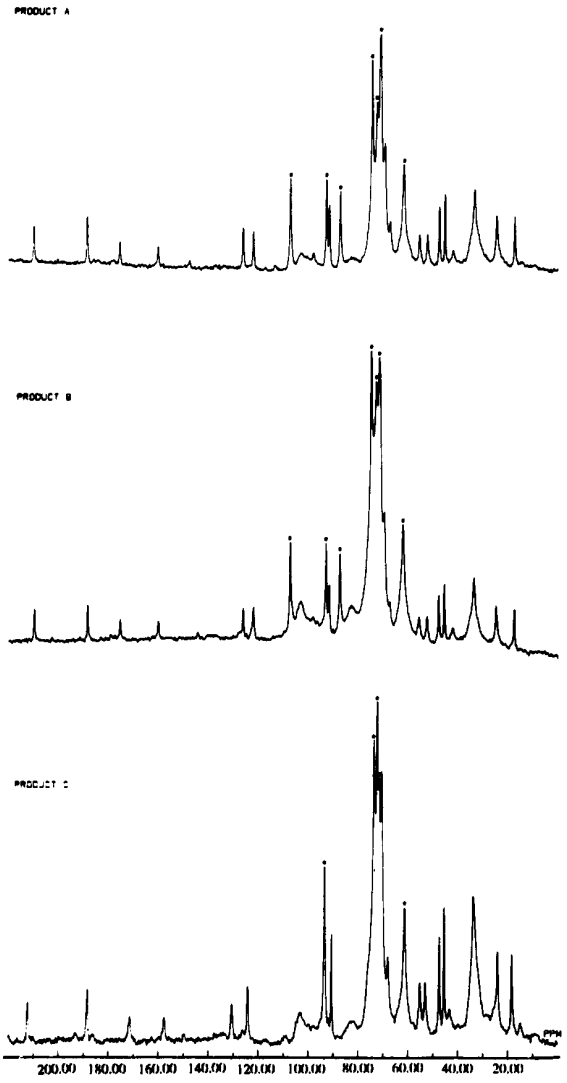


Figure 10. Solid-state ^{13}C CP/MAS NMR spectra of prednisolone tablets from three different vendors.[31]

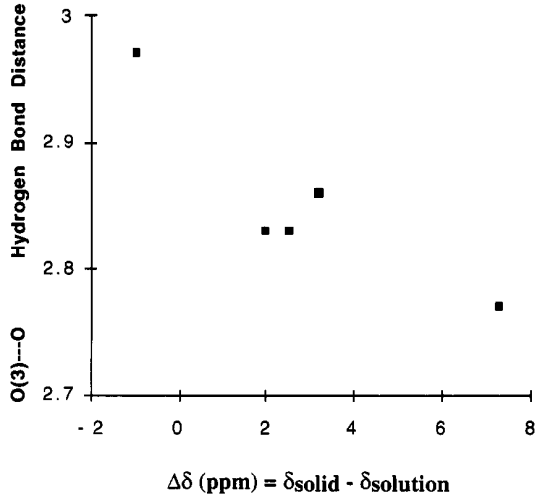


Figure 11. Plot of the difference in chemical shift for carbon 1 between the solid state and solution and the O(3)···O hydrogen bond distance.[32]

degradations of pharmaceuticals are related to molecular mobility.[32,44,45] In addition, Zografi has suggested that water absorption enhances the molecular mobility of amorphous pharmaceutical solids, perhaps explaining the

(36) Fyfe, C. A. *Solid-state NMR for chemists*; CFC Press: Toronto, Ontario, 1983.
(37) Lyerla, J. R. *Contemporary Topics in Polymer Science*; Shen, M., Ed.; Plenum Press: New York, 1979; Vol. 3, pp 143–213.
(38) Garroway, A. N.; Moniz, W. B.; Resing, H. A. In *Carbon-13 NMR in Polymer Science*; Pasika, W. M., Ed.; American Chemical Society: Washington, DC, 1979; pp 67–86.
(39) Tonelli, A. E.; G., M. A.; Tanaka, H.; Schilling, F. C.; Cozine, M. H.; Lovinger, A. J.; Bovey, F. A. *ACS Adv. Chem. Ser.*; Craver, C. D., Provder, T., Eds.; American Chemical Society: Washington, DC, 1990; Vol. 227, pp 409–451.
(40) Axelson, D. E. *Carbon-13 NMR in Polymer Science*; Pasika, W. M., Ed.; American Chemical Society: Washington, DC, 1979; pp 181–214.
(41) Menger, E. M.; Veeman, W. S.; de Boer, E. *Macromolecules* **1982**, *15*, 1406.
(42) Kitamara, R.; Horii, F.; Murayama, K. *Macromolecules* **1986**, *19*, 636–643.
(43) Earl, W. L.; VanderHart, D. L. *Macromolecules* **1979**, *12*, 762.

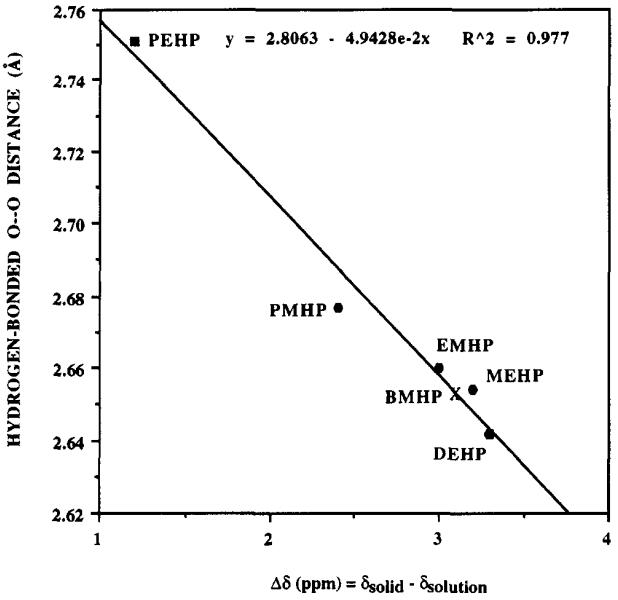


Figure 12. Plot of the hydrogen bonded O···O distances against the differences ($\Delta\delta$) between the ^{13}C chemical shifts of the pyridone carbonyl (O4) and the solid state (δ_{solid}) and the solution state ($\delta_{solution}$) of DAHPs. Although the crystal structure of BMHP is unknown, its hydrogen-bonded O···O distance can be estimated from the plot using the NMR chemical shift data (point X).[34]

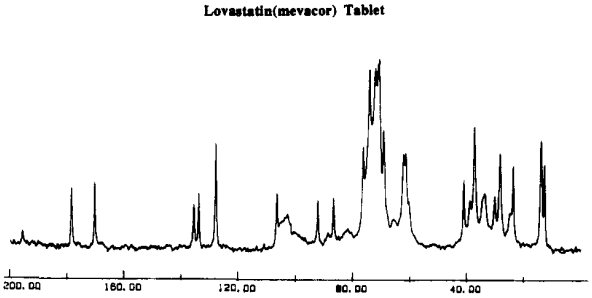
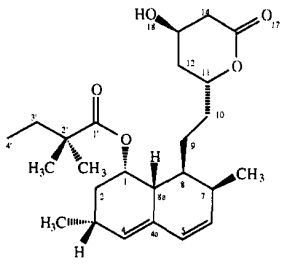


Figure 13. Solid-state CP/MAS NMR spectrum of a lovastatin tablet.

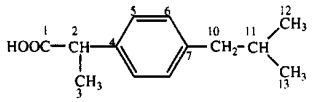
enhanced chemical reactivity of these materials in the presence of water.[46] Further study of the relationship between molecular mobility and solid-state reactivity requires the development of new approaches to determine molecular mobility especially in mixtures such as pharmaceutical dosage forms where single-crystal X-ray methods cannot be used.

Solid-state NMR offers several approaches to studying the molecular mobility of solids. These include (1) determination of the activation energies for T_1 relaxation of individual carbon atoms using variable-temperature solid-state NMR, (2) study of processes which result in peak coalescence of solid-state NMR resonances using variable-temperature solid-state NMR, (3) use of interrupted decoupling to detect methylene and possible methine groups with unusual mobility, and (4) comparison of solid-state MAS spectra measured with and without cross polarization.

Recent research at Purdue University is using all of these approaches but especially the first one to study the relative mobility of methyl groups in a number of drugs which contain multiple methyl groups including simvastatin, lovastatin, ibuprofen, and phenacetin.[47-49] The results of these studies will be published shortly.



Simvastatin



Ibuprofen

In addition, Maverick and Dunitz[50] have suggested that solid-state NMR activation energies and X-ray thermal parameters are related. Therefore, solid-state NMR appears to be a good method for study of the mobility of methyl groups in solids. Because solid-state NMR can be used to study pharmaceutical dosage forms and other mixtures,[31] this powerful method will find increased application in the determination of the molecular mobility of drugs in mixtures and dosage forms.

Surprisingly little research has been done on the solid-state NMR spectra of pharmaceutical dosage forms. To our knowledge, prior to the paper by Saindon et al.,[31] solid-state NMR has been used to study only two tablets both consisting almost entirely of pure drug: aspirin[51,52] and acetaminophen.[53] This paper shows that solid-state NMR is useful for the study of more complex pharmaceutical products.[31]

For example, Figure 13 shows the solid-state NMR spectrum of lovastatin tablets, which contain a rather large excess of excipients. The excipients, which have resonances in the 50–100 ppm range obscure resonances of lovastatin which appear at the same chemical shift but have little effect on resonances at other chemical shifts. Similar results were obtained for tablets of another closely related HMG-CoA reductase inhibitor, simvastatin.

E. Summary

In this review, areas of particular interest to Peggy Etter and her group were discussed including crystallization, hydrogen bonding, solvates and solid-state NMR. It is clear that her pioneering work has tremendously important implications for solid-state pharmaceutical chemistry.

(44) Byrn, S. R.; Lin, C. T. *J. Am. Chem. Soc.* **1976**, *98*, 4004.
(45) Byrn, S. R.; Kessler, D. W. *Tetrahedron* **1987**, *43*, 1335–43.
(46) Zografi, G. Z.; Ahlneck, K. V. *Int. J. Pharm.* **1990**, *62*, 87.
(47) Cauchon, N. Ph.D. Thesis, Purdue University, 1992.
(48) Saindon, P. Ph.D. Thesis, Purdue University, 1992.
(49) Toma, P. Ph.D. Thesis, Purdue University, 1993.
(50) Maverick, E.; Dunitz, J. *Mol. Phys.* **1987**, *62*, 451.
(51) Chang, C. J.; Diaz, L. E.; Morin, F.; Grant, D. *Magn. Reson. Chem.* **1986**, *1986*, 768.
(52) Diaz, L. E.; Frydman, L.; Olivieri, A.; Frydman, B. *Anal. Lett.* **1987**, *20*, 1657.
(53) Jagannathan, N. R. *Curr. Sci.* **1988**, *56*, 827.

COMMUNICATIONS CHEMISTRY

COMMENT

https://doi.org/10.1038/s42004-020-00388-9 OPEN

Open questions in organic crystal polymorphism

Aurora J. Cruz-Cabeza[1✉], Neil Feeder[2] & Roger J. Davey[1]

Polymorphs, crystals with different structure and properties but the same molecular composition, arise from the subtle interplay between thermodynamics and kinetics during crystallisation. In this opinion piece, the authors review the latest developments in the field of polymorphism and discuss standing open questions.

Be they medicines, foodstuffs, paints or electronics, many of the products that we consume contain active crystalline components. The structure and the properties of such crystalline solids are dictated by intermolecular interactions which bring molecules together in perfectly ordered symmetric arrangements—crystal structures (Fig. 1)[1]. The regularity of these structures is manifest to the naked eye in the form crystallites of regular and symmetric shapes (also known as crystal habits and morphologies), and their exquisite internal structures can be determined at the molecular level by techniques such as X-ray diffraction.

Crystallisation is the process by which molecular crystals are produced—with crystallisation from a liquid solution being the most common in industry. Two steps are involved in crystallisation: (i) nucleation, which is the process leading to the birth of a crystal nucleus and (ii) growth, which is the process by which molecules get incorporated into such nuclei, leading to macroscopic crystals. Because intermolecular interactions are soft 'bonds' and because molecules possess shape, the competition between maximum space filling and utilisation of strongest possible interactions can result in the nucleation and growth of different crystal structures (with identical composition and similar energies) under different crystallisation conditions (solvent, composition, purity, temperature, pressure). This phenomenon, known as crystal polymorphism (Fig. 1), was first noticed almost 200 years ago for inorganic compounds by Mitscherlich and soon after for organic compounds by the German chemists Liebig and Wöhler[2,3]. The phenomenon remained a curiosity at the time and was barely studied until, in the late 1960s, its importance to the development of drugs and other products began to be realised. Because each polymorph of a given molecule has a unique crystal structure, it would also have its own unique physical properties (such as mechanical hardness, solubility, colour, melting point etc). To manufacture and deliver crystalline based consumer products which perform consistently, therefore, it is vital to control and deliver the same polymorphic form across each batch of

[1] Department of Chemical Engineering and Analytical Science, The University of Manchester, Oxford Road, Manchester M13 9PL, UK. [2] Neil Feeder Consulting Ltd., 9 Betony Vale, Royston, Hertfordshire SG8 9TS, UK. ✉email: aurora.cruzcabeza@manchester.ac.uk

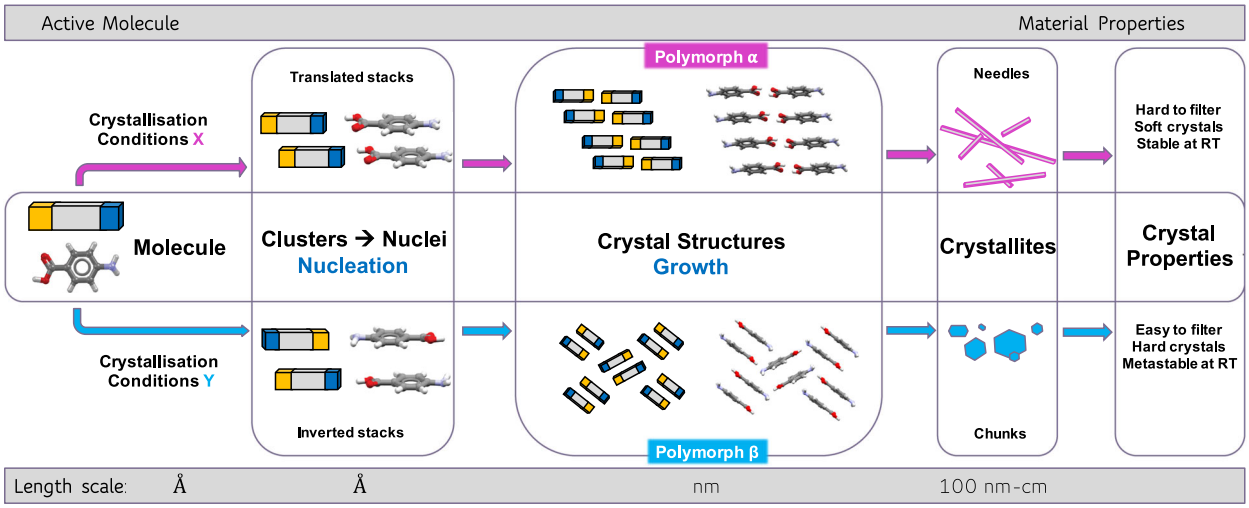


Fig. 1 Supramolecular assembly evolution of p-aminobenzoic acid (*p*ABA) from a single molecule into crystallites of two different polymorphs. The assembly occurs via two different routes (pink and blue) as a consequence of two different types of crystallisation conditions (X and Y), which leads to different early assembly, polymorphic structure, crystal shapes and material properties[1].

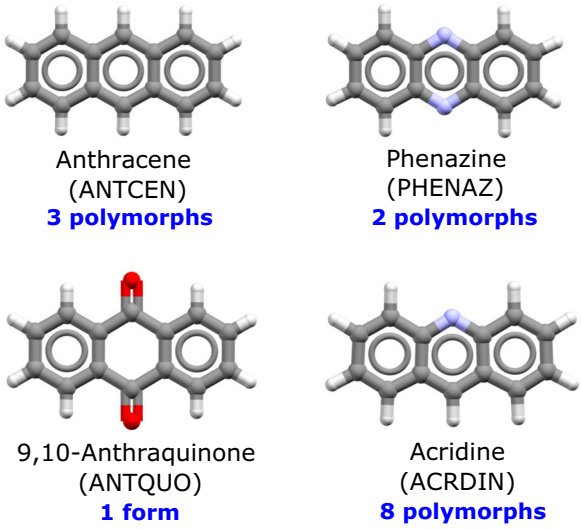


Fig. 2 Similar compounds can behave very differently when it comes to polymorphism. Molecular structure, Cambridge Structural Database six-letter family refcode and number of polymorphs for anthracene, phenazine, 9,10-anthraquinone and acridine.

crystals (Fig. 1). In this context, what have we learnt and what are the open questions in organic crystal polymorphism?

Molecular basis of polymorphism

Q1 Why are some compounds polymorphic and others not?. This is perhaps the first fundamental question which remains open. In some cases, compounds having very similar chemical structure behave in a completely different manner when it comes to polymorphism. To our knowledge, 9,10-anthraquinone crystallises in one unique crystal form, phenazine crystallises in two polymorphs, anthracene in three polymorphs, whilst acridine has been reported to have at least nine polymorphs (Fig. 2)[4]. We know from various databases that between 37–66% of compounds exhibit polymorphism[3]. The vast majority of polymorphic compounds are reported to only have a pair of polymorphs (89%), 9% three polymorphs and only 2% four polymorphs or more[2]. Yet, it remains impossible to know, based on molecular structure alone, whether a compound will be polymorphic or indeed how to decide if all possible polymorphs have been found in experimentation.

Q2 Are polymorphs predictable from molecular structure?. In the last 20 years or so, there has been enormous progress in the field of crystal structure prediction (CSP)[5]. CSP is a computational technique allowing for the generation of all possible crystal packings of a given compound. A polymorphic landscape is produced whereby hundreds of crystal structures are generated computationally, and their lattice energies calculated. These landscapes are sometimes successful at predicting the most stable low temperature crystal structure, if extremely accurate energy models are used[6]. Predicting which polymorphs might appear experimentally, however, still remains a major challenge. The fact that a crystal structure is generated computationally does not mean it can be obtained experimentally[7] and indeed making the link between prediction and practical realisation remains an unsolved, yet vital goal simply because while thermodynamic stability can be computed from structural information, rate constants for nucleation and growth cannot yet. However, some progress is being made here. Increasing evidence is appearing for the direct link between nucleation and growth rates with fast growers also being fast nucleators[8]. In this sense the problem may reduce to the computation of growth rates for which the literature is replete with methodologies. Here we mention the simple attachment energy methodology, the mechanistic models of Snyder and Doherty[9] and most recent work in which surface rugosity is used as a comparative measure of growth rates[10].

Experimental preparation of polymorphs

Q3 Why are some polymorphs so difficult to crystallise?. Nucleation, the origin of a crystal, is perhaps the least well understood step in the area of polymorphism. Kinetics and thermodynamics play a fine game in nucleation and crystal growth of various polymorphs. For example, theophylline form IV, despite being the most thermodynamically stable polymorph, is extremely difficult to crystallise because it is hard to nucleate and grows much slower than the common form II[11]. Ostwald's

rule of stages, with its central tenet that metastable forms will always appear first, has provided a useful experimental guide to the kinetics of solution crystallisation processes[12]. However, recently the rule has been shown to be only a special case of a much bigger experimental landscape, the details of which are currently beyond computation. Gaining a better understanding of the kinetics of crystal nucleation and growth for a wide range of polymorphic systems[13] is thus a must if we are able to establish better links between crystal forms and the conditions that afford them. Beyond detailed kinetic studies, the community would benefit from abundant and accurate reports of exact crystallisation conditions that lead to new polymorphs. The problem here, however, lies in the fact that often the presence of small amounts of impurities may play an important role. As a consequence, reports of irreproducibility of polymorphic observations or of disappearing polymorphs abound not only across labs but also within one's own[14]. Another aspect to consider in the crystallisation of polymorphs is the conformational problem whereby polymorphs with high energy conformers have been found to be very difficult to produce[2]. Other polymorphs cannot be nucleated directly from solution but have to be produced via desolvation of intermediate solvates[15] or through mechanochemistry[16].

Q4 Do polymorphs change stability under different conditions?. Most CSP landscapes only illustrate the system state at one unique set of conditions, usually 0 K and no external pressure. Polymorphs, however, are known to change in stability with conditions such as temperature, pressure and even particle size[17]. Therefore, the generation, understanding and prediction of phase diagrams under a number of conditions is an area that deserves careful further consideration within the context of polymorphism. In recent years, a number of approaches have been developed for the computation of crystal free energies[18] (beyond lattice energies) but these remain computationally expensive. Similarly, exploring polymorph stabilities experimentally with pressure may lead to stability changes between forms and the realisation of new polymorphs[19]. Finally, polymorph stability changes as a function of crystal size have rarely been studied although this has been shown to be important in the context of mechanochemistry[17] and crystallisation in nanoconfinement[20].

Q5 Can the crystallisation of polymorphs be directed by templating?. Many polymorphs can only be obtained by crystallisations in the presence of other compounds either in solution, with solid polymers[21] or crystallisation within gels[22]. Growing compounds onto isostructural (or mixed) seeds of related analogues has been proven as a way to produce some predicted forms but only in a handful of examples including form V carbamazepine[23] and ROY[24]. When such templating strategies are possible and how to achieve them remain open questions.

Characterisation of polymorphs

Q6 Are we able to detect and determine all polymorphs?. Despite advances in instrumentation over the last 50 years often compounds, especially large flexible pharmaceuticals, are difficult to crystallise as single crystals amenable to X-ray diffraction. In those cases, structure solution from powders or from a combination of methods may be the only possibility. In recent years, there has been some development in electron diffraction techniques which are able to solve complex structures, and even determine absolute configurations, from crystals of just a few hundreds of nm in size[25]. These techniques are still in need of further development so that they may be used more routinely in solid-state labs around the world. Related to this, tiny amounts of other polymorphs may be present in final products but are not detectable with current analytical techniques[26]. Increased sensitivity of analytical methods at the lab scale is therefore required, though this remains an issue of characterisation of materials in general. Finally, it is possible for true polymorphs to have very similar structures to the extent that that they may be overlooked experimentally, having only subtle differences in the X-ray diffraction patterns. Hence expert use of a combination of structural analysis techniques will be important in the future to uncover the true extent of polymorphism[27].

Structural basis for physical properties of polymorphs

Q7 Do crystal dynamics, defects and disorder effect polymorph properties?. The notion of an idealised perfect crystal is only true in theory. Real crystals are full of defects and many also have structural disorder. Beyond our average static view of crystals (averaged positions determined by XRD often at low temperatures), molecules are able to vibrate, librate and in some cases some of their groups are able to rotate (i.e. methyl group rotations or pedal motions). Our view of crystals and polymorphs is too static and to be able to better understand and model disorder or entropic contributions to free energies, we need to move towards a better understanding of crystal dynamics. This may require of further experimental data on high temperature structures and their dynamics as well as dynamic simulations of crystals. Disorder can manifest in many ways. It can be static or dynamic positional disorder of parts of the molecule within the unit cell, as well as more macroscopic phenomena such as mosaicity, twinning or stacking faults possibly also with loss of order at the crystal surfaces[28,29]. Each of these will have a precise effect on the physical properties of 'real' crystalline materials yet they remain difficult to characterise experimentally and model computationally even by expert practitioners.

Q8 Can we predict structure-property relationships?. We need to start establishing links between structure and properties in polymorphs so that we can enable computational prediction[30]. For this, first, properties of polymorphs need to be accurately measured, reported and reviewed. For example, Pudippeddi and Serajuddin compiled the solubility differences of a large set of polymorphs revealing solubility ratios between polymorphs is usually less than 2[31]. In recent years, with the development of nanoindentation there has been some novel work in trying to link crystal structure to mechanical properties of crystals[32]. More such studies would benefit the field tremendously since ultimately, the exploitation of polymorphs will be determined by their physical properties.

Outlook

In theory, one would want to generate the polymorphic landscape of a compound computationally, link it to crystal properties, retrieve the crystallisation conditions of the desired form and crystallise it. In practice, computationally generated polymorphic landscapes are challenging, structure-property relationships are not yet accurately predictable, we can rarely design crystallisation conditions for the discovery of specific polymorphic forms and crystallisation process design remains a challenging engineering exercise. Whilst we have learnt so much in the last fifty years or so, many fundamental questions remain open for us to solve in the coming decades.

Received: 17 September 2020; Accepted: 25 September 2020;
Published online: 19 October 2020

References

1. Cruz-Cabeza, A. J., Davey, R. J., Oswald, I. D. H., Ward, M. R. & Sugden, I. J. Polymorphism in p-aminobenzoic acid. *CrystEngComm* **21**, 2034–2042 (2019).
2. Cruz-Cabeza, A. J. & Bernstein, J. Conformational polymorphism. *Chem. Rev.* **114**, 2170–2191 (2014).
3. Cruz-Cabeza, A. J., Reutzel-Edens, S. M. & Bernstein, J. Facts and fictions about polymorphism. *Chem. Soc. Rev.* **44**, 8619–8635 (2015).
4. Schur, E. et al. The (current) acridine solid form landscape: eight polymorphs and a hydrate. *Cryst. Growth Des.* **19**, 4884–4893 (2019).
5. Neumann, M. A., Leusen, F. J. J. & Kendrick, J. A major advance in crystal structure prediction. *Angew. Chem. Int. Ed.* **120**, 2461–2464 (2008).
6. Hoja, J. et al. Reliable and practical computational description of molecular crystal polymorphs. *Sci. Adv.* **5**, eaau3338 (2019).
7. Price, S. L. Why don't we find more polymorphs? *Acta Crystallogr. Sect. B* **69**, 313–328 (2013).
8. Cruz-Cabeza, A. J. et al. Aromatic stacking—a key step in nucleation. *Chem. Commun.* **53**, 7905–7908 (2017).
9. Snyder, R. C. & Doherty, M. F. Predicting crystal growth by spiral motion. *Proc. R. Soc. Math. Phys. Eng. Sci.* **465**, 1145–1171 (2009).
10. Montis, R., Davey, R. J., Wright, S. E., Woollam, G. R. & Cruz-Cabeza, A. J. Transforming computed energy landscapes into experimental realities: the role of structural rugosity. *Angew. Chem. Int. Ed.* https://doi.org/10.1002/ange.202006939 (2020).
11. Bobrovs, R., Seton, L. & Dempster, N. The reluctant polymorph: investigation into the effect of self-association on the solvent mediated phase transformation and nucleation of theophylline. *CrystEngComm* **17**, 5237–5251 (2015).
12. Cardew, P. T. & Davey, R. J. The Ostwald ratio, kinetic phase diagrams, and polymorph maps. *Cryst. Growth Des.* **19**, 5798–5810 (2019).
13. Black, J. F. B. et al. Crystal nucleation and growth in a polymorphic system: Ostwald's rule, p-aminobenzoic acid and nucleation transition states. *CrystEngComm* **20**, 768–776 (2018).
14. Bučar, D.-K., Lancaster, R. W. & Bernstein, J. Disappearing polymorphs revisited. *Angew. Chem. Int. Ed.* **54**, 6972–6993 (2015).
15. Campeta, A. M. et al. Development of a targeted polymorph screening approach for a complex polymorphic and highly solvating API. *J. Pharm. Sci.* **99**, 3874–3886 (2010).
16. Day, G. M., Trask, A. V., Samuel Motherwell, W. D. & Jones, W. Investigating the latent polymorphism of maleic acid. *Chem. Commun.* **0**, 54–56 (2006).
17. Belenguer, A. M., Lampronti, G. I., Cruz-Cabeza, A. J., Hunter, C. A. & Sanders, J. K. M. Solvation and surface effects on polymorph stabilities at the nanoscale. *Chem. Sci.* **7**, 6617–6627 (2016).
18. Yang, M. et al. Prediction of the relative free energies of drug polymorphs above zero kelvin. *Cryst. Growth Des.* **20**, 5211–5224 (2020).
19. Fabbiani, F. P. A. et al. High-pressure recrystallisation—a route to new polymorphs and solvates. *CrystEngComm* **6**, 505–511 (2004).
20. Jiang, Q. & Ward, M. D. Crystallization under nanoscale confinement. *Chem. Soc. Rev.* **43**, 2066–2079 (2014).
21. Staab, E., Addadi, L., Leiserowitz, L. & Lahav, M. Control of polymorphism by 'tailor-made' polymeric crystallization auxiliaries. Preferential precipitation of a metastable polar form for second harmonic generation. *Adv. Mater.* **2**, 40–43 (1990).
22. Foster, J. A. et al. Pharmaceutical polymorph control in a drug-mimetic supramolecular gel. *Chem. Sci.* **8**, 78–84 (2016).
23. Arlin, J.-B., Price, L. S., Price, S. L. & Florence, A. J. A strategy for producing predicted polymorphs: catemeric carbamazepine form V. *Chem. Commun.* **47**, 7074–7076 (2011).
24. Lévesque, A., Maris, T. & Wuest, J. D. ROY reclaims its crown: new ways to increase polymorphic diversity. *J. Am. Chem. Soc.* **142**, 11873–11883 (2020).
25. Brázda, P., Palatinus, L. & Babor, M. Electron diffraction determines molecular absolute configuration in a pharmaceutical nanocrystal. *Science* **364**, 667–669 (2019).
26. Eddleston, M. D., Hejczyk, K. E., Bithell, E. G., Day, G. M. & Jones, W. Determination of the crystal structure of a new polymorph of theophylline. *Chemistry* **19**, 7883–7888 (2013).
27. Sacchi, P., Lusi, M., Cruz-Cabeza, A. J., Nauha, E. & Bernstein, J. Same or different—that is the question: identification of crystal forms from crystal structure data. *CrystEngComm* https://doi.org/10.1039/D0CE00724B (2020).
28. Bond, A. D., Boese, R. & Desiraju, G. R. On the polymorphism of aspirin: crystalline aspirin as intergrowths of two "polymorphic" domains. *Angew. Chem. Int. Ed.* **46**, 618–622 (2007).
29. Price, L. S. et al. A molecular picture of the problems in ensuring structural purity of tazofelone. *J. Mol. Struct.* **1078**, 26–42 (2014).
30. Nyman, J. & Day, G. M. Modelling temperature-dependent properties of polymorphic organic molecular crystals. *Phys. Chem. Chem. Phys.* **18**, 31132–31143 (2016).
31. Pudipeddi, M. & Serajuddin, A. T. M. Trends in solubility of polymorphs. *J. Pharm. Sci.* **94**, 929–939 (2005).
32. Varughese, S., Kiran, M. S. R. N., Ramamurty, U. & Desiraju, G. R. Nanoindentation in crystal engineering: quantifying mechanical properties of molecular crystals. *Angew. Chem. Int. Ed.* **52**, 2701–2712 (2013).

Acknowledgements

A.J.C.C. is thankful to the Royal Society for an Industry Fellowship in AstraZeneca. The authors are thankful to many colleagues in the Crystallography, Crystallisation and Crystal Engineering communities for helpful discussions. The authors are thankful to late Joel Bernstein for his past support and continued passion for polymorphism.

Author contributions

A.J.C.C. has led the writing of the comment and made the figures. N.F. and R.J.D. have contributed to discussions and to the writing of the comment.

Competing interests

The authors declare no competing interests.

Additional information

Correspondence and requests for materials should be addressed to A.J.C.-C.

Reprints and permission information is available at http://www.nature.com/reprints

Publisher's note Springer Nature remains neutral with regard to jurisdictional claims in published maps and institutional affiliations.

Open Access This article is licensed under a Creative Commons Attribution 4.0 International License, which permits use, sharing, adaptation, distribution and reproduction in any medium or format, as long as you give appropriate credit to the original author(s) and the source, provide a link to the Creative Commons license, and indicate if changes were made. The images or other third party material in this article are included in the article's Creative Commons license, unless indicated otherwise in a credit line to the material. If material is not included in the article's Creative Commons license and your intended use is not permitted by statutory regulation or exceeds the permitted use, you will need to obtain permission directly from the copyright holder. To view a copy of this license, visit http://creativecommons.org/licenses/by/4.0/.

© The Author(s) 2020

SUPERINTENDENCIA DE INDUSTRIA Y COMERCIO

NIT: 800.176.089-2

COMPROBANTE DE RECAUDO SISTEMA SIPI

Radicado: NC2021/0017366
Recibo: 25-157613
Fecha: 24/06/2025

CAROLINA MERCEDES DAZA MONTALVO
CC: 66.783.790
Pago PSE No: 1125978
CUS: 1575669509

Patente PCT
FORMA I ANHIDRA CRISTALINA DEL ATROPISÓMERO M DEL COMPUESTO 6-FLUORO-7-(2-FLUORO-6-HIDROXIFENIL)-1-(4-METIL-2-(2-PROPANIL)-3-PIRIDINIL)-4-((2S)-2-METIL-4-(2-PROPENOIL)-1-PIPERAZINIL)PIRIDO [2,3-D]PIRIMIDIN-2(1H)-ONA COMO INHIBIDOR SELECTIVO DE KRAS G12C

Detalle del pago

Id.	Rentístico	Concepto y Servicio	Cant.	Val. Unit.	Subtotal
1	50005-01-03	Modificaciones / Correcciones al registro Patente PCT (DESCUENTO INTERNET)	1	$ 225,000	$ 225,000
2	50005-01-01	Solicitud examen de patentabilidad Patente PCT (DESCUENTO INTERNET)	1	$ 1,522,000	$ 1,522,000
		TOTAL			$ 1,747,000

Sede Centro: Carrera 13 No.27-00 Pisos 3,4,5 y 10 Bogotá D.C. - Colombia
Web: www.sic.gov.co e-mail:contactenos@sic.gov.co Conmutador:(571)5870000 Contact Center: (571)5920400